2022

Ubiquitylation of Unphosphorylated c-myc by Novel E3 Ubiquitin Ligase SCFFbxl8

Sagar Bajpai
Medical University of South Carolina

Ubiquitylation of Unphosphorylated c-myc by Novel E3 Ubiquitin Ligase SCF^{Fbxl8}

Sagar Bajpai

A dissertation submitted to the faculty of the Medical University of South Carolina in partial fulfillment of the requirements for the degree of Doctor of Philosophy in the College of Graduate Studies.

Department of Biochemistry

2022

Pending Approval by:

Chairman, Advisory Committee	[Dr. John Alan Diehl]
	[Dr. Robin Muise-Helmericks]
	[Dr. Phil Howe]
	[Dr. David Long]
	[Dr. Antonis Kourtidis]

TABLE OF FIGURES:

ACKNOWLEDGEMENTS

First and foremost, I would like the thank Dr. John Alan Diehl for his mentorship. I appreciate all he has taught me, the patience and energy he invested me, and the guidance he gave. He truly encouraged me to explore with true freedom of scientific thought. Alan took the time and energy to consistently challenge my knowledge, methodology, and conclusions. His mentorship allowed me to develop a resilient, grounded, and confident mindset for which I will always be grateful. Thank you also to Hongri Jin, Bartosz Mucha, and Akihiro Yoshida taking the time out of their post-doctoral training to mentor a young trainee. I would also like to thank my committee members Phil Howe, David Long, Robin Muise-Helmericks, and Antonis Kourditis. These individuals provided critical insight into my scientific development. Perry Halushka, Amy Connolly, and Nancy DeMore have been an irreplaceable source of support. These individuals believed in my ability to overcome every hurdle I have faced during my MSTP training.

I would lastly like to thank my parents Ravi Shankar Bajpai and Anuradha Mishra Bajpai; without their life lessons, their love, and the risks they have taken for me, I would not be the person I am today.

"*To whom much is given, much is required"*

LIST OF FIGURES

LIST OF TABLES

LIST OF APPENDICES

LIST OF ABBREVIATIONS

5-FU – Fluorouracil

ACC – Adenoid Cystic Carcinoma

AML – Acute myeloid leukemia

ARF – Adenosine diphosphate-Ribosylation Factor

BAX – BCL2 Associated X, Apoptosis Regulator

BCL2 – B-cell lymphoma 2 protein

BIM – B-cell lymphoma 2 like protein 11

BRCA – BReast CAncer gene

BrdU – Bromodeoxyuridine

CDK – Cyclin-dependent kinases

CDK4 – Cyclin-dependent kinase 4

CESC – cervical squamous and endocervical adenocarcinoma

CHIP – The carboxy-terminus of Hsc70 interacting protein

CIP2A – Cellular Inhibitor of PP2A

CLL – Chronic lymphocytic leukemia

CML – Chronic myeloid leukemia

CRISPR – Clustered regularly interspaced short palindromic repeats

D3T283A – Cyclin D3 T→A amino acid change at 283rd residue

DDB – DNA-binding protein complex

DLBCL – Diffuse Large B-cell Lymphoma

DUB – deubiquitylating enzyme

E6AP – ubiquitin ligase E6 associated protein

ERK – extracellular signal-regulated kinases

FACS – fluorescence-activated single cell sorting

Fbx29 – also known as Fbxw8 (F-Box and WD Repeat Domain Containing 8)

Fbxl2 – F-box protein leucine rich repeat

Fbxl8 – F-Box and Leucine Rich Repeat Protein 8

Fbxo4 – F-Box Protein 4

Fbxw7 – F-Box and WD Repeat Domain Containing 7

Fbxw8 – F-Box and WD Repeat Domain Containing 8

GCS – (glutamyl-cysteine synthetase)

GFP – Green Florescent protein

GSK3β – Glycogen synthase kinase-3β

HAT – histone acetyltransferase

HLH-LZ – helix-loop-helix/leucine zipper

HSC – Hematopoietic stem cells

Hsp70 – 70 kilodalton heat shock protein

Hsp90 – 90 kilodalton heat shock protein

IHC – Immunohistochemistry

IKK – IκB kinase *complex*

Il-1β – Interleukin 1 beta

IRF5 – interferon regulatory factor 5

K (K48, K63) – Lysine (48) Lysin (63)

LUSC – Lung Squamous Carcinoma

Max – MYC Associated Factor X

MBII – Myc box II

MEF – Mouse Embryonic Fibroblasts

MEK – Mitogen-activated protein kinase kinase

MG132 – carbobenzoxy-L-leucyl-L-leucyl-L-leucinal

MIZ1 – "Myc-interacting zinc finger" protein

MXD – MAX Dimerization Protein 1

NEDD4 – neural precursor cell expressed developmentally down-regulated protein 4

NEMO – NF-kB essential modulator

NF-kB – Nuclear factor kappa B

NLS – Nuclear Localization Signal

OV- Ovarian Cancer

p53 – (TP53) tumor protein p53

PAAD – Pancreatic adenocarcinoma

PI3K – Phosphoinositide 3-kinases

Pin1 – Peptidyl-prolyl cis-trans isomerase NIMA-interacting 1

PP2A – Protein phosphatase 2

RBX1 - RING-box protein 1

RING - Really Interesting New Gene

S62 – Serine 62

SCF: Skp1 Cul1 F-box (complex)

shRNA – short hairpin RNA

siRNA – short interfering RNA

SKCM – Skin Cutaneous Melanoma

SWI-SNF – (SWItch/Sucrose Non-Fermentable) ATP dependent chromatin remodeling complex

T-ALL – T-cell acute lymphoblastic leukemia

T58 – Serine 62

TAD – transactivation domain

TCGA – The Cancer Genome Atlas

TCGT – Tenosynovial Giant Cell Tumor

THCA – Thyroid Cancer

TRIM32 – Tripartite Motif Containing 32

TRRAP – transactivation /transformation associated protein

TRUSS – tumor necrosis factor receptor-as-associated ubiquitous scaffolding and signaling protein

Ub – Ubiquitin

UCEC – Uterine Corpus Endometrial Carcinoma

UCS – Uterine Carcinoma

UPS – Ubiquitin Proteasome System

USP28 – ubiquitin specific protease 28

USP36 – ubiquitin specific protease 36

USP7 – ubiquitin specific protease 36

β-TrCP – *Beta*-Transducin Repeat Containing E3 Ubiquitin Protein Ligase

ABSTRACT

Overexpression of c-myc via increased transcription or decreased protein degradation is common to many cancer etiologies. C-myc protein degradation is mediated by ubiquitin-dependent degradation and this ubiquitylation is regulated by several E3 ligases. The primary regulator is Fbxw7 which binds to a phospho-degron within c-myc. Here, we identify a new E3 ligase for c-myc, Fbxl8 (F-box and Leucine Rich Repeat Protein 8), as an adaptor component of the SCF (Skp1-Cullin1-F-box protein) ubiquitin ligase complex, for selective c-myc degradation. SCFFbxl8 binds and ubiquitylates c-myc, independent of phosphorylation revealing that it regulates a pool of c-myc distinct from SCFFbxw7. Reduction of Fbxl8 expression is correlated in 11 distinct tumor tissue types. Loss of Fbxl8 increases c-myc protein levels, protein stability, and cell division while overexpression of Fbxl8 reduces c-myc protein levels. Concurrent loss of Fbxl8 and Fbxw7 trigger a robust increase in c-myc protein levels consistent with targeting distinct pools of c-myc. This work highlights new mechanisms regulating c-myc degradation.

Chapter 1: Introduction and Review of Literature

Introduction

The c-myc protein is dysregulated in about 70% of all human cancers and is often considered a driver of human cancers [1]. This stems from the fact that c-myc oncoprotein occupies 15 [2, 3] percent of the total genome promoters and plays a heavy hand in many contexts of tumorigenesis including cell cycle, differentiation, proliferation, and metabolism. The significance of c-myc deregulation is documented in T cell acute lymphoblastic leukemia, multiple myeloma, and certain subsets of Burkitt's lymphoma [4, 5]. Its involvement in such aggressive malignancies suggests that therapeutic efforts aimed at inhibiting MYC expression or activity should have an important clinical relevance. However, attempts to directly disrupt MYC function have been met with limited pharmacological success as there are still no clinically available MYC targeting therapies [6].

C-myc is a highly labile protein with a half-life of less that 30 minutes [7, 8]. Degradation of c-myc occurs via the ubiquitin-proteasome system (UPS). Rapid protein turnover by the UPS is an essential mechanism responsible for tight control of physiological levels of c-myc [9]. A well-defined process in c-myc degradation is the sequential phosphorylations of the serine 62 (S62) and threonine 58 (T58) residues. C-myc is stabilized upon phosphorylation of S62 by ERK.[10, 11] This priming step by ERK allows for the subsequent phosphorylation at the T58 residue by GSK3β.[12] The S62 residue is then dephosphorylated by PP2A although this has recently been shown to not be essential [8]. This monophosphorylated c-myc (T58 only) is recognized by the E3 ubiquitin ligase Fbxw7 and degraded by the 26S proteasome [13, 14] Highlighting the importance

of this degradation pathway in cancer, many of the signaling proteins (i.e. PP2A and Pin1) implicated in the MYC S62/T58 phosphorylation are often deregulated in tumor cells, resulting in altered c-myc phosphorylation and increased c-myc protein stability.[9, 15]

In this study we describe the identification and characterization of Fbxl8, an F-box protein that has only just recently been shown to function as an E3 ubiquitin ligase. As described in Chapter 2, Fbxl8, directly polyubiquitylates cyclins D3 in a phosphorylation-dependent manner in vivo and in vitro thereby determining the rate of degradation. Loss of Fbxl8 results in cyclin D3 accumulation, cell cycle dysregulation and oncogene-driven transformation revealing tumor suppressor potential. As described in Chapter 3, the main body of work from this investigation, Fbxl8 directly polyubiquitinates c-myc independent of the canonical phosphorylation sites (T58 and S62) in vitro and in vivo. Loss of Fbxl8 results in c-myc accumulation and cell cycle dysregulation revealing tumor suppressor potential.

Review of literature

Research on c-myc took place during a time where the genetic foundation of cancer largely uncharacterized. Only until the 1980's did the overall understanding of the c-myc protein really start to begin to take shape (Fig. 1.1). [16] Now decades later, thousands of c-myc papers have been published investigating a broad range of disciplines, including development, signal transduction, apoptosis, cell cycle, stem cell biology, non-coding RNAs, transcriptional and post-transcriptional mechanics, and of course the molecular basis of cancer and tumorigenesis. MYC has 3 related human genes *c-myc, l-myc, n-myc,* where c-myc is expressed consistently in cancer conditions.

The molecular basis of cancer is of particular interest to many since this context of study allowed for immense insight into overall c-myc function and regulation. Three novel mechanisms identified for c-myc oncogenic activation. The first mechanism was insertional mutagenesis. C-myc was the first cellular oncogene discovered to be activated by retroviral promoter insertion [17, 18]. The resulting leukemogenesis was induced by the avian myelocytomatosis retrovirus MC29, producing a chimeric *v-gag-myc*. This phenomenon was a clear example of neoplastic transformation through activation of a non-mutated gene and became a trailblazer for insertional mutagenesis being applied as a tool for oncogene discovery.

The second mechanism for oncogenic activation is chromosomal translocation. This is observed in mouse plasmacytomas and human Burkitt's lymphoma in which there is recombination between the immunoglobulin (Ig) heavy chain and the *Myc* oncogene [18-20]. Once again overexpression of a non-mutated gene was sufficient for tumorigenesis. This specific translocation has been modeled in *Eμ-Myc* construct [21].

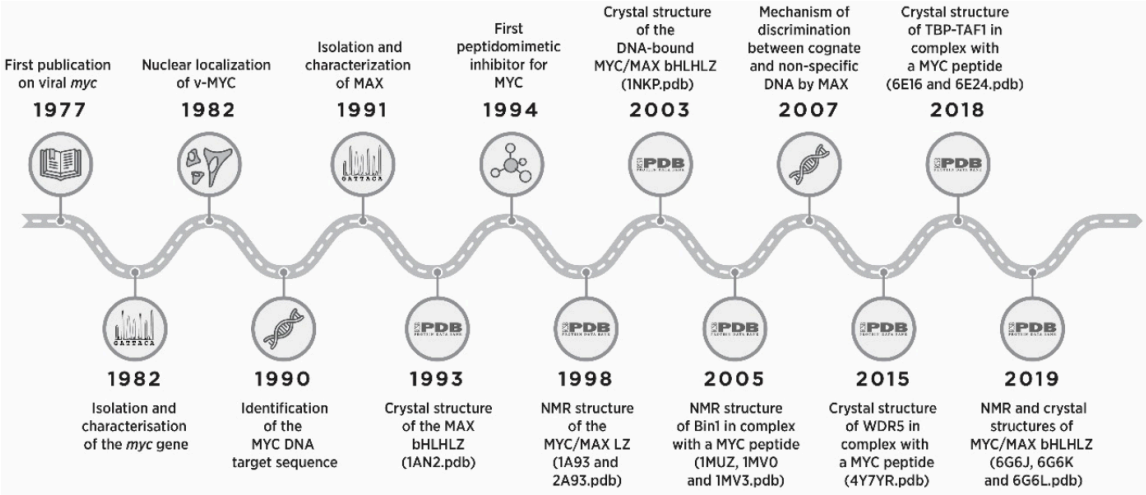

Figure 1.1 c-Myc Discoveries Over Time in Biology, Pharmacology, and Biophysics
(Beaulieu et al, 2020)

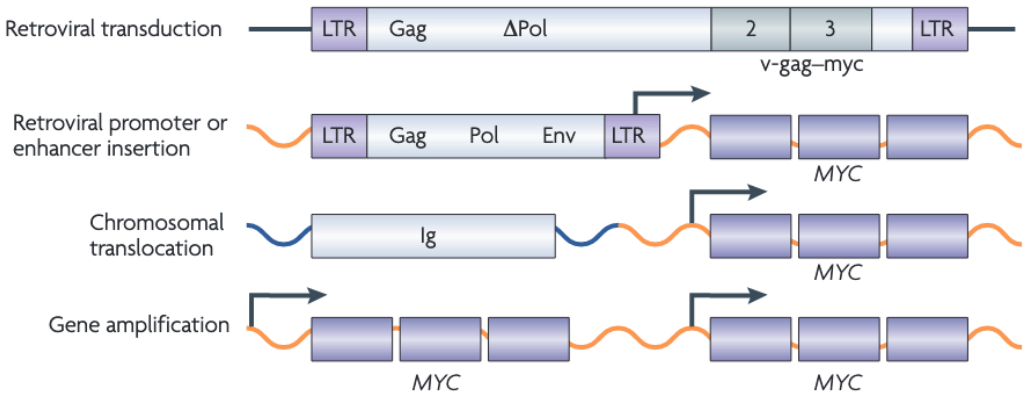

Figure 1.2 Genetic mechanisms of c-myc deregulation (Penn and Meyer et al 2008).
The v-gag-myc element from retroviruses were originally discovered to drive tumorigenesis. This led to the subsequent discovery that deregulation can occur through genetic alterations at the *MYC* locus. These genetic alterations include insertion of a retroviral promotor / enhancer, chromosomal translocation, and gene amplification.

Not only does this mouse acquire B-cell lymphoma but has been used in countless studies thereafter to advance understanding of c-myc overexpression in the context of cancer.

The third mechanism for oncogenic activation is genomic amplifications [18]. Cancer cells are prone to many karyotypic abnormalities and activation of the *Myc* genes via amplification is commonly observed in human solid tumors, unlike chromosomal translocations.

C-myc expression control

Different laboratory groups uncovered key aspects of c-myc regulation. The Eisenman group showed that v-myc directly binds to double stranded DNA [22]. Shortly after this S. Hann confirmed nuclear localization for the endogenous form of the protein. The Leder group showed that c-myc is also highly responsive to mitogenic stimulation and c-myc RNA rapidly reaches maximal levels within 2 hours of mitogenic treatment [23]. Inversely, anti-proliferative signaling was also shown to trigger sharp downregulation of c-myc expression. With regards to transcription, c-myc was the first gene discovered to be regulated by transcription elongation control. This block is seen in cell differentiation and look of this block is found in cancer [24]. The MYC promoter itself is the convergence of multiple signaling pathways that will either augment or mitigate MYC transcription. Post transcription mRNA turnover can also be influenced by translation dependent mechanisms. Poly (A) tail shortening will increase turnover in a translation dependent fashion while the coding determinant region on the carboxy terminus and the body of c-myc RNA influences RNA turnover in a translation dependent fashion [25]. Increased stability in c-myc mRNA in human cancers is influenced both via direct and indirect mechanisms (Fig. 1.3).

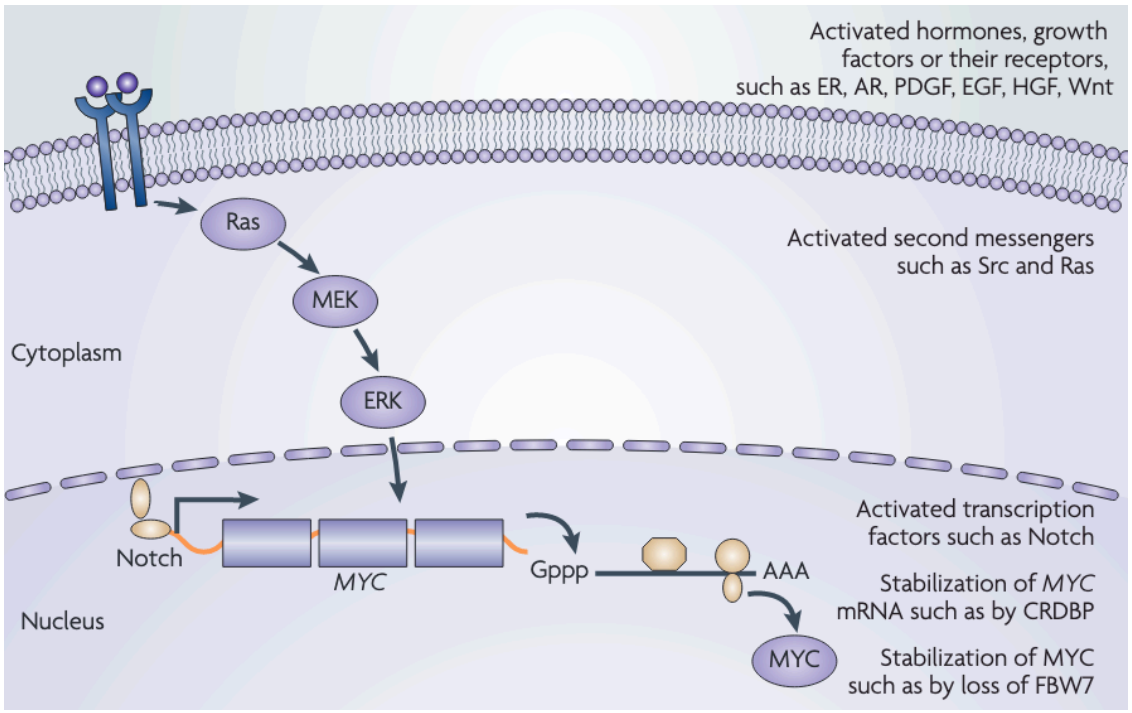

Figure 1.3 External Mechanisms of c-myc Deregulation (Penn and Meyer et al, 2008)
MYC can be deregulated by activation of hormones of growth factors, their corresponding receptors, second messengers, and transcriptional effectors that converge and integrate on MYC expression. Alterations in these mechanisms will directly or indirectly stabilize MYC mRNA and/or protein.

Oncogenic Cooperation

One concept that c-myc was crucial to uncovering was the idea of oncogene cooperation. The idea that malignant transformation of cells can occur and alter not only latency of disease but manifest a complete alteration in the tumor spectrum. In the laboratory of Dr. Rob Weinberg, an attempt was made to transform primary rat embryo fibroblasts instead of established, immortal fibroblasts. In this experiment Ras alone was not sufficient to transform these cells but when co-transfected with c-myc, these cells formed in vitro foci [26]. Bcl2, an anti-apoptotic protein was also found to collaborate with c-myc in the Adams laboratory. Both expressed genes together induce malignant transformation in lymphocytes [27]. The overarching trend that held true was that this oncogenic cooperation with c-myc was often related to mitigating apoptosis induced by oncogenic c-myc. The Cory laboratory further illustrated this in vivo when they crossed *Eμ*-myc mice with *Eμ*-Bcl2 mice [28]. This cooperation model was also recapitulated in humans as well [29].

Overall c-myc function was nebulous up until the late 1980s. Until this time what was known was that c-myc's expression was strongly associated with cell growth and that overexpressing c-myc was associated with reduced serum dependence for rapid proliferation [30]. This led to expensive study into whether c-myc played a role as a regulator of DNA replication or as a regulator of gene transcription. Over time it became clear that the latter was more clearly and reproducibly demonstrated.

Overarching Control of c-myc Expression

In 1983 it was discovered that stimulation of quiescent cells induced rapid transcription of c-myc RNA. Once cells were in the cell cycle both mRNA and protein were expressed at constant levels. The phosphorylation pattern of c-myc was also invariant throughout the cell cycle. Anti-proliferative signals triggered downregulation of c-myc protein levels. This data suggests that c-myc transcription is very tightly regulated in the context of normal non-transformed cells and is very sensitive to external cellular signals.

C-myc The Transcriptional Activator

C-myc heterodimerizes with its partner Max to induce its transcriptional and oncogenic activity [31]. However, this association is balanced through c-myc association with other cofactors of the Mxd family to add another layer of transcriptional activity of c-myc. Cofactor TRRAP (transactivation /transformation associated protein) that is essential for transformation activity by binding to the MBII region [32]. TRAPP also associations with c-myc to recruit histones acetylation complexes to chromatin [33]. INI1 (integrase interactor 1) another identified c-myc partner responsible for chromatin remodeling as a part of the SWI-SNF (SWItch/Sucrose Non-Fermentable) ATP dependent chromatin remodeling complex [34]. RNA polymerase II is also subject to recruitment by Myc through the PTEFb (positive transcription elongation factor complex). Cowling and Cole even presented evidence that c-myc can induce RNA polymerase II phosphorylation at the C-terminal domain along with mRNA cap methylation [35].

C-myc The Transcriptional repressor

C-myc does participate in its own negative feedback loop. Several lab groups have documented the non-translocated normal *MYC* allele in Burkitt's lymphoma does not even express; in fact, overexpressing exogenous c-myc downregulated endogenous c-myc expression in a dose dependent manner [36]. In transformed cells we there is a loss of this normal auto suppressive feedback and c-myc protein levels are no longer inhibited [37]. Genome wide analysis shows that c-myc suppresses just as many gene targets as it activates, adding further depth to the role of transcriptional repression in c-myc function.

How Does c-myc Transform Cells?

In cells with activated c-myc, G1 phase is shortened as cells enter the cell cycle and is essential for G1-S phase progression [38]. Transcription of CDK inhibitors and cell cycle checkpoint genes are overridden by c-myc and cell cycle progression is activated through c-myc's positive regulation of Cyclin D1, Cyclin D2, Cyclin E1, Cyclin A2, CDC25A, E2F1, and E2F2 [39]. These diverse roles of c-myc being involved if different pathways show how multiple cellular signals contribute to one overall biological program. Its already known that ectopic c-myc blocks differentiation in many cell types, and that downregulation of c-myc expression allows cell cycle exit and differentiation. C-myc prevents differentiation and promotes migration leading to more tumorigenic, more metastatic cancers. However, this regulation of differentiation by c-myc is strongly tied to cell fate.

In the latter part of the 1990s, c-myc became famous for two actions promoting tumorigenesis: regulating cell size and induction of the angiogenic switch. When c-myc activity is induced, cellular growth is no longer a rate limiting step to cell proliferation.

Increased metabolism and protein synthesis is backed by c-myc's ability to provide plenty of basic cellular building blocks to allow this process to perpetuate [40]. This occurs through c-myc activating an assortment of target genes to promote this biological program.

Dr. A. Thomas-Tikhonenko first showed that angiogenesis was associated with c-myc deregulation [41]. Several lab groups showed that thrombospondin downregulation through c-myc induced MiR17-92; a microRNA that is vital to angiogenesis[42]. It was also showed in pancreatic cells that Il-1B along with increased c-myc expression is needed for the angiogenic initiation [43]. These finding suggest that c-myc may have an interweaving role in regulation of normal vascular development and inflammatory responses in the angiogenic context.

C-myc and Apoptosis

Deregulated c-myc by itself promotes hyperproliferation with a compensatory increase in cell death [44]. For transformation to occur, c-myc potentiated apoptosis must be overridden. This is evident in c-myc null cells showing resistance to apoptotic stimuli [45]. The most well characterized pathway for apoptotic activity is the ARF-MDM2-p53 axis, caused by c-myc deregulation and concludes with p53 inducing the cell death program.

In the *Eμ*-Myc mouse model c-myc suppresses anti-apopotic proteins BCL2 and BCL-X indirectly, which is consistent with c-myc triggering apoptosis through BAX, which in turn releases cytochrome C from the mitochondria and inducing downstream caspase activity [46]. The Prendergast laboratory showed that c-myc sensitizes cells to undergo apoptosis via p53 dependent and p53 independent mechanisms. The p53

Table 1: C-myc Regulated activities and Target Genes (Penn & Meyer et al, 2008).

Functional class	Description of function	Examples of responsible genes*
Cell cycle	MYC–ER activation drives quiescent cells to enter and transit through the cell cycle; primary cells from conditional knockout mice arrest in the absence of MYC expression	Cyclin D2, CDK4 (induced); p21, p15, GADD45 (repressed)
Differentiation	Deregulated MYC blocks differentiation of many cell systems; MYC accelerates epidermal differentiation	CEBP (repressed)
Cell growth, metabolism and protein synthesis	MYC expression levels are associated with body size owing to regulation of cell size and cell number	Lactate dehydrogenase, CAD, ODC, ribosomal proteins, EIF4E, EIF2A (induced)
Cell adhesion and migration	MYC drives tumorigenesis in part by allowing for anchorage-independent growth	N-cadherin, integrins (both repressed)
Angiogenesis	MYC induces angiogenesis in a wide range of tissues	IL1β, miR-17–92 microRNA cluster (induced), thrombospondin (repressed)
ROS, DNA breaks and chromosomal instability	MYC can contribute to instability, trigger telomere aggregation and increase ROS production	MAD2, TOP1, BUBR1, cyclin B1, MT-MCI
Stem cell self-renewal and/or differentiation	Ectopic MYC can potentiate induced pluripotent stem cells; MYC can control the balance between stem cell self-renewal and differentiation	To be determined, potentially genes associated with cell cycle, immortalization, adhesion and migration
Transformation	MYC can drive focus formation and anchorage-indepenent growth *in vitro* and full tumorigenesis *in vivo*; MYC is often deregulated in primary human cancers	Multiple targets are thought to contribute to transformation

independent mechanism works through upregulation of BIM, a pro-apoptotic molecule [47]. Restarting apoptotic pathways in the presence of deregulated c-myc could prove an effective anti-tumor growth strategy in therapeutics.

As stated, before a major pathway in which c-myc levels are controlled is through selective degradation by the ubiquitin proteasome system (UPS). Here we discuss various mechanisms by which the UPS controls c-myc protein levels and overall c-myc stability along with how this relates to c-myc transcription and therapeutic strategy.

Aside from UPS dependent degradation it is noteworthy to mention calpain dependent cleavage. This cleavage occurs in the cytoplasm where the calpains inactivate c-myc transcriptional activity via removal of the C-terminus in a calcium dependent fashion. This cleavage generates what is known as the MYC-Nick (Fig. 1.4), a 298 amino acid sequence from the N-terminus that has been show to play a role in muscle differentiation through regulation of microtubules, particularly in the context of muscle differentiation [48].

Regarding the degradation by the ubiquitin proteasome system, a highly specific ATP-dependent process, proteins are degraded in 2 key steps; The first step involves ubiquitin being covalently added to the target protein substrate and the second step being the ubiquitylated substrate being degraded by the 26s proteasome (Fig 1.6). Addition of ubiquitin occurs through activation if ubiquitin by the E1 ubiquitin activating enzyme. Then, activated ubiquitin is then transferred to the E2 conjugating enzyme to work in tandem with the E3 ubiquitin ligase, which is already bound to the substrate target protein, to transfer the activated ubiquitin to a Lysine (K) residue on the substrate target protein. Subsequent ubiquitin units are attached to one another at their respective K residues.

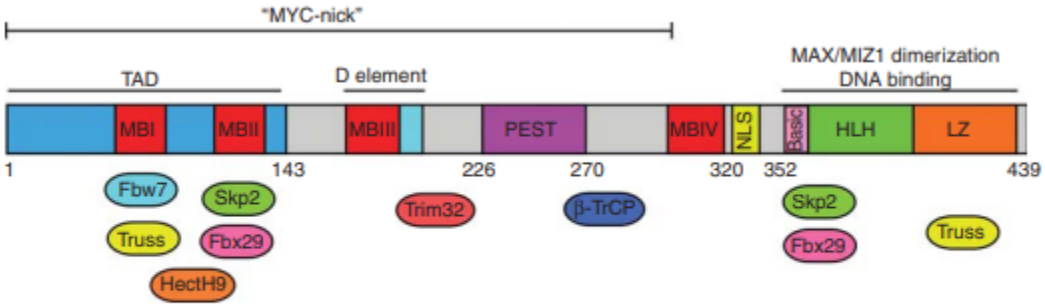

Figure 1.4 Structure of MYC (Farrell & Sears et al, 2014). E3 ligases known to regulate MYC stability, function, and localization

The K48 polyubiquitin chain linkage is recognized by the proteasome and hence strongly correlated with proteasomal degradation. Recent literature however suggests that other ubiquitin moieties are recognized by the proteasome for proteasomal degradation. [49]

Any given cell contains a handful of E1 activating enzymes, around 50 E2 conjugating enzymes, and about 500 E3 ligases. This is a reflection of how E3 ligases are particularly responsible for substrate specificity [50]. There are several categories of E3 ligases which all differ in homology and mechanism of action. The first the E3 ligase family is the RING-FINGER/U-BOX family. This E3 acts as a scaffold bringing together the E2 and the substrate target for ubiquitylation. The E3 is a multi-unit complex that has a RING-FINGER domain (like Rbx), a Cullin scaffold, an adaptor (like Skp1), and a substrate specific binding element (F-box protein). The last category is the HECT (homologous to E6AP carboxyl terminus) domain E3 ligases. These E3s, unlike others, form a catalytic intermediate with ubiquitin and directly transfer ubiquitin onto the substrate. Regions of c-myc affected by UPS protein contain elements that control their own degradation.

Fbxw7, shown in Fig. 1.5, is the most well characterized E3 ligase for c-myc. It is a part of the SCF (Skp1-Cul1-F Box) complex [51, 52] and has about 90 total characterized substrates target including c-myc, making it very interesting in a slew of biological and disease contexts. There are 3 isoforms including Fbxw7 α, β, and γ. They localize in the nucleoplasm, cytoplasm, and nucleolus respectively with the α isoform being responsible for binding and degrading c-myc. Fbxw7 ubiquitylates c-myc with K48 linked polyubiquitin chains for degradation and only does so after c-myc is phosphorylated at the T58 and S62 residues by ERK and GSK3β respectively [14].

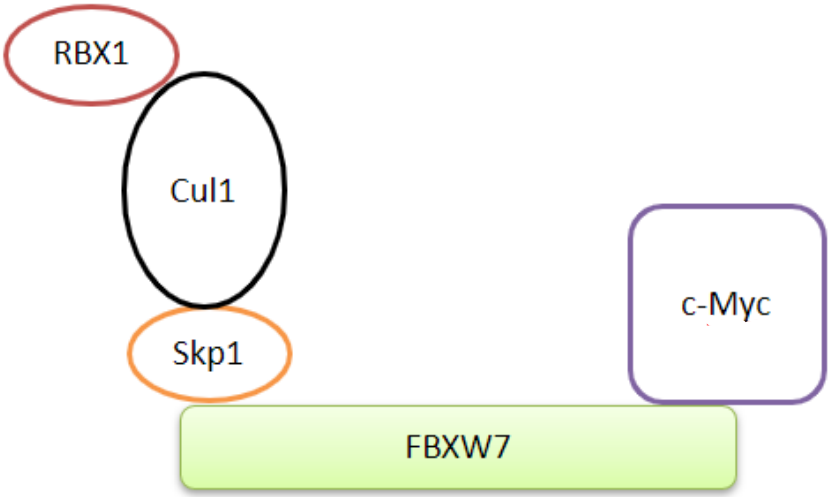

Figure 1.5 E3 Ubiquitin ligase SCF^{Fbxw7}
Schematic of Fbxw7 interfacing with c-myc substrate and core E3 ubiquitin ligase machinery

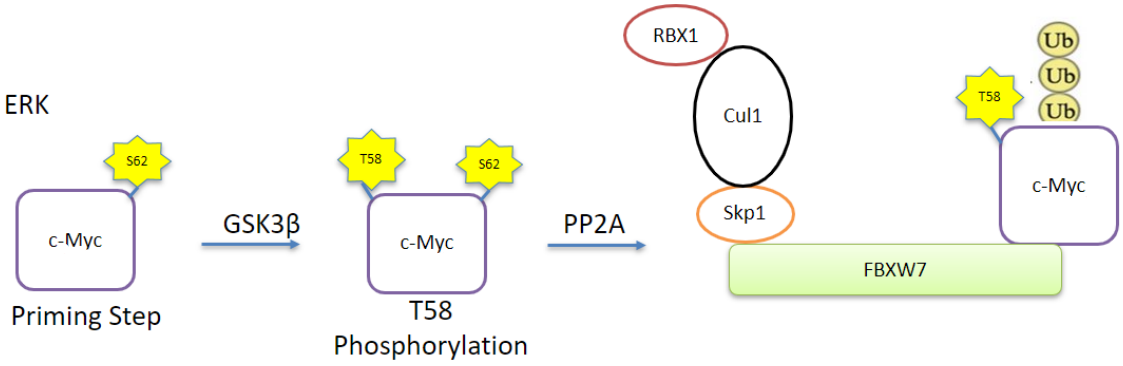

Figure 1.6 MYC Ubiquitylation by E3 Ubiquitin ligase SCF^{Fbxw7}

c-myc phosphorylation sequence needed for ubiquitylation activity by Fbxw7. The first step is S62 phosphorylation by ERK kinase followed by the T58 phosphorylation by GSK3β. Once PP2A dephosphorylates the S62 residue then and only then with Fbxw7 bind, ubiquitylate, and degrade c-myc.

Fbxw7 activity is primarily present in the G1 and early S phase of the cell. Mutations in Fbxw7 are seen in as many as 31 percent of human cancers and hence has been termed a *Bona fide tumor suppressor* [53].

Ubiquitylation of c-myc by Fbxw7 has primarily been characterized to be essential for controlling c-myc levels in the G1 and early S phase of cell cycle. However, in following phases of cell cycle progression c-myc ubiquitylation is attributed to another RING-FINGER E3 ligase known as $SCF^{\beta\text{-}TrCP}$. F-box protein β-TrCP, unlike Fbxw7, binds to the 278-283 amino acid residues and stabilizes c-myc in a ubiquitin mediated fashion [54]. The ubiquitin chains formed by β-TrCP are heterotypic linkages composed of both K48 and K63 linkages, whereas SCF^{Fbxw7} only forms K48 ubiquitin linkages. C-myc ubiquitylation by β-TrCP is essential for cell cycle re-entry after S-phase arrest thus mechanistically opposing the activity of Fbxw7 in a cell cycle specific context [54].

PIN1 (peptidyl-prolyl isomerase) is an enzyme that isomerizes a proline from a cis to trans to a cis confirmation or vice versa [55, 56]. These isomerization steps happen at two points in the c-myc phosphorylation process (Fig. 1.7). The trans to cis confirmation occurs after the S62 phosphorylation at the 63rd proline residue. This phosphorylation step increases overall c-myc protein stability, and the first isomerization enhances c-myc's DNA binding and facilitates transcriptional activity. This then catalyzes the cis to trans isomerization of proline 63 which allows for dephosphorylation of S62 by PP2A, thus allowing c-myc to be ubiquitylated and degraded by the Fbxw7 E3 ubiquitin ligase [57]. There is now accumulating evidence that Pin1 could be a therapeutic target for various cancers by inhibiting metastasis, proliferation, and maintenance of genomic stability [56].

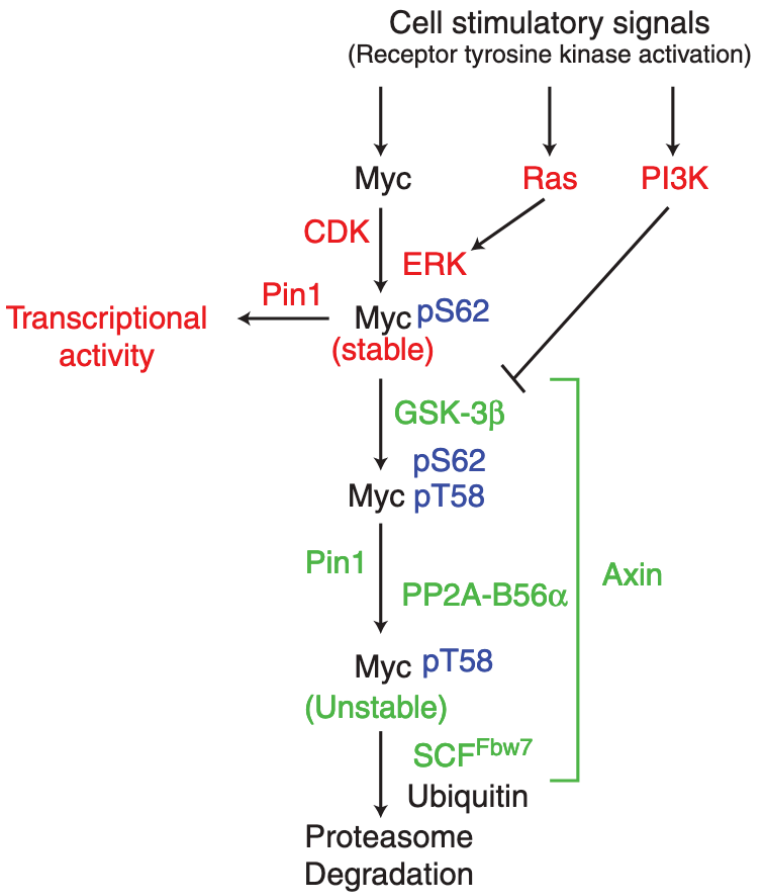

Figure 1.7 pS62 / pT58 MYC degradation pathway (Farrell & Sears et al, 2014)
Protein in red stabilize and / or activate c-myc. Proteins in green help facilitate degradation.

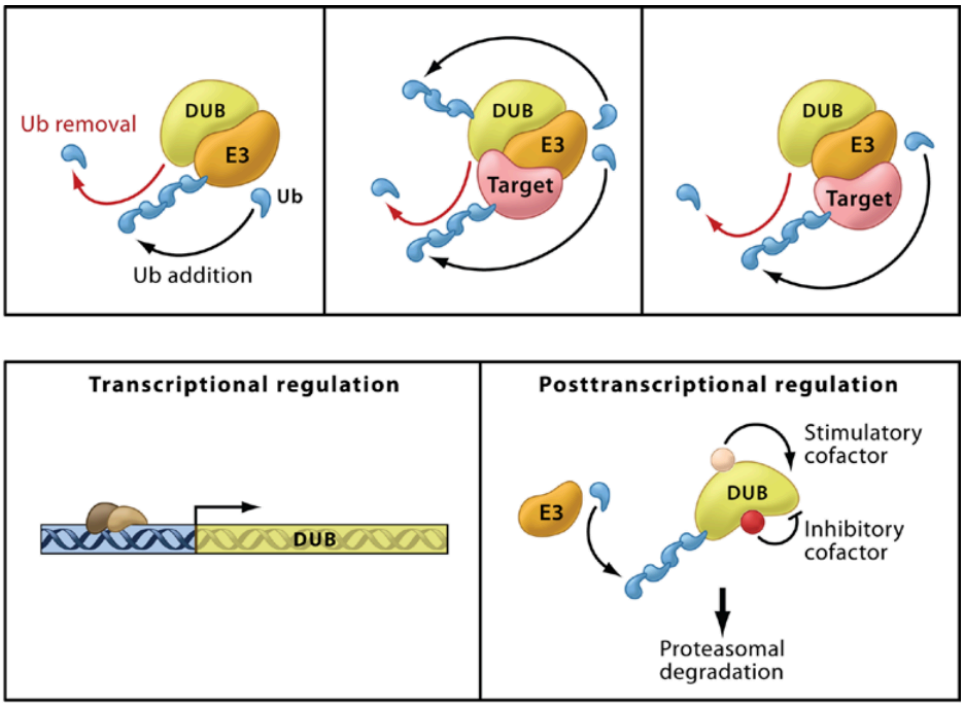

Figure 1.8 Deubiquitylation Model and regulation (Nijman S et al, 2005)
DUBs and E3s are often found in complex together. DUBs are regulated during transcription and post translationally through the actions of stimulatory and inhibitory cofactors that induce conformational changes to adject specificity.

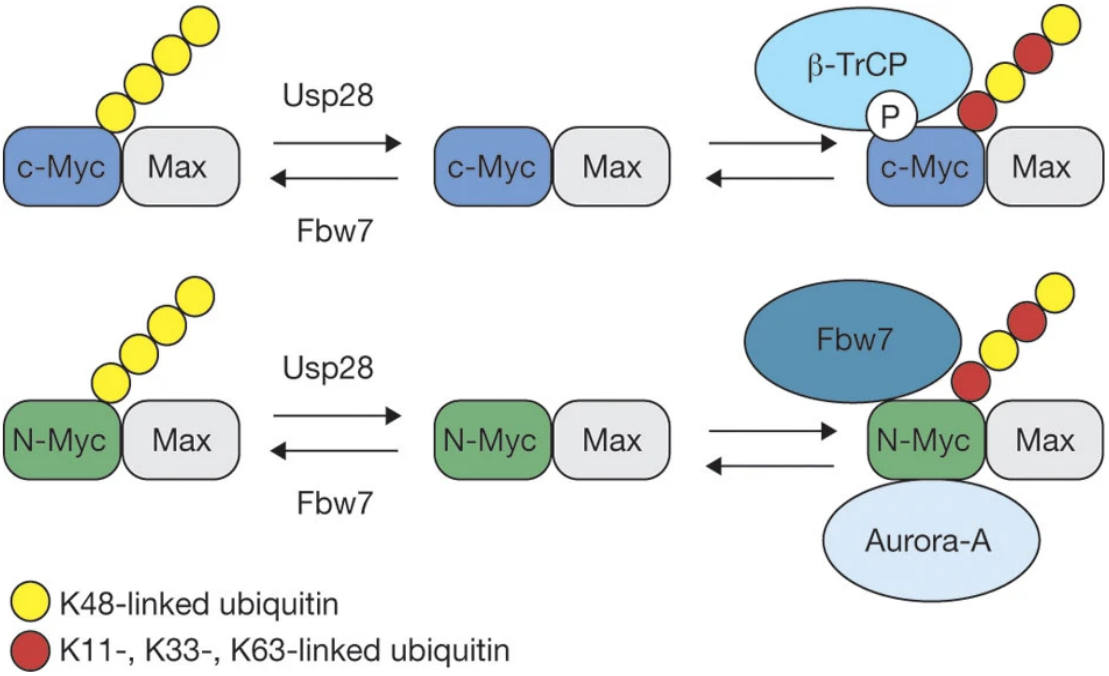

Figure 1.9 c-myc ubiquitylation interplay between Fbw7, Usp28 and β-TrCP (Popov N et al, 2010)
DUBs and E3s are often found in complex together. DUBs are regulated during transcription and post translationally through the actions of stimulatory and inhibitory cofactors.

Usp28 (ubiquitin specific protease 28) is a deubiquitylating enzyme that directly opposes Fbxw7α activity as discovered from an shRNA screen to identify genes responsible for c-myc function [58]. USP28 therefore antagonizes the polymerization of ubiquitin chains thereby opposing the E3 ligases that produce them. USP36 localized in the nucleolus, directly interacts with, and opposes Fbxw7γ [59]. Opposition to Fbxw7 by these USP's leads to overall stabilization of c-myc and is essential for tumor cell proliferation. USP28 is also being screened as a therapeutic target to modulate c-myc [60].

SKP2 is a known characterized oncogene and has been implicated in the protein degradation of many substrate targets [61]. Skp2 binds to c-myc through the MBII and HLH-LZ region and then catalyzes its polyubiquitylation and subsequent degradation [62]. A dominant ubiquitin linkage has not been associated with Skp2 ubiquitylation of c-myc but K48 is a likely candidate and other linkages may have ancillary roles. Other notable substrates include P27, Cyclin E and Cyclin A [63].

Interestingly, there is also evidence showing Skp2 expression stimulated c-myc induced cell cycle entry into S phase. In this context unlike Fbxw7, Skp2 promotes c-myc transcriptional activity while binding with the E3 ligase via the F-box domain.

Furthermore, Skp2 was found to associate with c-myc target gene promoters suggesting possible evidence of interplay between Skp2 ubiquitylation, c-myc transcriptional activation, and degradation. It is also noteworthy to mention that Skp2 itself is a c-myc target gene [64] meaning that c-myc itself can induce Skp2 expression adding another facet of control for c-myc protein levels.

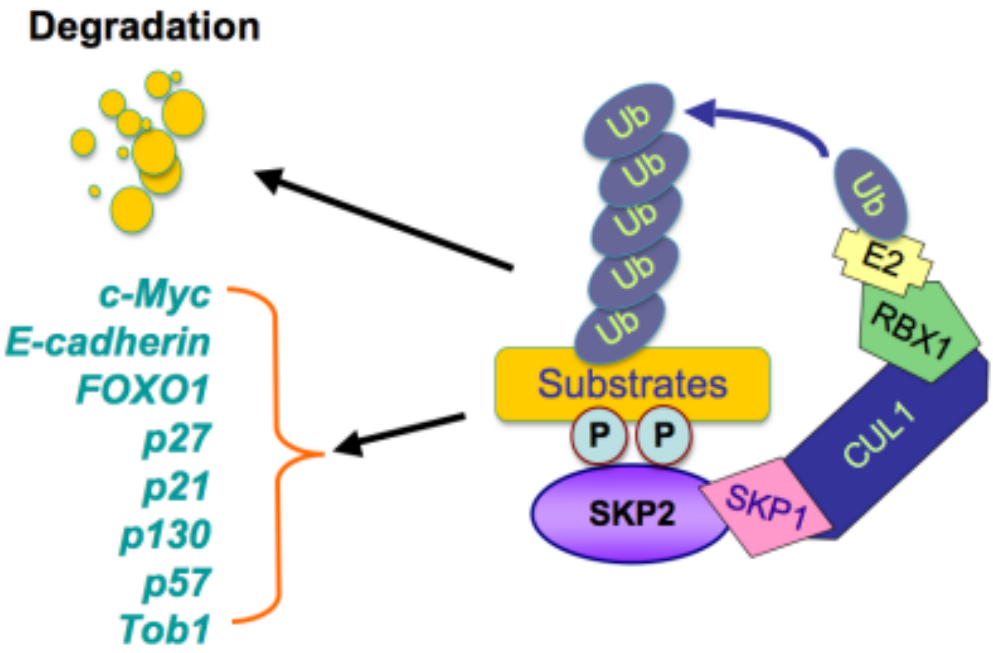

Figure 1.10 SCF^{Skp2} with target substrates (Wang Z et al, 2012)
Skp2 interfaces with Skp1, Rbx1, and Cul1 E3 ligase machinery to ubiquitylate and degrade c-myc along with other target substrates.

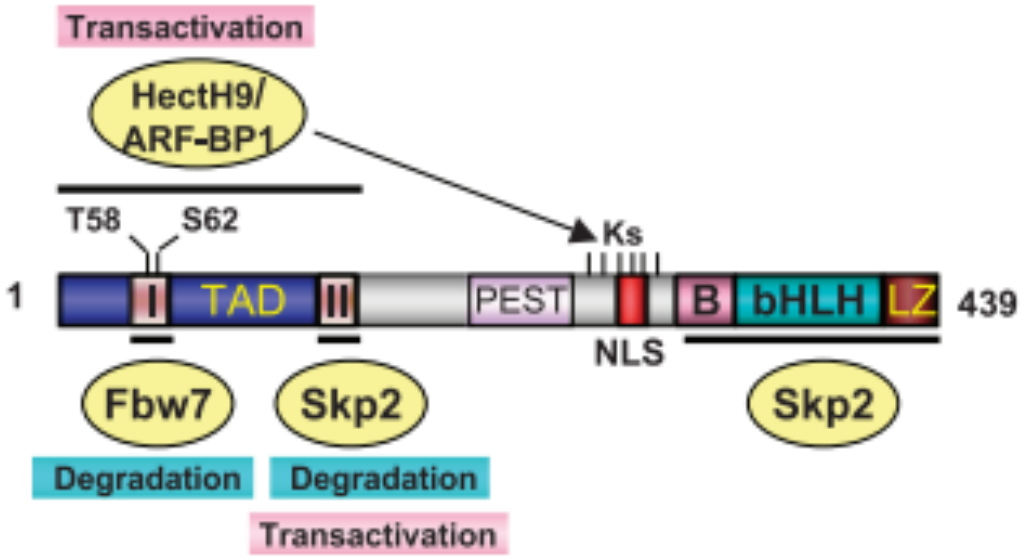

Figure 1.11 HECTH9 Regulation of c-myc (Dai M et al, 2006)
HECTH9 along with other mention E3 ligases regulate c-myc. HECTH9 ubiquitylates one or more of six lysines residues around the NLS nuclear localization signal by binding to the TAD (transactivation domain). This ubiquitylation leads to c-myc activation.

HECTH9 belongs to the HECT domain family of E3 ubiquitin ligases. This E3 ligase interacts with the TAD domain of c-myc and catalyzes K63 ubiquitin linkages of lysine residues in proximity to the nuclear localization signal (Fig. 1.11). This ubiquitylation does not trigger degradation of c-myc but rather increases c-myc transcriptional activity through recruitment of p300, activation of c-myc target genes, and induction of cell proliferation by c-myc [65]. It does however associate with MIZ1 and repression HECTH9 will stabilizes MIZ1 which results in repression of c-myc activated target genes [66].

TRUSS (tumor necrosis factor receptor-as-associated ubiquitous scaffolding and signaling protein) is responsible for degradation of both c-myc and N-myc [67]. This interaction takes place between c-myc and the DDB-CUL4 E3 ubiquitin ligase complex [68]. TRUSS interacts with the carboxy terminus of c-myc that contains the HLH-LZ motif along with additional elements located at the N-terminus. However TRUSS' activity is cell cycle specific (Fig. 1.12) The ubiquitylation of c-myc by TRUSS results in degradation and reduced transactivation of c-myc target genes [68]. Thus, Truss regulated c-myc function is controlled by reduction in protein levels in a similar manner by which Fbxw7 regulates c-myc function [69].

TRIM32 is vastly less characterized relative to other E3 ligases. It is a part of the RING-FINGER family of E3 ubiquitin ligase and has been documented to regulate stability of a smattering of protein and microRNAs, particularly Let-7a in the context of balancing differentiation and progenitor daughter cell types produced in the murine neocortex (Fig. 1.13). Recent data suggests that Trim32 does in fact ubiquitinate N-myc in human neuro blastoma cells at the spindle pole [70]. There is also new evidence showing how Trim32

expression overlaps with expression of USP7, a deubiquitylation enzyme, during neuronal differentiation in vitro and in vivo experimental conditions [71].

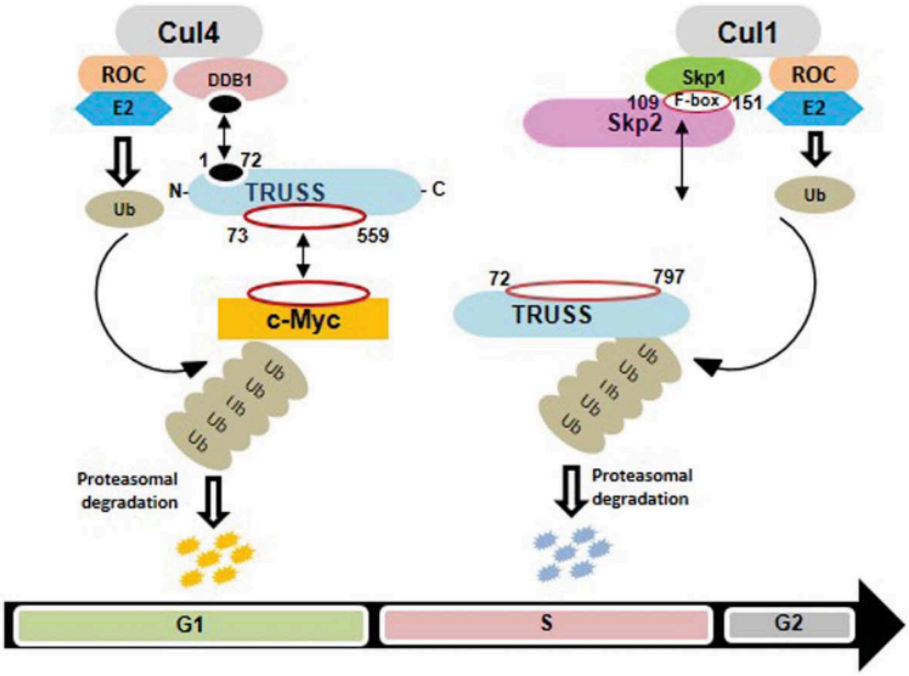

Figure 1.12 TRUSS regulation of c-myc (Jamal A et al, 2015)
TRUSS oscillates it association with Cul1 and Cul4 scaffolds to regulate c-Myc in a cell cycle specific manner. During G1 phase TRUSS Associates with the DDB-Cul4 E3 ligase complex to ubiquitylate and degrade Myc. Then when the cell proceeds to S-phase TRUSS itself become ubiquitylated and degraded.

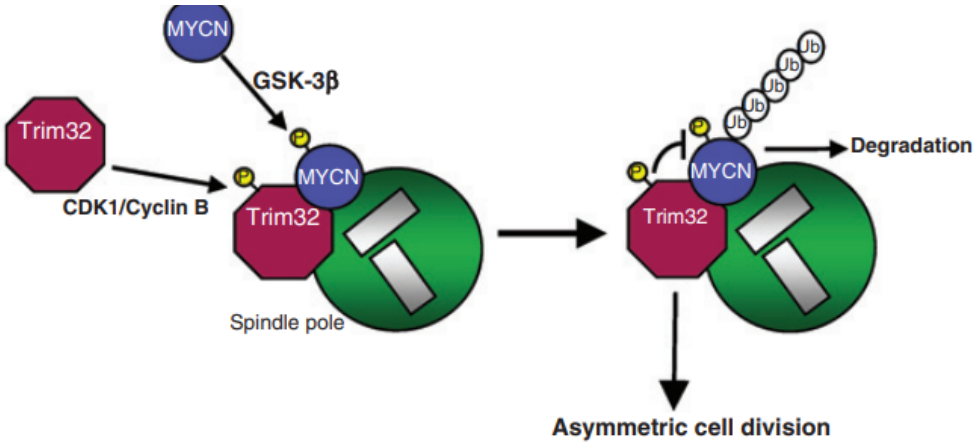

Figure 1.13 TRIM32 regulation of c-myc (Izumi H et al, 2014)
Schematic model of Fbx29 (Fbxw8) associating with the Skp1 Cul7 E3 ligase complex machinery to ubiquitylate and degrade MYCN

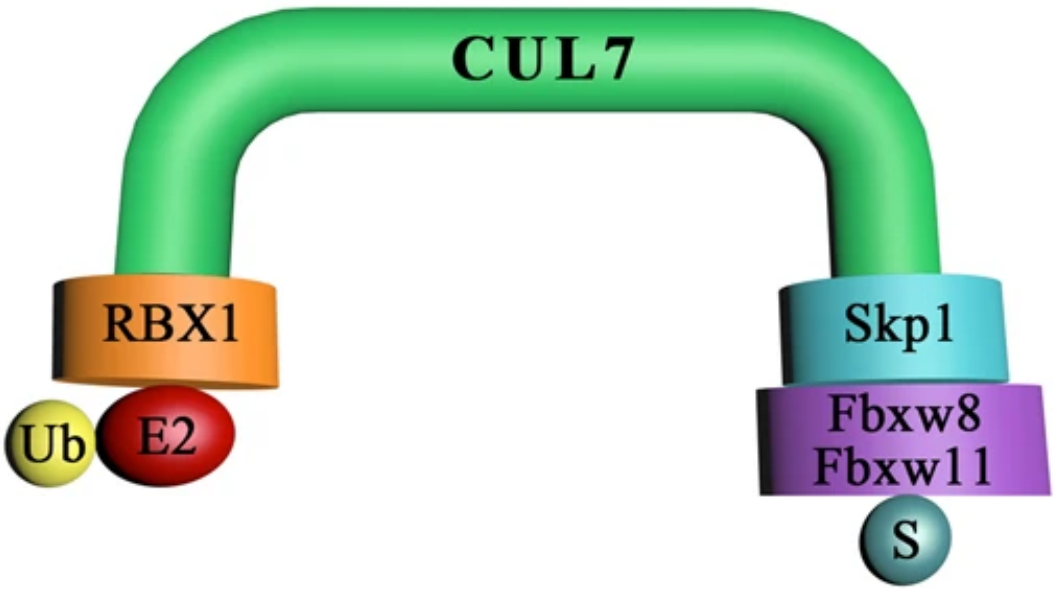

Figure 1.14 Fbx29 (Fbxw8) regulation of c-myc (Shi L et al, 2020)
Schematic model of Fbx29 (Fbxw8) associating with the Skp1 Cul7 E3 ligase complex machinery.

Fbx29, also known as Fbxw8, is the F-box adapter component of the Skp1-Cul7 ROC1 E3 (Figure 1.14) ubiquitin complex [72]. Fbx29 interacts with c-myc at the MBII and the HLH-LZ domain at the carboxy terminus. Overexpression of Fbx29 decreases protein levels and transactivation however studies did not directly measure overall c-myc ubiquitylation [73]. Thus, it is still unclear if c-myc is a direct substrate of Fbx29 or not. It may also be possible that Fbx29 competes with Skp2 for c-myc binding since they bind to the same regions.

CHIP (carboxyl terminus of Hsc50-interacting protein) is a more recently characterized U-box E3 ligase linked to the 26s proteasome via chaperone association [74]. The chaperone in this case is Hsp70 and to a lesser extent Hsp90 (Fig. 1.15). CHIP associates with and ubiquitylates c-myc along with decreasing its transcriptional activity and reducing expression of c-myc target genes [75].

SIRT2 and NEDD4

SIRT2 a class histone deacetylase (HDAC) has also been documented to indirectly stabilize c-myc. It shows a strong preference for H4K16 [76] an acetylation mark commonly lost in cancer cells [77]. This mechanism works by SIRT2 repressing transcription of NEDD4, an E3 ubiquitin ligase that has been characterized to ubiquitylate and degrade c-myc [78].

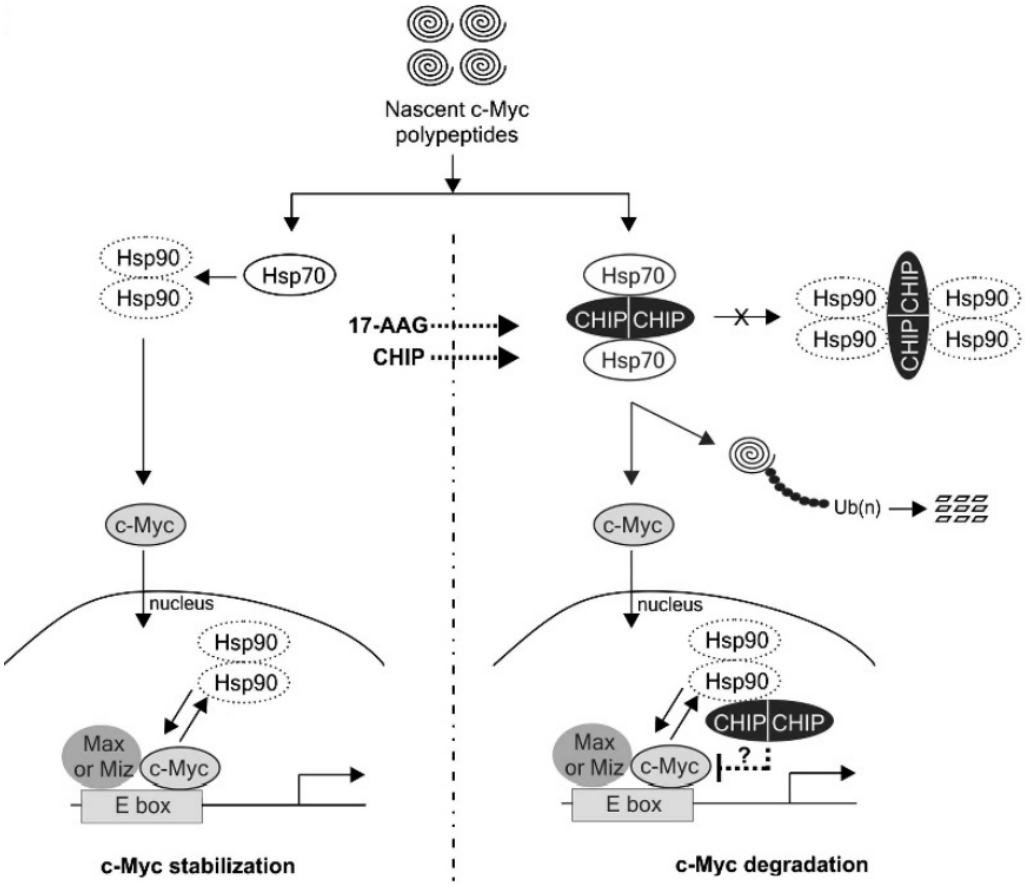

Figure 1.15 CHIP regulation of c-myc (Paul I et al, 2013)
Schematic model of CHIP associating with Hsp90 and Hsp70 proteins to differentially regulate c-myc.

NEMO (NF-kB essential modulator) is also an indirect c-myc stabilizer. NEMO is a scaffold in the IKK complex, a necessary factor for activation of the NF-kB pathway [79]. NEMO stabilizes c-Myc in two ways. First it directly interacts with c-myc in the nucleus. Second, NEMO also reduces overall ubiquitylation of c-myc by inhibiting Fbxw7 ubiquitylation activity. It is also documented that this c-myc stabilization upregulated expression of GCS (glutamyl-cysteine synthetase), a downstream target of c-myc [80]. GCS expression increases intracellular levels of glutathione which allows cells to become more resistant to ionizing radiation. Thus, addressing a NEMO / c-myc interaction based therapeutic strategy for combating radiotherapy resistance.

Link Between c-myc Ubiquitination and Acetylation

Interaction between c-myc and cofactors that have histone acetyltransferase (HAT) activity. Examples of these HAT cofactors include P300, TIP60, and GCN5 [81]. C-myc itself is an acetylation target, being that acetylation and ubiquitylation both occur on lysine residues. This allows not only for dual interplay between these processes but also competition. P53, Runx3, ReLA and SMAD 7 are documented substrates which ubiquitylation and acetylation compete for. P300 acetylates c-myc with no effect on DNA binding but ubiquitylation is reduced and c-myc is stabilized [81]. Similar findings are shown with GCN5 mediated acetylation where nuclear localization is not affected, and Max dimerization is also not affected [82]. C-myc can also be a target for deacetylation as documented specifically by Sirt1 [83]. Not only does SIRT1 deacetylate c-myc but it is also a c-myc gene target; thus it was proposed that this relationship is in actuality a negative feedback loop where SIRT1 acts as a tumor suppressor [83].

Protein	Effect on MYC stability	Effect on MYC activity	Phase of cell cycle
Fbw7	Decrease	Decrease	G_1–S
Pinl	Decrease	Increase	—
Usp28	Increase	Increase	G_1–S
β-TrCP	Increase	Increase	S–G_2
Skp2	Decrease	Increase	G_1–S
HectH9	—	Increase	G_1–S
Truss	Decrease	Decrease	—
Trim32	Decrease	—	—
Fbx29	Decrease	Decrease	—
CHIP	Decrease	Decrease	—
SIRT2	Increase	—	—
NEDD4	Decrease	—	—
NEMO	Increase	Increase	—

Table 1.2 Table summary of regulation of c-myc by various F-box's (Farrell & Sears et al, 2014)

Link Between c-myc Ubiquitylation and Transcriptional Activation

Based on the work done on various E3 ligases, specifically Skp2, HectH9, and Pin1/Fbxw7, came the idea of "transcription factor licensing". The underpinning assumption in the model implies that the activation of some transcription factors is coupled to their own ubiquitylation and degradation [84]. Lysine residues on murine c-myc have been identified in the TAD domain for the induction of c-myc targets gene important for cellular transformation [85]. Loss of this TAD ubiquitylation induces Egr1, a non-canonical c-myc target, resulting in apoptosis. This apoptotic event, mediated by ARF, disrupts the interaction between c-myc and Skp2, resulting in reduced ubiquitylation and increased c-myc protein stability. When Skp2 is overexpressed ARF recruitment and ARF induced apoptosis is reduced. This points to the phenomena that c-myc ubiquitylation not only controls protein levels but also biological activity that may involve competition between sites that are prone to ubiquitylation as well as acetylation [85].

Negative feedback loop is another context to look at myc activity. Where c-myc expression / activation is linked or could to its own downregulation and degradation. Proteasomal subunits have been detected at c-myc target gene promoters [57]. Linking transcriptional activity to degradation adds another layer of tuning to c-myc related cell fate determinations.

The other facet that contributes to optimal c-myc transcriptional activity is its dynamic nature of binding to DNA. In normal cells, Pin 1 regulates c-myc's binding to target gene promoters, recruiting cofactors, leading to transcriptional activation, and release from the promoters associated with degradation via Fbxw7 [57].

However, in cancer when c-myc is stabilized via pT58 or pS62 defect, Pin 1 no longer facilitate Fbxw7 mediated degradation but still modulates transcriptional activation. Cancers cells with more stable c-myc have rapid c-myc dissociation from its target gene promoters which was partially restored upon inhibition of protein synthesis in a Pin 1 dependent manner because remaining pS62-myc present in cancer cells.

C-myc Stability and Cancer

Dysregulated c-myc expression plays a large role in tumorigenesis. Majority of cancers have myc overexpression but only a minority of these cancers have a gene amplification and / or translocation to justify this increase in overall c-myc levels [86]. This suggests that c-myc stability is the larger player in the context of cancer and E3 ligases themselves contribute to overall c-myc levels and stability. Various E3 ligases, particularly Fbxw7, a known tumor suppressor [87], have been documented to be inactivated by point mutations or even lost in various human cancers. Roughly 30 percent of cancers have mutated Fbxw7 [88] and primary human tumors themselves show Fbxw7 to have an overall 6 percent mutation rate [89]. Thus c-myc's stability determined by the ubiquitin proteasome system needs thorough characterization. Tumorigenic phenotypes of different tumors with deregulated c-myc types can vary widely as c-myc mediates transcription of 15% of all the genome's promotors with a large rolodex of transcriptional programs.

TRUSS another E3 ligase that negatively regulates c-myc has also been shown to be expressed at lower levels in many human cancer cell lines [67]. A similar trend has been observed with CHIP in the context of breast cancer [90]

Skp2 and HectH9 however seem to have a relationship contrasting with the E3 ligases mentioned previously being that they enhance c-myc transcriptional activity. Skp2

is widely accepted as an oncogene and is overexpressed in human cancer. HectH9 is also upregulated in 43% of breast cancers, 46% of lung tumors, 52% of colon tumors, 18% of liver tumors, 20% of pancreatic carcinomas and 9% of thyroid tumors from tissue microarrays [65].

Altered Cell Signaling Pathways That Impact c-myc Stability In Cancer

Elements of the pT58 and pS62 degradation pathway involved with Fbxw7 dependent degradation of c-myc turnover are commonly deregulated in cancer (Fig. 8). Therefore c-myc T58 and S62 phosphorylation status along with c-myc stability should explain c-myc common overexpression profile in cancer without the presence of gene amplification.

Normal phosphorylation of c-myc occurs in a sequential manner involving the first phosphorylation step of the pS62 residue by ERK kinase followed by a second phosphorylation step by GSK3b kinase. After this step PP2A phosphatase acts on the S62 residue, and only after this occurs does Fbxw7 mediated ubiquitylation and degradation take place (Figure 7). Subsets of Burkitt's lymphoma contain c-myc mutations at or around the T58 residue that impair phosphorylation and increase S62 phosphorylation and inhibit binding, ubiquitylation, and degradation by Fbxw7.

Hematopoietic stem cells transduced with T58A c-myc mutant constructs or S62A knock-in mice conditionally expressed in the mammary glands showed increased tumorigenic potential [91]. When the T58 mutant is knocked into the c-myc locus, hematopoietic progenitors exhibit self-renewal late appearing myeloid and lymphoid neoplasia. Despite these phospho mutations being present in certain subsets of Burkitt’s lymphoma, human leukemia, and breast cancer cell lines along with primary human tumors

show a low T58/S62 phosphorylation ratio relative to their normal controls. Meaning higher levels of S62 phosphorylation is detected relative to controls and c-myc was also aberrantly more stable as well [92, 93]. Such was also exhibited in pancreatic samples with regards to phosphorylation and stability [94].

This pS62 c-myc in conjunction with Pin 1 is very transcriptionally active [57]. Activation of MEK/ERK signaling along with decreased expression of PP2A-B-56a and altered splicing of Axin 1 in cancer cell lines that express stabilized S62 phosphorylated c-myc [95]. This information taken in overall presents an avenue for therapeutic targeting within the T58/S62 phosphorylation and Fbxw7 mediated degradation pathway.

Targeting c-myc with PP2A inhibitor, BRD4, CIP2A, and SET

PP2A is the predominant serine/threonine phosphatase in mammals. It is a part of a family of heterotrimeric proteins phosphatases consisting of a conserved catalytic C unit and a variable array of regulatory B subunits [96]. It is also a well characterized tumor suppressor that negatively regulates a host of signal transduction pathways aside from c-myc [97]. In the context of c-myc, PP2A dephosphorylates the S62 residue and destabilizes c-myc. Inhibiting PP2Ais essential for cell transformation and this inactivation can occur by oncogenic viruses, subunit mutations, or by overexpression of endogenous inhibitors [96]. Examples of these naturally expressed inhibitors include SET (I2PP2A) and Cell Inhibitor of PP2A (CIP2A).

CIP2A is quite notable as a PP2A inhibitor. Overexpression cooperates with Ras and c-myc to transform murine embryonic fibroblasts and its suppression conversely prevents tumor growth [96]. CIP2A not only interacts with PP2A and c-myc but it also

disrupts dephosphorylation of c-myc at the S62 residue, increasing overall c-myc stability. CIP2A levels are above normal in head and neck squamous carcinoma, GI cancers, and colon cancer and has been correlated with reduced survival [98]. One third of breast cancers overexpress CIP2A [99] and CIP2A overexpression in human pancreatic malignancies is also frequent.

SET is upregulated in CML, Wilm's tumors, Brain malignancies, headband neck tumors, and testicular cancers [100]. Correlation of disease aggressiveness has been documented in ovarian cancer (Ouellet et al. 2006), AML, [101], and CLL [102]. Frequent overexpression is also seen in breast and pancreatic cancer types [94, 103].

Targeting these naturally occurring PP2A inhibitors presents a mechanistic approach to inhibiting post translational activation of c-myc in human cancers. What has been documented suggests that knocking down SET or CIP2A increases PP2A activity subsequent c-myc degradation leading to reduced tumorigenic potential in breast and pancreatic cell lines in vitro and in vivo conditions [94, 103]. Although no CIP2A pharmacological antagonists have been developed, SET inhibitor OP449 [102] has shown success in breast and pancreatic cancer cell lines. Particularly with the activation of PP2A, increased c-myc degradation, reduced proliferation, reduced proliferative, and survival signaling [94, 103].

Targeting c-myc In Cancer

Aside from exploiting natural inhibitors of c-myc there have also been ongoing research endeavors to characterize c-myc as a direct cancer target. Since c-myc is often dysregulated in cancer it's an attractive target in a wide range of malignancies. Lipid nanoparticles were synthesized to deliver siRNA particles to tumor cells leading to reduced

c-myc protein expression however therapeutic results were not as robust as expected (Tolcher A et al. 2015). In more recent studies, the inhibitor, Omomyc, a dominant negative c-myc analogue, has been shown to reduce tumor progression [104] in various cancer types even in tumor where c-myc was not the driving oncogene, further qualifying c-myc as a potential therapeutic target.

Considerations and Challenges in Targeting c-myc

c-myc has been well characterized as a maser and integral regulator of normal cell survival and proliferation making it a potentially risky therapeutic target. Germline knock out mice substantiated this claim when homozygous ablation of c-myc alleles proves to be embryonically lethal [105]. However, mouse studies with animals expressing Omomyc, had almost no side effects in normal tissue [104]. Major side effects were noted in high turnover tissues such as the skin but were reversed after cessation of Omomyc expression.

Homing in on c-myc specificity is another challenge with drug targeting. C-myc is an intrinsically disordered protein and lacks a lot of “hot spots” and hydrophobic pockets that are paramount for efficient drug targeting approaches. IDPs have been shown to form liquid droplets inside the cell and are often referred to as “membrane-less organelles”. This phase transition may limit inhibitor efficiency and accessibility within the target protein. On top of that the location of c-myc in the nucleus adds to the therapeutic limitation. However, despite these difficulties inhibiting c-myc interactions with Max and Miz1 has shown some promise [106] and has garnered significant interest from pharmaceuticals .

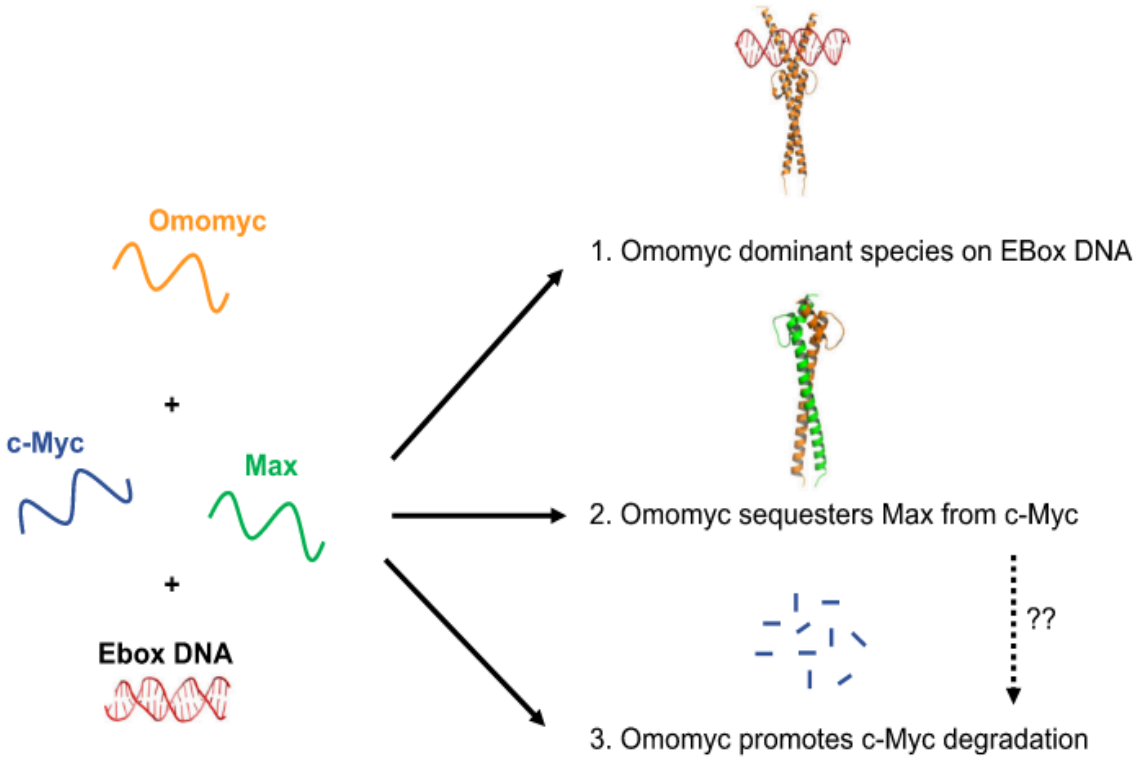

Figure 1.16 Proposed Mechanisms of action for Omomyc (Madden S, 2021)
First, Omomyc (Orange) homodimer blocks c-myc/Max dimer from binding to E-box DNA (Red). Second, Omomyc binds to Max therefore sequestering it from c-Myc binding. Lastly the presence of Omomyc, c-myc levels are reduced due to compensatory proteasomal degradation.

Properties of small molecules, peptides, and protein that inhibit c-myc activity

Inhibitor type	Inhibitor	Mechanism of action (A, B or C)[a]	Inhibitor of Myc/ Max binding to DNA in vitro	Activity in vitro	Reduction of cancer cell growth/ proliferation	Tumor reduction in animal models
Small Molecules	IIA6B17	B	Yes	IC_{50} = 50 ± 25 μM (EMSA, inhibition of E-box binding)	Yes	–
	NY2267	B	Yes	IC_{50} = 36.5 μM (EMSA, inhibition of E-box binding)	–	–
	10,058-F4	B	Yes	K_D = 42 μM (Binding to c-Myc) 15 μM (SPR)	Yes	No
	10,074-G5	B	Yes	IC_{50} = 146.8 μM (EMSA, inhibition of E-box binding) K_D = 20 μM (Binding to c-Myc) 18 μM (SPR)	Yes	No
	JY-3-094	B	Yes	IC_{50} = 33 μM (EMSA, inhibition of E-box binding)	Yes	–
	3jc48–3	B	Yes	IC_{50} = 34.8 μM (EMSA, inhibition of E-box binding)	Yes	–
	Mycro1, Mycro2	B	Yes	IC_{50} = 30 ± 5 μM (Mycro1) and 23 ± 4 μM (EMSA, inhibition of dimerization and E-box binding)	Yes	–
	Mycro3	B	Yes	IC_{50} = 40 ± 13 μM (FP competition assay, inhibition of E-box binding and dimerization)	–	Yes
	MYCMI-6	B	–	K_D = 1.6 ± 0.5 μM (SPR, binding to c-Myc)	Yes	Yes
	KJ-Pyr-9	B	Yes	K_D = 6.5 ± 1.0 nM (Backscattering Interferometry, binding to c-Myc)	Yes	–
	MYCi361	B, C	Yes	K_D = 3.2 μM (FP competition assay, binding to c-Myc)	Yes	Yes
	MYCi975	B, C	–	K_D = 2.5 μM (FP competition assay, binding to c-Myc)	Yes	Yes
	Celastrol and analogues	A,C	Yes	IC_{50} = 67 ± 2 μM (Celastrol) (EMSA, inhibition of E-box binding)	Yes	Yes [b]
	JKY-2-169	A	Yes	IC_{50} = 11.6 ± 2.3 μM (EMSA, inhibition of E-box binding)	–	–
	EN4	B	Yes	IC_{50} = 6.7 ± 2.3 μM (inhibition of E-box binding)	Yes	Yes
(Poly)peptide/ mini-protein	Omomyc	A, B, C	Yes	K_D of Omomyc homodimer = nM range (Circular Dichroism spectroscopy, binding to E-box)	Yes	Yes
	Max bHLHZ	A, B	–	–	Yes	–
	Mad1	A, B	Yes	–	Yes	–
	ME47	A	Yes	K_D = 15.3 ± 1.6 nM (EMSA, binding to E-box)	Yes [c]	Yes [c]
	Monoclonal antibody	B	Yes	–	–	–
	H1 peptide	B	Yes	–	Yes	Yes
	aMax/aMip	B	Yes	K_D = 460 μM (aMax), 250 μM (aMip) (Thermal denaturation monitored by CD, binding c-Myc in absence of DNA)	–	–
	Linked basic regions	A	–	–	–	–

Table 1.3 Table of small molecules that inhibit c-myc activity (Madden S et al, 2021)

A = E-box inhibitor

B = Inhibitor of c-myc / Max binding

C = c-myc degradation Promotor

[b] shown to inhibit tumor growth but likely due to another mechanism

[c] Transgene, not as a peptide alone

*Indicates that this is currently unknown

Many cellular controls operate on c-myc vast array of functions in both cell growth and metabolism. A key control mechanism is the modulation of c-myc levels via ubiquitin mediated proteasomal degradation. Several E3 ubiquitin ligases have been characterized to act on c-myc but they do not act in equivalent activity or magnitude. These E3 ligases can either stimulate c-myc protein degradation or increase c-myc protein stability. These destabilizing E3 ligases themselves can either inhibit c-myc activity or increase c-myc activity suggesting a link between c-myc ubiquitylation and transcriptional activity. There is also interplay between c-myc ubiquitylation and acetylation. All these relationships are needed to understand regulation of c-myc in normal cells and how deregulation occurs in the context of cancer. More needs to be uncovered regarding c-myc's post translational dependent regulation of its own stability and turn over.

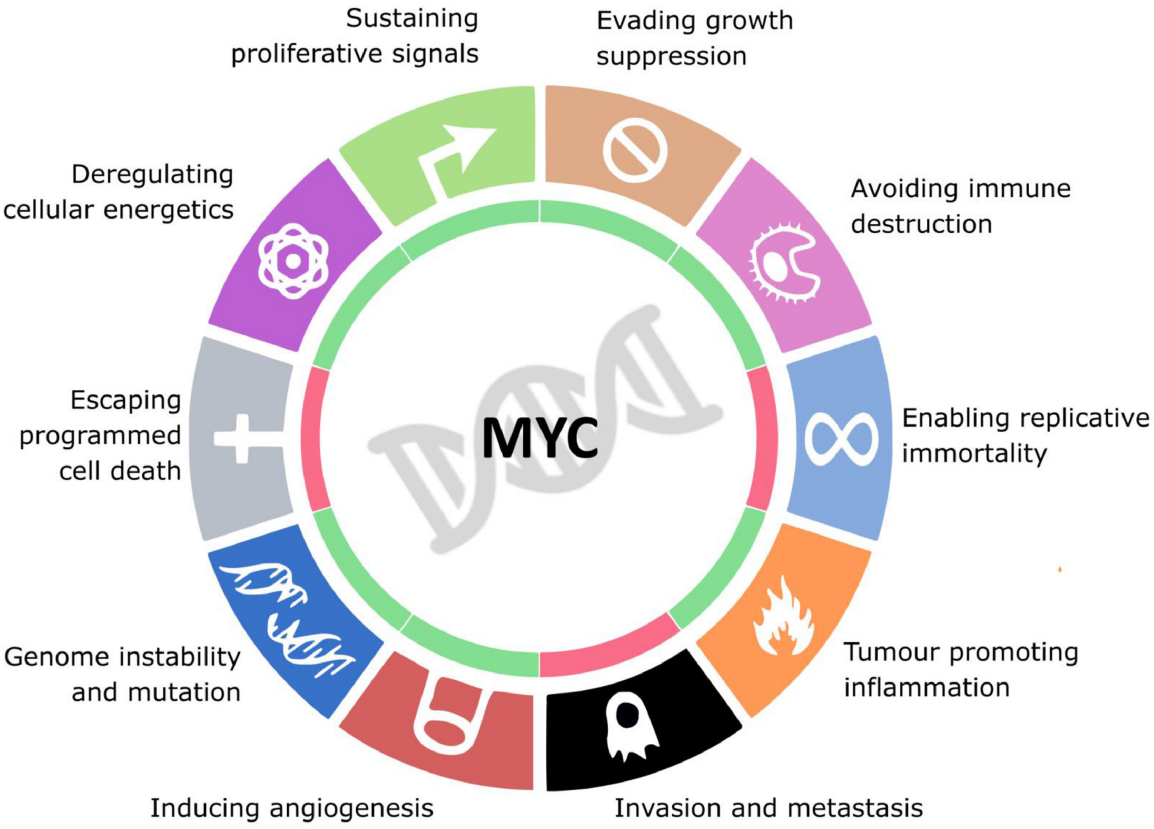

Figure 1.17 Myc Regulates all Hallmarks of Cancer (Lombart and Mansour, 2022)

Fbxl8 Background

For much of this chapter, we have covered c-myc and its importance and relevance to protein degradation and ubiquitylation. In this investigation c-myc is investigated in the context of Fbxl8 activity therefore it important that we understand the current knowledge available regarding Fbxl8 (F-box and Leucine Rich Repeat Protein 8). Up until recently Fbxl8 was what was known as an orphan F-box protein; an F-box adaptor with no confirmed or characterized substrates. The first publication mentioning Fbxl8 was published in 2005 in an expression analysis screen for tumor suppressor genes [107]. In this study chromosome 16q was being screened for tumor suppressors specifically for breast cancer. Fbxl8 was a candidate for this study however it did not show any expression differences or mutations in breast cancer cells lines with loss of chromosome 16q22 heterozygosity. Only in year 2020 did another publication regarding Fbxl8 surface once more [108]. Here Fbxl8 was identified as a novel E3 ligase that promotes BRCA metastasis by stimulating tumor cytokines and inhibition of cyclin D2 and IRF5. Although cell culture experiments supported this hypothesis there was no mechanistic evidence citing the downregulation of these substrates was mediated by ubiquitin mediated degradation.

This same lab group followed up this publication with another one indicating Fbxl8 collaborates and counters other E3 ligases associated with cyclin F modulation in the context of BRCA [109]. Once again cell culture experiments supported this hypothesis but little to no mechanistic data verifying the F-box substrates as direct ubiquitylated targets was presented.

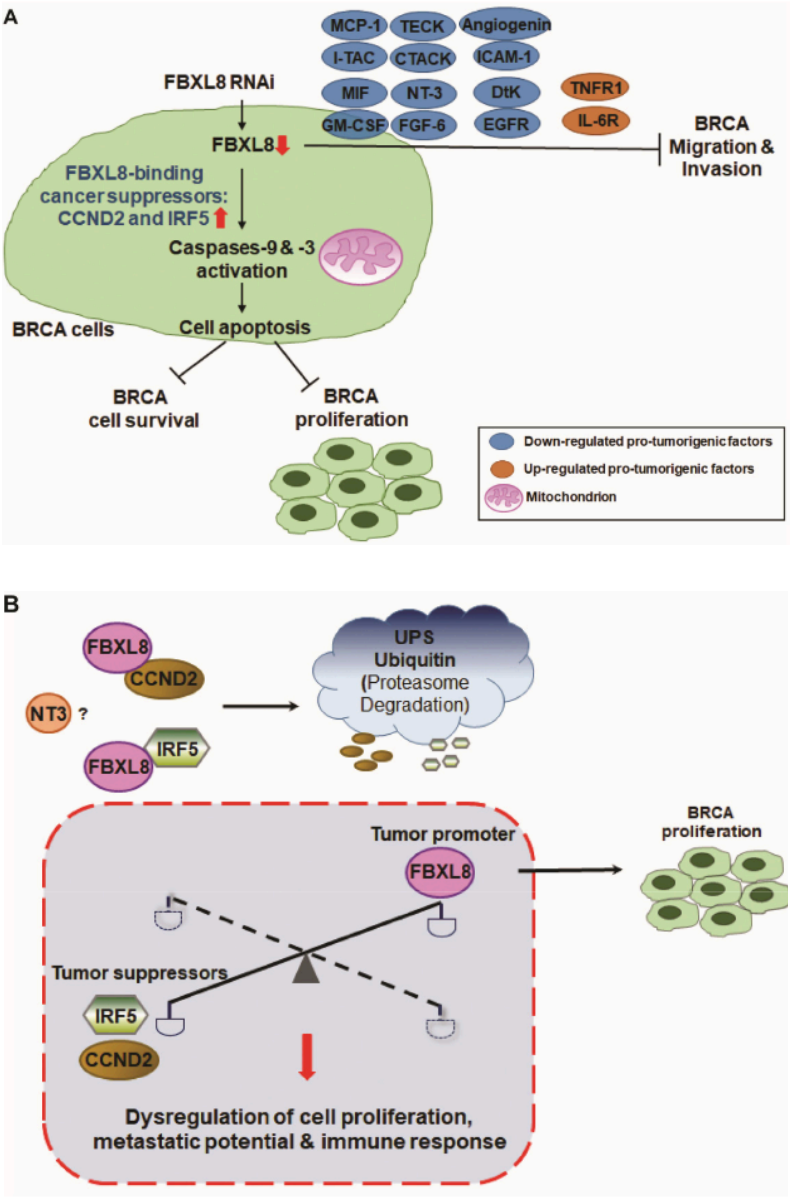

Figure 1.18 A model from illustrating how Fbxl8 attenuates CCND2 and IRF5 factors while upregulating pro-tumorigenic cytokines and suppressing apoptosis and promoting metastasis potential in BRCA. Fbxl8 plays a key role in anti-apoptosis in BRCA. (Chang et al 2020)

a. Knockdown of FBXL8 increased expression of cancer suppressors CCND2 and IRF5, thus inhibiting cell growth and proliferation in BRCA, driven by: (i) increase in early apoptosis, (ii) activation of Caspase-9 and -3, and (iii) inhibition of the production of cancer-promoting cytokines, including MCP-1, I-TAC, TECK, CTACK, MIF, GM-CSF, NT-3, FGF-6, Angiogenin, ICAM-1, DtK and EGFR. Therefore, FBXL8 promotes pro-tumorigenic microenvironment, contributing to BRCA metastasis and progression.

b. FBXL8 interacts and downregulates cancer suppressors CCND2 and IRF5 via protein degradation system. Hence, upregulated FBXL8 in BRCA causes the reduction of CCND2 and IRF5 proteins, and leads to dysregulated cell proliferation, immune response, and metastatic potential of BRCA cells.

The most robust data regarding Fbxl8 was recently published from the Alan Diehl Laboratory. In this work cyclin D3 was observed to be a direct target of Fbxl8 mediated ubiquitylation and degradation [110]. Cyclin D3 is overexpressed in ~50% of Burkitt's lymphoma correlating with a mutation of Thr-283. However, the E3 ligase that regulates phosphorylated cyclin D3 and whether a stabilized, phosphorylation deficient mutant of cyclin D3, has oncogenic activity was previously undefined. This lab group found that SCF^{Fbxl8} was identified as the E3 ubiquitin ligase for the Thr-283 phosphorylated cyclin D3 and that SCF^{Fbxl8} poly-ubiquitylates p-Thr-283 cyclin D3 targeting it to the proteasome. Functional investigation clearly demonstrated that Fbxl8 antagonizes cell cycle progression, hematopoietic cell proliferation, and oncogene-induced transformation through degradation of cyclin D3, which is abolished by expression of cyclin D3T283A, a non-phosphorylatable mutant. Clinically, the expression of cyclin D3 is inversely correlated with the expression of Fbxl8 in lymphomas from human patients implicating Fbxl8 functions as a tumor suppressor [110]. This the first seminal work that demonstrates direct ubiquitin mediated degradation by this E3 ligase that was substantiated by clinical relevance.

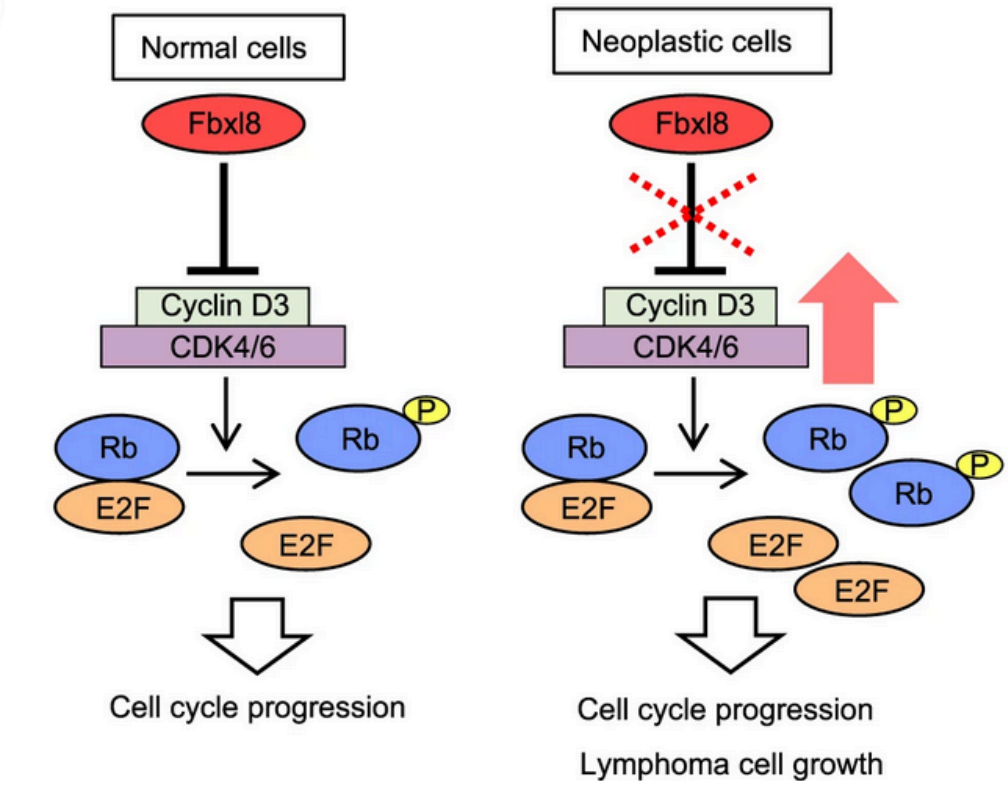

Figure 1.19 Model of Lymphoma Cell Growth by Fbxl8-Cyclin D3 Axis (Yoshida et al, 2020)
Fbxl8 control levels of cyclin D3 in a proteasome mediated fashion thus modulating cell cycle progression. Inhibiting Fbxl8 mediated degradation will stabilize Cyclin D3 and induce cell cycle progression and malignant transformation.

Chapter 2

Fbxl8 suppresses lymphoma growth and hematopoietic transformation through degradation of cyclin D3

The following work was produced largely by Akihiro Yoshida and Jaewoo Choi. I contributed supplementary but essential data for this investigation as I was also working to uncover other biochemical roles of Fbxl8.

Results

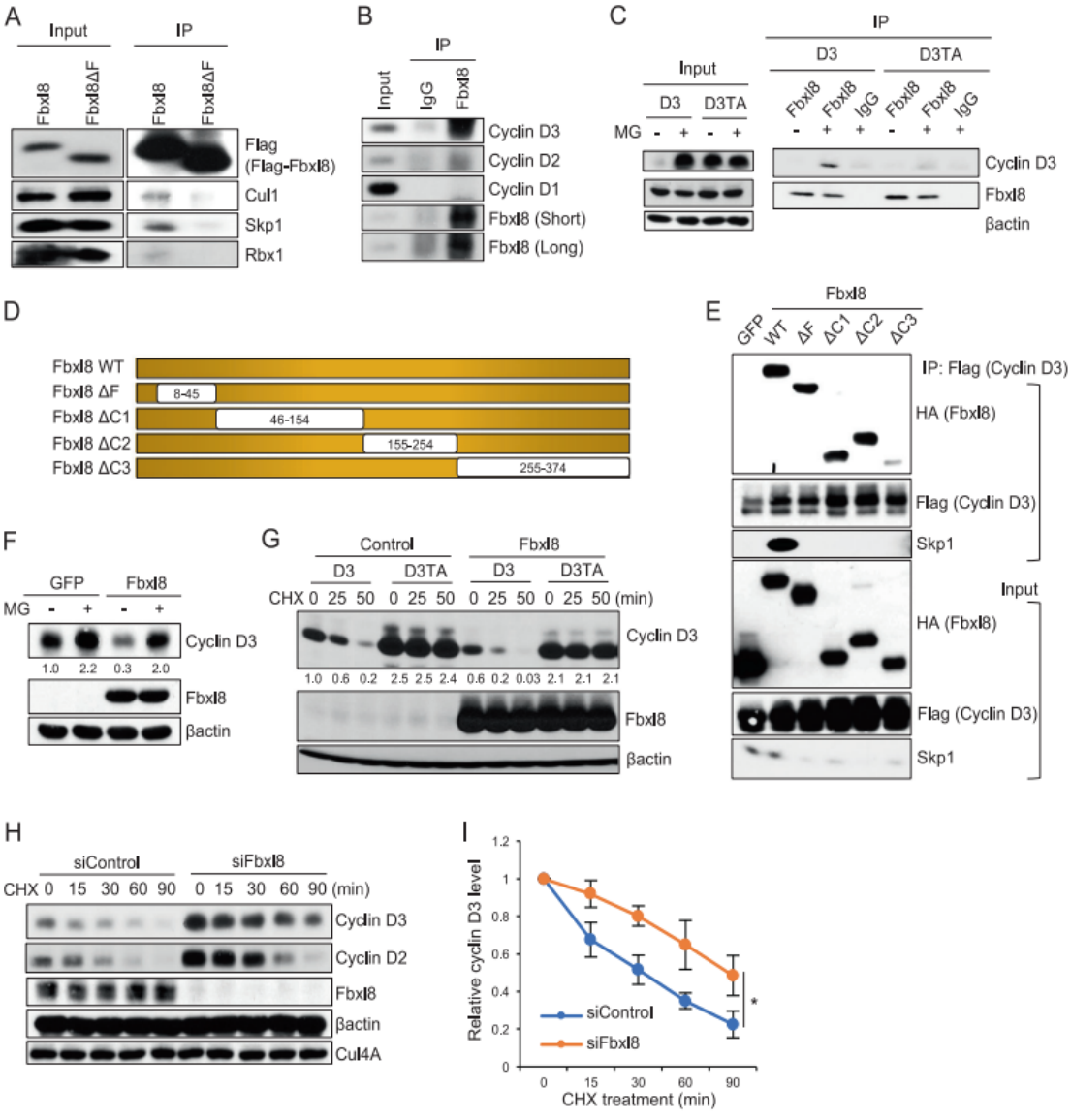

Figure 2.1

Fig. 2.1 Fbxl8 binds to and regulates cyclin D3 in proteasome and phosphorylation-dependent manner. a Lysates from NIH3T3 cells transfected with Flag-Fbxl8 or Flag-Fbxl8-ΔF and treated with a proteasome inhibitor MG132 (20 μM) for 4 hours were immunoprecipitated with anti-Flag beads. Immune complexes were analyzed by western blot for Flag-Fbxl8, Cul1, Skp1, and Rbx1. b Lysates from NIH3T3 cells treated with a proteasome inhibitor MG132 (20 μM) for 4 h were immunoprecipitated with normal IgG or an antibody specific for Fbxl8. Immune complexes were analyzed by western blot for cyclin D3, cyclin D2, cyclin D1, and Fbxl8. c Lysates from HEK293T cells co-transfected with Flag-tagged cyclin D3 or cyclin D3Thr283A (D3TA), with HA-Fbxl8, and treated with or without MG132 (20 μM) for 4 h were subjected to immunoprecipitation with normal IgG or anti-HA. Immune complexes were analyzed by western blot for cyclin D3 and Fbxl8. d Schematic model of deletion mutants of Fbxl8. e Lysates from NIH3T3 cells co-transfected with HA tagged GFP or Fbxl8 mutants described in d with Flag-D3 and treated with a proteasome inhibitor MG132 (20 μM) for 4 h were precipitated with anti-Flag beads. Immune complexes were analyzed by western blot. f Lysates from NIH3T3 cells co-transfected with Flag-GFP or FlagFbxl8 with or without treatment of MG132 (20 μM) for 4 h were analyzed by western blot for cyclin D3, Fbxl8, and βactin. The numbers indicate quantifications of cyclin D3 normalized by βactin. g Lysates from NIH3T3 cells co-transfected with cyclin D3 or cyclin D3Thr283A (D3TA) and empty plasmid (Control) or Flag-Fbxl8 and treated with 100 μg/mL of cycloheximide (CHX) for the indicated time periods were analyzed by western blot using antibodies against cyclin D3, Fbxl8 and βactin. The numbers indicate quantifications of cyclin D3 normalized by βactin. h Lysates from NIH3T3 cells transfected with si-Control or siFbxl8 for 3 days were treated with 100 μg/mL of cycloheximide for the indicated time periods and analyzed by western blot for cyclin D3, Cyclin D2, and Fbxl8, βactin and Cul4A. i Quantitative analysis of cyclin D3 from h to determine half-life. Data represent mean ± SD, *$p < 0.05$ (two-tailed Student's t test, $n = 3$).

Fbxl8 co-precipitates with Cyclin D3, But not Cyclins D1 and D2

There is a paucity of data characterizing cyclin D3 phosphorylation in vivo. Therefore, we immunopurified Flag-cyclin D3 from NIH3T3 cells, and using mass spectrometry analysis identified phosphorylation of 8 distinct serine/threonine residues including Thr-283 (Appendix A). Mutation of individual residues to alanine demonstrated that only a Thr-283 to alanine mutation (T283A) altered the kinetics of cyclin D3 degradation (Appendix A). To identify the E3 ligase that regulates Thr-283 phosphorylation-dependent ubiquitylation of cyclin D3, we expressed tagged wild type cyclin D3 or cyclin D3T283A alleles in NIH3T3 fibroblasts and used mass spectrometry to identify co-purifying proteins. Fbxl8 was enriched with cyclin D3 but not cyclin D3T283A. We confirmed that Fbxl8 forms an SCF complex in vivo and in vitro (Figs.

2.1A and Appendix A) and subsequently demonstrated that endogenous Fbxl8 binds to cyclin D3 in NIH3T3 cells and Burkitt's lymphoma, Raji cells (Figs. 2.1b and Appendix A). Since cyclin D2 and D3 are both expressed in lymphoid cells and exhibit analogous regulation [111], we tested whether Fbxl8 interacts with cyclin D2. Immunoprecipitation revealed that endogenous Fbxl8 co-precipitates with cyclin D3 and no specific association was apparent with cyclin D1 or D2 (Figs. 1b and S1E). It is worth noting that cyclin D2 and cyclin D3 were properly phosphorylated under these immunoprecipitation conditions (Appendix A). To further examine the contribution of cyclin D3 phosphorylation for binding to Fbxl8, we assessed binding of cyclin D3T283A to Fbxl8. Co-immunoprecipitation revealed weak to undetectable binding of Fbxl8 with D3T283A (Fig. 2.1c). To identify the domain of Fbxl8 that recognizes cyclin D3, Fbxl8 deletion mutants were generated (Fig. 2.1d). HA-Fbxl8 (wild type, ΔF, ΔC1, ΔC2, and ΔC3) or HA-GFP was transfected into NIH3T3 cells along with Flag-D3; reduced binding of cyclin D3 to Fbxl8-ΔC3 was observed (Fig. 2.1e). Consistently, in vitro binding revealed direct binding of Fbxl8 to cyclin D3, but not to cyclin D2 (Appendix G). In addition, no binding of cyclin D3 with Fbxo4, an ubiquitin ligase for cyclin D1 [112], was observed (Appendix A).

Fbxl8 Regulates Cyclin D3 Protein Stability

We next assessed whether Fbxl8 regulates cyclin D3 protein stability. Overexpression of Fbxl8 resulted in reduced expression of cyclin D3 relative to control, in an MG132- dependent manner (Fig. 2.1f). Fbxl8 overexpression accelerated degradation of cyclin D3 and this rapid turnover was not apparent with cyclin D3T283A (D3TA) (Fig. 2.1g). Cyclin D3 degradation was not accelerated by overexpression of Fbxl2, Fbxo4,

Fbxo31 or Fbxo11 (Appendix B), demonstrating specificity. Consistently, knockdown of Fbxl8 increased basal levels of endogenous cyclin D3 (Fig. 2.1h). Cycloheximide (CHX) chase experiments revealed that knockdown of Fbxl8 extended half-life of cyclin D3 while cyclin D2 protein stability was unaffected (Fig. 2.1h-i). These results demonstrate that Fbxl8 regulates the stability of cyclin D3 in a phosphorylation-dependent manner.

Fbxl8 catalyzes polyubiquitylation for cyclin D3

To further test the function of Fbxl8, we established CRISPR-mediated knockout cell lines (clones 1, 2 and 3) in NIH3T3 cells (Fig. 2.2a top). Stabilization of cyclin D3 was noted in Fbxl8 KO cell lines (Fig. 2.2a bottom; Appendix B). To assess mechanisms, cells were transfected with vectors encoding Flag-D3 together with HA-Ub+MG132. No ubiquitylation of cyclin D3 was observed in KO-Fbxl8 clones, while polyubiquitin of cyclin D3 was observed in control cells (Fig. 2.2b). Ectopic Fbxl8 restored polyubiquitylation of cyclin D3 while Fbxl8-ΔF was impaired in polyubiquitylation of cyclin D3 (Fig. 2.2c). Consistent with phosphorylation-dependence, wild type cyclin D3 was polyubiquitylated by Fbxl8 while the cyclin D3TA mutant was refractory (Fig. 2.2d). Finally, we demonstrated that recombinant SCF-Fbxl8 purified from Sf9 cells, polyubiquitylated cyclin D3, but not cyclin D2, in an F-box dependent manner demonstrating cyclin D3 is a direct substrate (Figs. 2.2e–g and Appendix B).

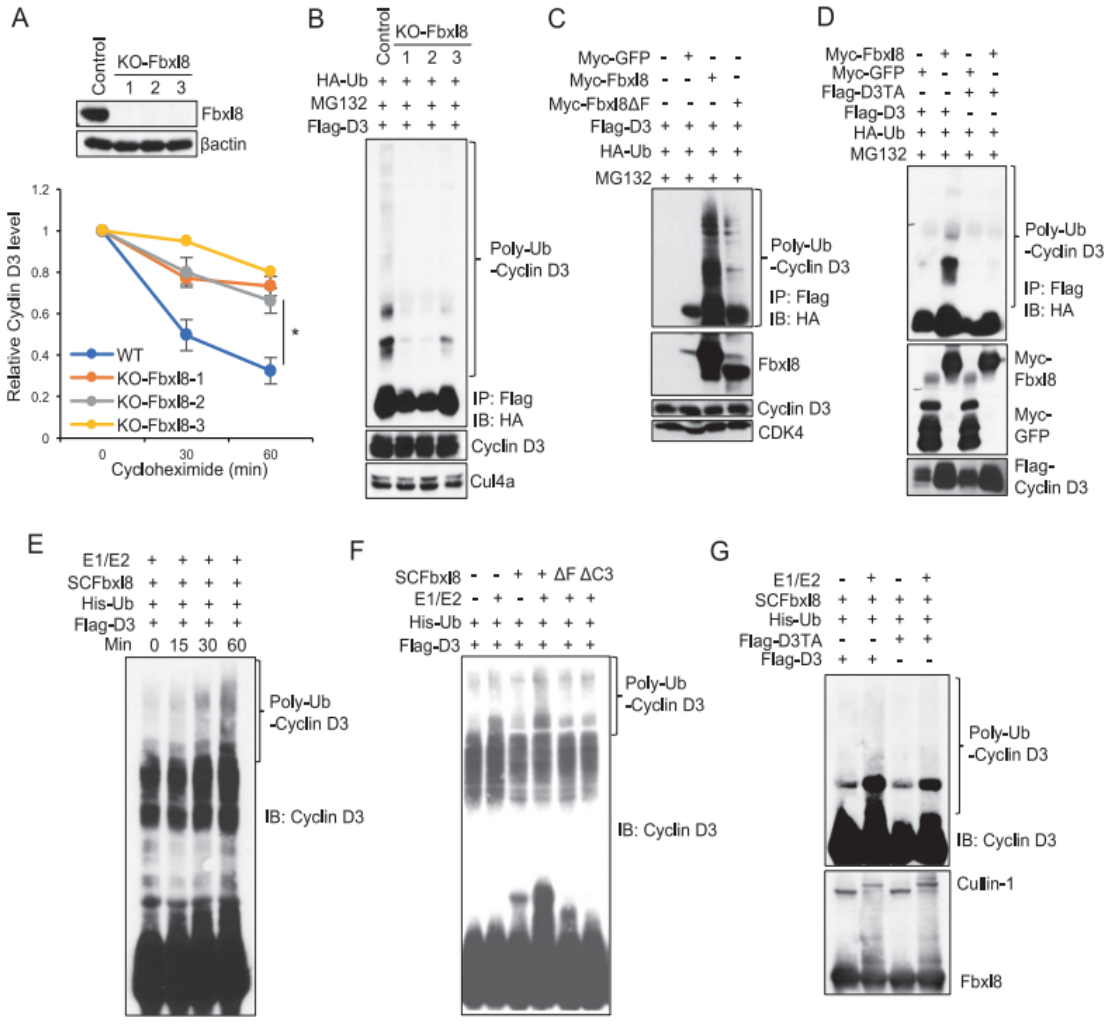

Figure 2.2

Fig. 2.2 Fbxl8 ubiquitylates cyclin D3 in a phosphorylation dependent manner

a Lysates from parental NIH3T3 cells versus clones (1, 2, and 3) with CRISPR/Cas9 mediated knock out of Fbxl8, were analyzed by western blot for Fbxl8 and βactin (top panel). Lysates from NIH3T3 cells or KO-Fbxl8 clones from (top panel) were treated with 100 μg/mL of cycloheximide for the indicated time periods and analyzed by western blot for cyclin D3 and βactin. Quantitative analysis of cyclin D3 is shown. Data represent mean ± SD, *p < 0.05 (two-tailed Student's t test, n = 3). b Lysates from NIH3T3 (Control) or NIH3T3 KO-Fbxl8 clones were co-transfected with HA-Ub and Flag-D3 for 40h, and treated with MG132 (20 μM) for 4 h prior to immunoprecipitation with anti-Flag beads. Immune complexes were analyzed by western blot for ubiquitinated proteins (α-HA), cyclin D3 and Cul4a as a loading control. c, d Lysates from HEK293T cells co-transfected with indicated plasmids were treated with MG132 (20 μM) for 4 h prior to immunoprecipitation with anti-Flag beads. Immune complexes were analyzed by western blot for HA-ubiquitylated proteins, total Fbxl8, cyclin D3 and CDK4. e–g In vitro ubiquitylation assays were performed in reaction mixtures containing the presence or absence of the indicated reaction mixture components. Lysates from assays were analyzed by western blot using antibodies against indicated antibodies.

Fbxl8 loss accelerates G1-Sphase Transition

Since overexpression of cyclin D3 accelerates G1-S phase progression [113], we reasoned that Fbxl8 loss should accelerate G1-S phase transition. Cells with si-Control or siFbxl8 were arrested in G0/G1 by contact inhibition and cell cycle reentry was analyzed at 0, 6, 12, 16, 24, 32 and 48 h following replating at subconfluence (Fig. 2.3a). siFbxl8 was transfected into the cells before cells were synchronized resulting in cyclin D3 accumulation at the 0 h time point (Fig. 2.3b). Cells arrested with equal efficiency, but siFbxl8 cells transitioned from G1 to S phase with accelerated kinetics (Fig. 2.3a).

To focus on the impact of Fbxl8 during the G1-S phase transition, cells with si-Control or siFbxl8 were synchronized in G0/G1 and cell cycle progression was analyzed at multiple time points after release. Cells transfected with siFbxl8 progressed to S phase faster than cells with siControl due to accelerated progression of G1/S phase. As a result, we observed increased S + G2/M phase populations, eventually leading to more cells entering the next cell cycle at 27 h time point (Fig. 2.3c and Appendix C). Consistent with FACS analyses, cyclin D3 levels increased earlier in siFbxl8 cells (Fig. 2.3d). In addition, increased phosphorylation of Rb at Ser-780, a substrate for cyclin D-CDK4/6 was observed in siFbxl8 cells relative to control cells (Fig. 2.3d). This is consistent with elevated kinase activity of cyclin D/CDK4/6, reflecting increased cyclin D3 and reduced degradation of phosphorylated cyclin D3. To further establish increased kinetics of S phase entry upon knockdown of Fbxl8, we utilized BrdU incorporation. Consistently, knockdown of Fbxl8 accelerated G1-S phase transition (Figs. 2.3e and Appendix C) and increased only the S phase population in asynchronous cells (Fig. Appendix C). Together, these results suggest that knockdown of Fbxl8 shortens G1 phase of the cell cycle by upregulating cyclin D3.

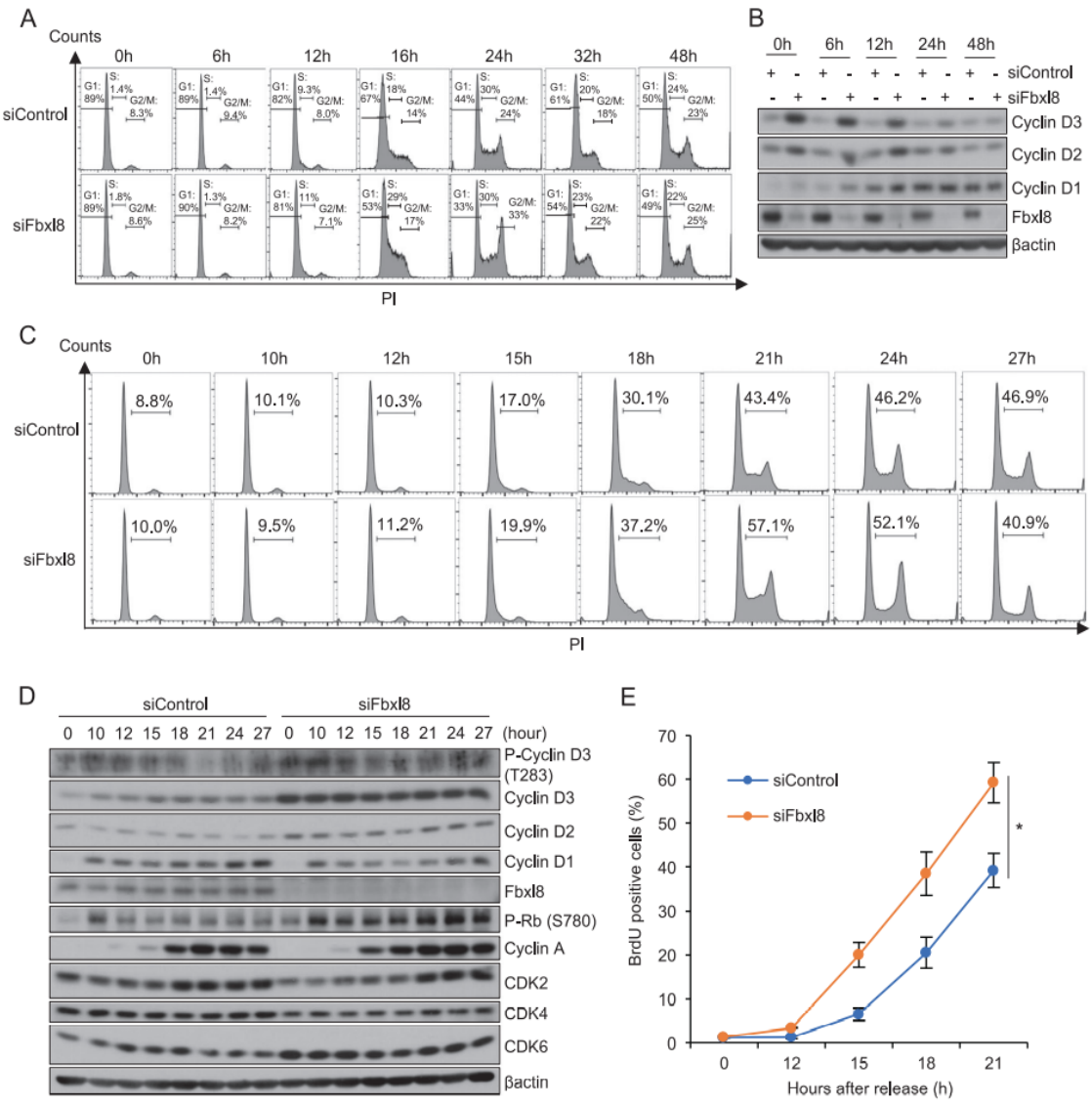

Fig. 2.3 Knockdown of Fbxl8 promotes G1-S phase transition of cell cycle.

a NIH3T3 cells were transfected with siControl or siFbxl8 and arrested at G0/G1 by contact inhibition for 36 h. Following release by replating at low density, the cell cycle was analyzed at 6, 12, 16, 24, 32, 48 h by FACS. b Western analysis of lysates from a. c NIH3T3 cells were transfected with either siControl or siFbxl8 and arrested at G0/G1 by contact inhibition for 36 h. Following release by replating at low density, the cell cycle was analyzed at 10, 12, 15, 18, 21, 24, and 27 h by FACS. Representative FACS profiles were shown. d Western analysis of lysates from c for phospho-cyclin D3, cyclin D3, cyclin D2, cyclin D1, Fbxl8, phospho-Rb (S780), cyclin A, CDK2, CDK4, CDK6 and βactin. e NIH3T3 cells were transfected with siControl or siFbxl8 and arrested at G0/G1 phase by contact inhibition for 36 h. S phase entry was assessed by BrdU incorporation (30 min) and FACS at 0, 12, 15, 18, and 21 h post release. Quantification of BrdU positive cells; mean ± SD, *$p < 0.05$ (two-tailed Student's t test, n = 3).

Enforced Expression of Fbxl8 Delays G1-S Phase Transition

Since Fbxl8 opposes cyclin D3 accumulation, we reasoned that Fbxl8 overexpression should delay cell cycle progression. A bicistronic plasmid encoding Fbxl8/IRES GFP or Fbxl8ΔF/ IRES GFP was expressed in NIH3T3 cells. The bicistronic nature of this vector permits sorting on GFP positive cells that are co-expressing Fbxl8 or Fbxl8-ΔF versus GFP negative cells that serve as a control for FACS assessment of cell cycle progression (Fig. 2.4a). We confirmed reduced expression of cyclin D3 in cells with ectopic Fbxl8, while Fbxl8-ΔF had no impact on cyclin D3 (Fig. 2.4b). BrdU incorporation revealed that cells expressing Fbxl8 progressed to S phase slower than cells expressing only GFP, while Fbxl8-ΔF mitigated Fbxl8 mediated S phase reduction (Figs. 2.4c and Appendix D). Consistently, all GFP negative populations that do not express GFP, Fbxl8 or Fbxl8-ΔF progressed to S phase with similar kinetics (Appendix D). Finally, we assessed whether overexpression of Fbxl8 delays G1 phase progression through degradation of cyclin D3. Cyclin D3TA, a non-phosphorylatable mutant, was expressed together with or without Fbxl8 (Fig.2. 4d). BrdU incorporation revealed that cyclin D3TA hampers Fbxl8 function regulating G1-S phase (Figs. 2.4e and Appendix D). Together these results indicate that Fbxl8 regulates G1-S phase transition through degradation of cyclin D3.

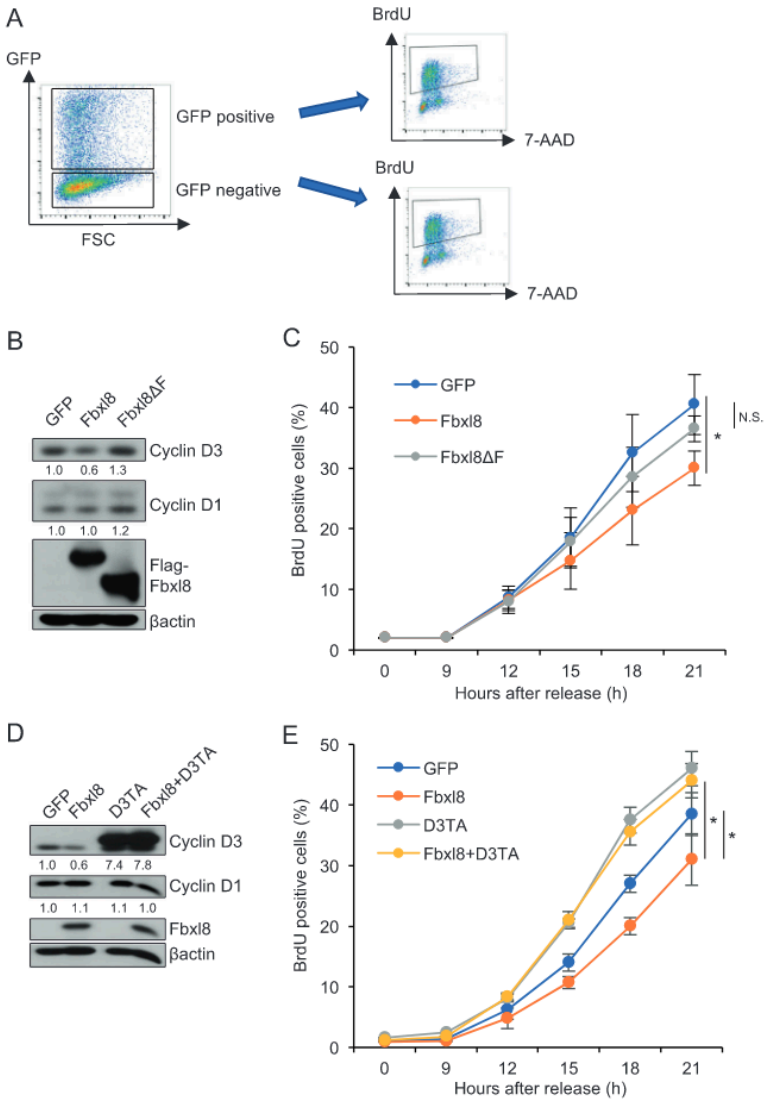

Fig. 2.4 Overexpression of Fbxl8 recedes G1-S phase transition of cell cycle through degradation of cyclin D3.

a Schematic model of experiment. NIH3T3 cells were transfected with MigR1 IRES-GFP, MigR1Fbxl8 IRES-GFP or MigR1Fbxl8ΔF IRES-GFP, and arrested at G0/G1 phase by serum starvation for 36 h. GFP positive cells and negative cells were FACS sorted, and S phase entry was assessed by BrdU incorporation (30 min). b Western analysis of lysates from sorted GFP positive NIH3T3 cells expressing GFP, Fbxl8, or Fbxl8ΔF for cyclin D3, cyclin D1, Flag-Fbxl8 and βactin. The numbers indicate quantifications of cyclin D3 and cyclin D1 normalized by βactin. c GFP and BrdU double-positive cells were analyzed 9, 12, 15, 18, 21 h after release from G0/G1 phase by re-splitting cells in DMEM with 10%FBS. Quantification of GFP and BrdU double-positive cells; mean ± SD, *$p < 0.05$ (two-tailed Student's t test, n = 3). N.S. Not Significant (two-tailed Student's t test, n = 3). d Western analysis of lysates from sorted GFP positive NIH3T3 cells expressing GFP, Fbxl8, cyclin D3TA or Fbxl8+cyclin D3TA for cyclin D3, cyclin D1, Flag-Fbxl8 and βactin. The numbers indicate quantifications of cyclin D3, cyclin D2 and cyclin D1 normalized by βactin. e GFP and BrdU double-positive cells were analyzed 9, 12, 15, 18, 21 h after release from G0/G1 phase by re-splitting cells in DMEM with 10%FBS. Quantification of GFP and BrdU double-positive cells; mean ± SD, *$p < 0.05$ (two-tailed Student's t test, n = 3).

Cyclin D3 co-localizes with Fbxl8 during S-phase in the cytoplasm in a phosphorylation-dependent manner

D-type cyclins are localized in nucleus during G1 phase, where they initiate phosphorylation-dependent inactivation of Rb [114-116]; however, they translocate to the cytoplasm during S-phase as a mechanism to restrict dysregulation of cell division. We therefore assessed the subcellular localization of cyclin D3 and Fbxl8 during G1 and S phases. Cells were synchronized at G0/G1 and cell division was monitored in parallel by FACS. Immunofluorescence microscopy revealed nuclear cyclin D3 during G1 phase (8 h after release), but cytoplasmic during S phase (16 h after release). We next determined whether CRM1-dependent nuclear export of cyclin D3 is responsible for cytoplasmic localization during S-phase. Cyclin D3 re-localization to the cytoplasm was inhibited following Leptomycin B treatment consistent with CRM1-dependent nuclear export (Fig. Appendix E). Conversely, Fbxl8 was cytoplasmic throughout the cell cycle suggesting cyclin D3 stability during G1 phase is ensured through differential subcellular localization of cyclin D3 versus Fbxl8. Importantly, cyclin D3T283A remained nuclear during S phase consistent with p-T283 regulating cytoplasmic localization (Appendix E). Consistently, immunoprecipitation experiments revealed that Leptomycin B treatment prevented the binding of Fbxl8 and cyclin D3 while D3T283A is refractory to binding to Fbxl8 (Fig. Appendix E), indicating that p283 coordinates nuclear export followed by its direct binding to Fbxl8 for degradation in cytoplasm

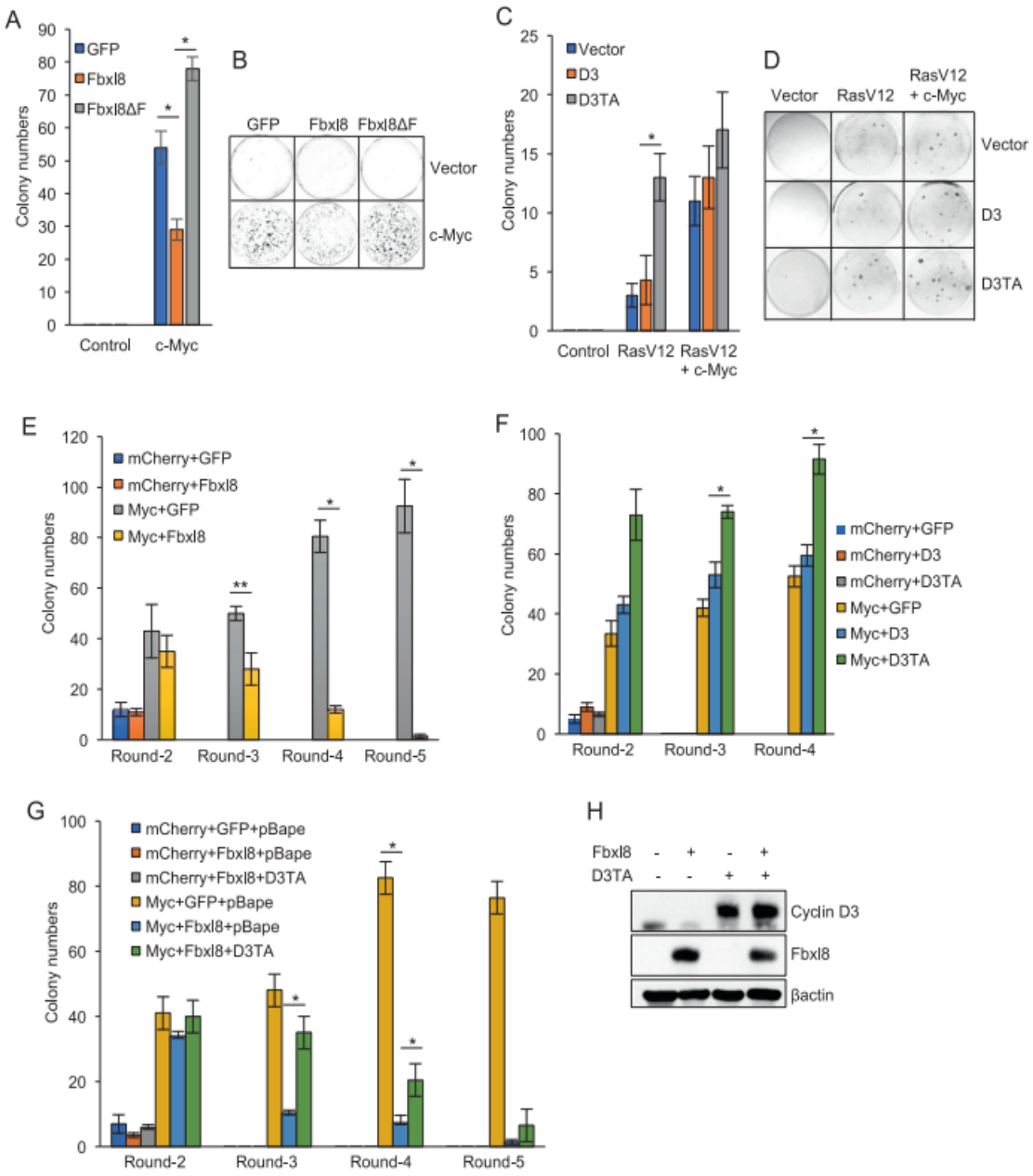
A
Colony numbers
GFP
Fbxl8
Fbxl8ΔF
Control
c-Myc
B
GFP
Fbxl8
Fbxl8ΔF
Vector
c-Myc
C
Vector
D3
D3TA
Colony numbers
Control
RasV12
RasV12 + c-Myc
D
Vector
RasV12
RasV12 + c-Myc
Vector
D3
D3TA
E
mCherry+GFP
mCherry+Fbxl8
Myc+GFP
Myc+Fbxl8
Colony numbers
Round-2
Round-3
Round-4
Round-5
F
mCherry+GFP
mCherry+D3
mCherry+D3TA
Myc+GFP
Myc+D3
Myc+D3TA
Colony numbers
Round-2
Round-3
Round-4
G
mCherry+GFP+pBape
mCherry+Fbxl8+pBape
mCherry+Fbxl8+D3TA
Myc+GFP+pBape
Myc+Fbxl8+pBape
Myc+Fbxl8+D3TA
Colony numbers
Round-2
Round-3
Round-4
Round-5
H
Fbxl8
D3TA
Cyclin D3
Fbxl8
βactin

Figure 2.5

Fig. 2.5 Fbxl8 suppresses c-myc-induced transformation through phosphorylation-dependent cyclin D3 degradation.

a,b NIH3T3 cells were co-transfected with empty vector (Vector) or c-Myc + either MigR1 (GFP), MigR1 Fbxl8 (Fbxl8) or MigR1 Fbxl8-ΔF (Fbxl8-ΔF), plated and cultured for 21 days. Quantification of colony numbers (a) and representative images (b). Data represent mean ± SD, *p < 0.05 (two-tailed Student's t test, n = 3). c, d NIH3T3 cells were cotransfected with empty vector (Vector), c-Myc or c-Myc+RasV12 and MigR1 (Vector), MigR1 cyclin D3 (D3) or MigR1 cyclin D3Thr283A (D3TA), plated in soft agar medium and cultured for 21 days. Quantification of colony numbers (c) and representative images (d) are shown. Data represent mean ± SD, *p < 0.05 (two-tailed Student's t test, n = 3). e Bone marrow derived HSC cells from 5-FU (150 mg/kg) treated mice were co-transduced with retrovirus encoding the indicated cDNA and plated in methycellulose media. Colony numbers were quantified and subjected to 5 rounds of serial replating. Data represent mean ± SD, *p < 0.01, **p < 0.05 (two-tailed Student's t test, n = 3). f Bone marrow HSC from mice treated with 5-FU (150 mg/kg) were co-transduced with retrovirus encoding the indicated cDNA and plated in methycellulose media and colony numbers were quantified over 4 rounds of serial replating. Data represent mean ± SD, *p < 0.05 (twotailed Student's t test, n = 3). g Bone marrow HSC from mice treated with 5-FU (150 mg/kg) were co-transduced with retrovirus encoding the indicated cDNA and plated into methycellulose media and colony numbers were quantified and subjected to 5 rounds of serial replating. Data represent mean ± SD, *p < 0.05 (two-tailed Student's t test, n = 3). h Lysates from g were analyzed by western blot using antibodies against cyclin D3, Fbxl8 and βactin.

Cyclin D3T283A has oncogenic properties

Data thus far suggests a hypothesis wherein Fbxl8 should exhibit tumor suppressive properties reflecting its ability to antagonize cyclin D3. Because cyclin D3T283 mutations co-occur coordinately with c-myc translocation in Burkitt's lymphoma, we assessed Fbxl8 activity in the context of c-myc overexpression. Transformation assays revealed that c-Myc driven transformation was suppressed by Fbxl8 and enhanced by Fbxl8ΔF, suggesting tumor suppressive function of Fbxl8 (Fig. 2.5a, b). To address whether cyclin D3 or cyclin D3T283A has oncogenic functions and contributes to neoplastic transformation, we performed soft agar assays with D3 versus D3TA. D3TA increased H-RasV12 or H-RasV12/c-Myc-dependent transformation, while cyclin D3 was less potent (Fig. 2.5c, d). Because overexpression of cyclin D3 or mutation of D3 at Thr283 is frequently observed in Burkitt's lymphoma and leukemia [6] and c-Myc driven murine lymphomas [117, 118] (Appendix F), we further defined whether Fbxl8 has tumor suppressive function in

hematopoietic cells. Bone marrow cells isolated from 5-FU treated mice were infected with bicistronic retrovirus encoding c-myc/Cherry, Fbxl8/GFP or c-myc/Cherry+Fbxl8/GFP were plated on methyl cellulose medium and carried through 5 rounds of replating. While cells expressing c-myc accumulated through 5 rounds consistent with transformation, co-expression with Fbxl8 inhibited colony formation driven by c-myc (Fig. 2.5e), indicating Fbxl8 is a tumor suppressor. We next assessed whether Fbxl8-dependent growth suppression is cyclin D3- dependent. Consistently, cells overexpressing c-myc accumulated through 4 rounds, whereas co-expression with cyclin D3T283A remarkably enhanced colony formation, in contrast with cyclin D3 which was less effective (Fig. 2.5f). Finally, we assessed whether cyclin D3T283A rescues the Fbxl8 mediated reduction in colony formation that is driven by c-myc. Cells expressing c-myc or cmyc+Fbxl8 formed same numbers of colonies through round 2, but by round 3–4 Fbxl8 dramatically diminished c-myc induced colony formation (Fig. 2.5g). Critically, cyclin D3T283A, a documented mutant expressed in some B-cell lymphomas that also express high levels of c-myc, significantly rescued Fbxl8 mediated hematopoietic cell growth attenuation and this rescue was maximized at round 3 (Fig. 2.5g). We confirmed developed colonies still maintain the expression of cyclin D3T283A and Fbxl8 (Fig. 2.5h).

Fbxl8 attenuates lymphoma cell growth and lymphoma formation in vivo

To address tumor suppressive function of Fbxl8 in an in vivo model, a Burkitt's lymphoma cell line CA46 expressing GFP, GFP/Fbxl8, or GFP/Fbxl8ΔF was generated (Fig. 2.6a). CA46 were chosen as they will form xenograft tumors [117] and retain wild type cyclin D3, maintaining phosphorylation-dependent regulation of cyclin D3 by Fbxl8.

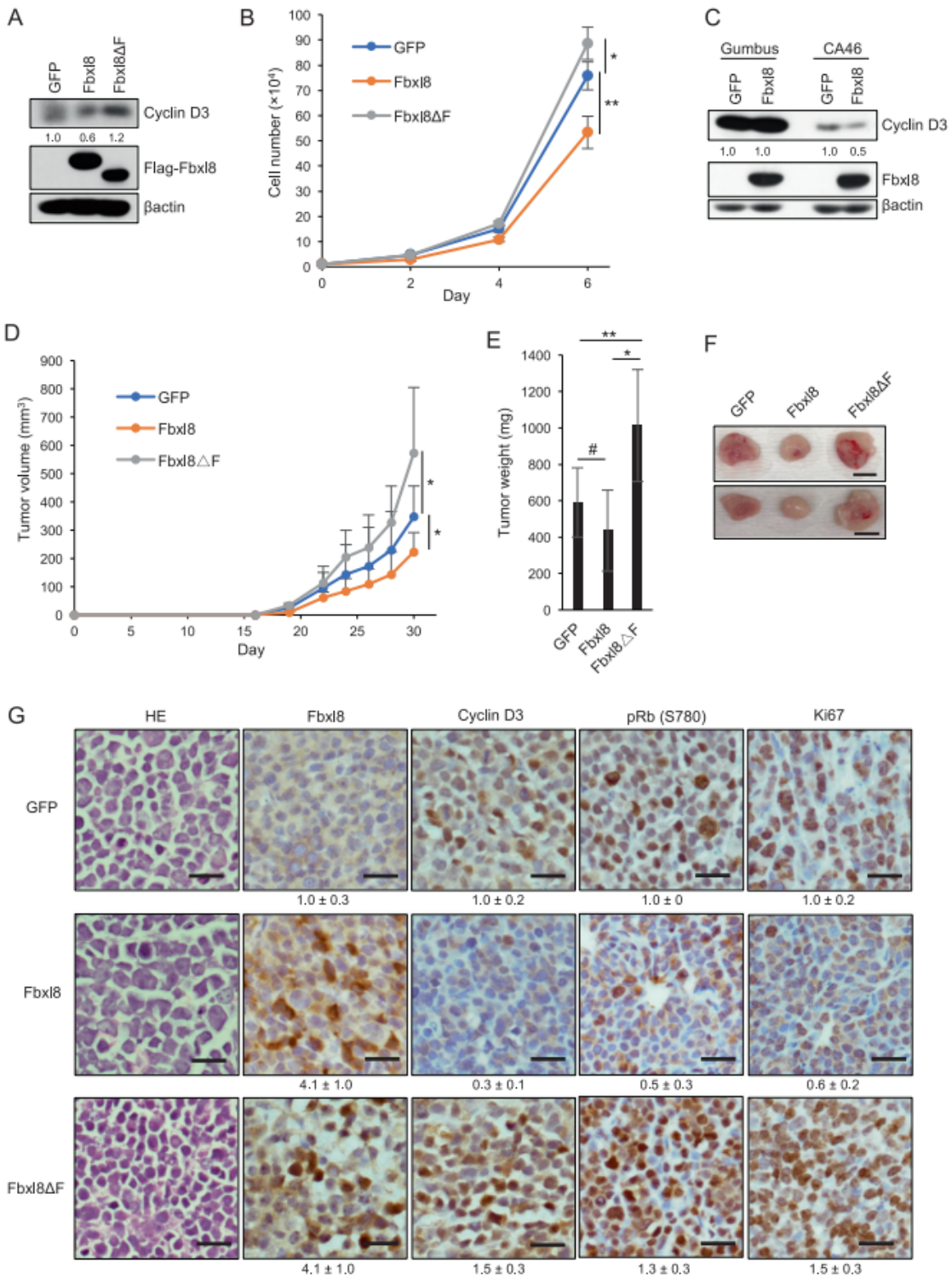
A
GFP
Fbxl8
Fbxl8ΔF
Cyclin D3
1.0 0.6 1.2
Flag-Fbxl8
βactin
B
Cell number (×10⁴)
GFP
Fbxl8
Fbxl8ΔF
Day
C
Gumbus
CA46
GFP
Fbxl8
GFP
Fbxl8
Cyclin D3
1.0 1.0 1.0 0.5
Fbxl8
βactin
D
Tumor volume (mm³)
GFP
Fbxl8
Fbxl8△F
Day
E
Tumor weight (mg)
GFP
Fbxl8
Fbxl8△F
F
GFP
Fbxl8
Fbxl8ΔF
G
HE
Fbxl8
Cyclin D3
pRb (S780)
Ki67
GFP
1.0 ± 0.3
1.0 ± 0.2
1.0 ± 0
1.0 ± 0.2
Fbxl8
4.1 ± 1.0
0.3 ± 0.1
0.5 ± 0.3
0.6 ± 0.2
Fbxl8ΔF
4.1 ± 1.0
1.5 ± 0.3
1.3 ± 0.3
1.5 ± 0.3

Figure 2.6

Fig. 2.6 Fbxl8 suppresses lymphoma growth in vivo.
a Lysates from CA46 cells infected with GFP, GFP/Flag-Fbxl8, or GFP/FlagFbxl8ΔF were analyzed by western blot for Flag-Fbxl8, cyclin D3 and βactin. The numbers indicate quantifications of cyclin D3 normalized by βactin. b 1 × 104 CA46 cells from a were plated at low density and cell were counted every 2 days. Data represent mean ± SD, *p = 0.02, **p < 0.01 (two-tailed Student's t test, n = 4). c Lysates from Gumbus cells and CA46 cells infected with GFP, GFP/FlagFbxl8 were analyzed by western blot for Flag-Fbxl8, cyclin D3 and βactin. The numbers indicate quantification of cyclin D3 normalized to βactin. d 2 × 106 CA46 cells from a were subcutaneously injected into 8-week-old SCID mice with matrigel. Tumor volumes were measured by caliper every 2 days after tumors developed and calculated by the following formula V = (Length × width × height)/2. Data represent mean ± SD, *p = 0.02 (two-tailed Student's t test, n = 10). e The average of tumor weight from d. Data represent mean ± SD, # p = 0.02, **p = 0.03, *p < 0.01 (two-tailed Student's t test, n = 10). f Representative images of the xenograft tumors from e. Scale bar indicates 1 cm. g Representative H&E staining and IHC staining images for Fbxl8, cyclin D3, pRb (S780), and Ki67 from f. Scale bar indicates 50 μm. The numbers indicate quantification of intensity determined by IHC scoring from three independent experiments. The IHC score in each experiment was defined by the following formula: Intensity = [staining positive population (1 to 3) × staining intensity (1 to 3)]

While Fbxl8 overexpression has no impact on cyclin D3 levels or cell proliferation in Gumbus cells (Gumbus harbor an endogenous cyclin D3 T283A mutant), Fbxl8 overexpression in CA46 downregulates wild type cyclin D3 and attenuates cell proliferation (Figs. 2.6c and Appendix G). Conversely, knockdown of Fbxl8 promoted lymphoma cell proliferation with upregulated cyclin D3 expression (Appendix G). Immune compromised mice injected with CA46 cells expressing GFP, Fbxl8, or Fbxl8-ΔF were monitored every 2 days for tumor progression. CA46 cells with Fbxl8 overexpression formed tumors slower than cells expressing GFP and cells expressing Fbxl8-ΔF developed tumors faster than cells expressing GFP, indicating tumor suppressive function of Fbxl8 and consistent with cell growth curve (Fig. 2.6d–f). H&E staining revealed that tumors exhibited typical histology of lymphoma (Fig. 2.6g). IHC staining for Fbxl8 and cyclin D3 revealed that tumors maintained Fbxl8 or Fbxl8-ΔF accompanied with reduced or increased expression of cyclin D3, respectively (Fig. 2.6g). While Fbxl8 overexpression resulted in reduced phospho-Rb (S780) and Ki67 in xenograft tumors, Fbxl8-ΔF increased

positivity of phospho-Rb (S780) and Ki67 (Fig. 2.6g). We finally tested whether Fbxl8 reduces lymphoma proliferation through degradation of cyclin D3. Cyclin D3TA was expressed together with or without Fbxl8 (Fig. Appendix G). Cyclin D3TA overcomes Fbxl8 mediated attenuation of lymphoma proliferation (Fig. Appendix G). Together these results demonstrate that Fbxl8 functions as a tumor suppressor through degradation of cyclin D3 in lymphoma.

Fbxl8 is negatively correlated with cyclin D3 in human lymphomas

We subsequently evaluated the relevance of the Fbxl8-cyclin D3 axis in human patients. Normal lymph node tissues, spleen, tonsil, and lymphomas arrayed on slides (US Biomax, Inc.) were stained with cyclin D3 and Fbxl8 specific antibodies (Fig. 2.7a) and IHC scores of each core were calculated (details in Materials & Methods). We categorized cyclin D3 expression as low, medium, and high in all samples and plotted on the x axis to compare with IHC scores for Fbxl8 (Fig. 2.7a, b). Patient samples with low, medium, or high expression of cyclin D3 have high, medium, or low expression of Fbxl8, respectively, underscoring Fbxl8 negatively regulates cyclin D3 expression in human lymphomas in a dose dependent manner. We further used a recently developed online tool to assess the lymphoma patients' overall survival with gene expression [119], and observed that the low expression of Fbxl8 mRNA significantly correlated with reduced overall survival for lymphoma patients while the expression of cyclin D3 mRNA does not (Fig. 2.7c). We suggest this is consistent with our conclusions that Fbxl8 regulates cyclin D3 at posttranslational level and Fbxl8 has a tumor suppressive function. This further suggested that cyclin D3-dependent kinase might be a novel therapeutic target in certain lymphomas that harbor low expression of Fbxl8 or high expression of cyclin D3.

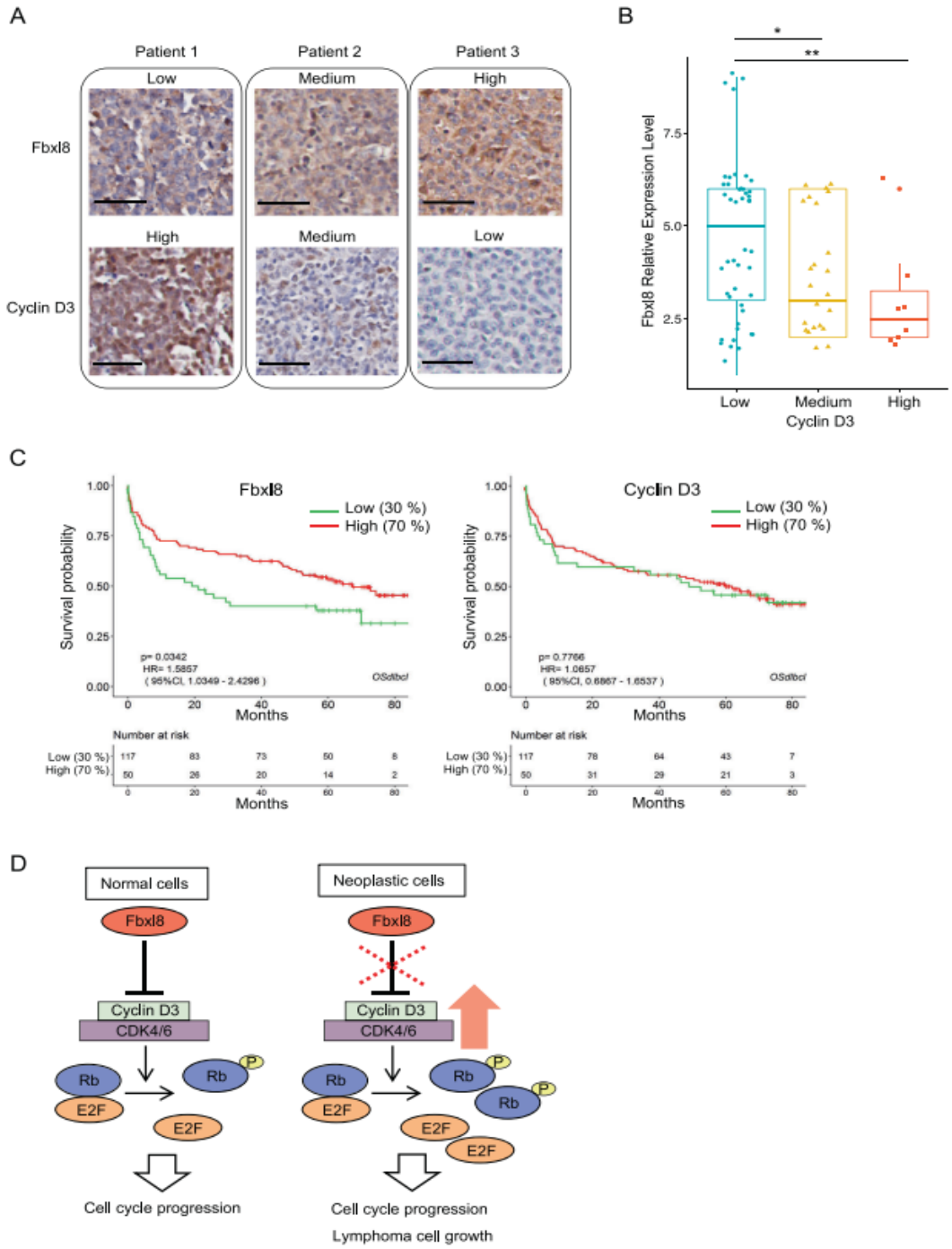

Figure 2.7 Fbxl8 expression is negatively correlated with cyclin D3 expression in human lymphomas

a. Representative IHC staining images from human patients for low, medium, and high expression of cyclin D3 or Fbxl8. Scale bar indicates 50 μm. b Each IHC score was calculated as described in the Materials & Methods. The box plot with scatters and statistics are shown, *p = 0.046, **p = 0.017 (Wilcoxon rank sum test, n = 77). c Kaplan–Meier survival curve for overall survival in lymphoma patients with low and high expression of Fbxl8 (left panel) or cyclin D3 (right panel). d Model of lymphoma cell growth by Fbxl8- cyclin D3 axis.

Cyclin D3 overexpression renders cells to susceptible to CDK4/6 small molecule inhibitors

CDK4/6 inhibitors (CDK4/6i) have been evaluated in clinical trials in many cancer types with promising results [120]. Given that cyclin D3TA has oncogenic properties and promotes oncogenic-driven transformation (Fig. 2.5), we assessed the efficacy of the CDK4/6i, palbociclib, on cells expressing wild type versus mutant cyclin D3. We confirmed robust expression of both cyclin D3 and cyclin D3TA (Appendix H). As expected, cyclin D3TA expression is elevated relative to wild type cyclin D3, reflecting increased stability of cyclin D3TA by circumventing phosphorylation-dependent degradation by Fbxl8 while mRNA level is unchanged between wild type cyclin D3 and cyclin D3TA (Appendix H). While NIH3T3 cells expressing vector control were relatively refractory to palbociclib, those overexpressing either cyclin D3 or cyclin D3TA were sensitive to palbociclib and arrested at G1 (Appendix H), consistent with a previous report that palbociclib-induced senescence is linked to CDK4 hyperactivation [121].

GSK3β does not phosphorylate cyclin D3 for degradation

Previous reports implicated p38 as a potential kinase that phosphorylates cyclin D3 at Thr-283 [122]. We assessed whether p38 affects cyclin D3 expression in CA46 Burkitt's lymphoma cells. Surprisingly, SB203580 (p38 inhibitor) did not significantly impact cyclin D3 (Appendix I). The GSK3β inhibitor SB216763 marginally increased cyclin D3 protein level and slightly reduced p-cyclin D3 (T283) (Appendix I). Given that D-type cyclins function during G1-S phase transition of the cell cycle, we next assessed the impact of p38 on cyclin D3 expression during G1-S phase. We confirmed that cells either with or without treatment of inhibitors entered S phase 15 h after release from G1 phase (Appendix I).

While SB216763 (GSK3β inhibitor) increased cyclin D1 expression in late G1 to S phase as we previously demonstrated [116], SB203580 and SB216763 had a marginal impact on cyclin D3 (Appendix I). The collective data suggest that the kinase that regulates cyclin D3 remains to be identified conclusively.

Chapter 3: Ubiquitylation of Unphosphorylated c-myc by Novel E3 Ligase SCF^{Fbxl8}

RESULTS

c-myc associates with Fbxl8 in vivo.

To identify Fbxl8 substrate targets, Flag-Tagged Fbxl8 was expressed in 293T cells; Flag-Fbxl8 was precipitated from lysates and co-precipitating proteins were identified by mass spectroscopy analysis to identify bound protein partners (Appendix J). Among numerous co-precipitating proteins, the presence of the oncogenic transcription factor, c-myc, was of particular interest. C-myc stability and activity are regulated by numerous E3 ligases and the possibility that Fbxl8 might contribute to the regulation of c-myc warranted further investigation.

We first confirmed binding c-myc-Fbxl8 binding following co-expression in U2OS cells (Fig 3.1A). We subsequently assessed binding of endogenous c-myc and Fbxl8. Endogenous Fbxl8 was precipitated from U2OS cells and the presence of c-myc was assessed by immunoblot. As a positive control, we assessed co-precipitation of cyclin D3 since we have already established cyclin D3 as a direct Fbxl8 substrate.[110] Both c-myc and cyclin D3 were detected in Fbxl8 precipitates (Fig 3.1B). To address binding specificity, we assessed the ability of c-myc to bind to a panel of Fbxl8 deletion mutants. Specific mutations of interest include c-terminal deletions that should impact Fbxl8 binding with substrates (ΔC1-3; Fig 3.1C). Flag-tagged wild-type and mutant Fbxl8 expressing vectors were expressed in U2OS cells; we also expressed Fbxw7 as a positive control versus Fbxo31 as a negative control. Flag-Fbxl8-ΔF, a catalytically deficient mutant lacking its F-box motif and therefore unable to bind with Skp1, was also overexpressed. Cells were treated with MG132 to inhibit degradation of c-myc prior to generating cell

lysates. Complexes were precipitated with Flag antibodies and co-precipitating, endogenous c-myc was assessed by immunoblot (Fig 3.1D). Binding of c-myc with Fbxw7 and wild type Fbxl8 was readily detected with no binding of c-myc with Fbxo31 (Fig 3.1C). Significant loss of c-myc-Fbxl8 association was observed with the Fbxl8-ΔC3 mutation demonstrating a c-myc binding domain within residues 255-374 of Fbxl8 (Fig 3.1D).

SCF^{Fbxl8} polyubiquitylates c-myc.

F-box proteins frequently function as substrate specific adaptors of the Skp-Cullin1 E3 ligase family. We hypothesized that Fbxl8 in association with the Skp-Cullin1 E3 ligase (SCF^{Fbxl8}) might direct c-myc polyubiquitylation. To test this, wild type Fbxl8, Fbxl8-ΔF (inactive mutant) and c-myc were overexpressed in U2OS cells along with His-tagged ubiquitin. Fbxw7 was used as a positive control for c-myc polyubiquitylation. Following transfection, cells were treated with MG132, and complexes were precipitated from cell lysates with antibodies directed to the His-tagged ubiquitin. We noted increased c-myc polyubiquitin chains in the presence of wild type Fbxl8 and reduced polyubiquitin chains with Fbxl8-ΔF (Fig 3.2A). To determine if polyubiquitylation was direct we purified SCF^{Fbxl8} or $SCF^{Fbxl8\Delta F}$ from Sf9 cells (Fig 3.2B). Recombinant, purified SCF^{Fbxl8} but not $SCF^{Fbxl8\Delta F}$ polyubiquitylated purified c-myc (Fig 3.2C) demonstrating that c-myc is a direct SCF^{Fbxl8} substrate.

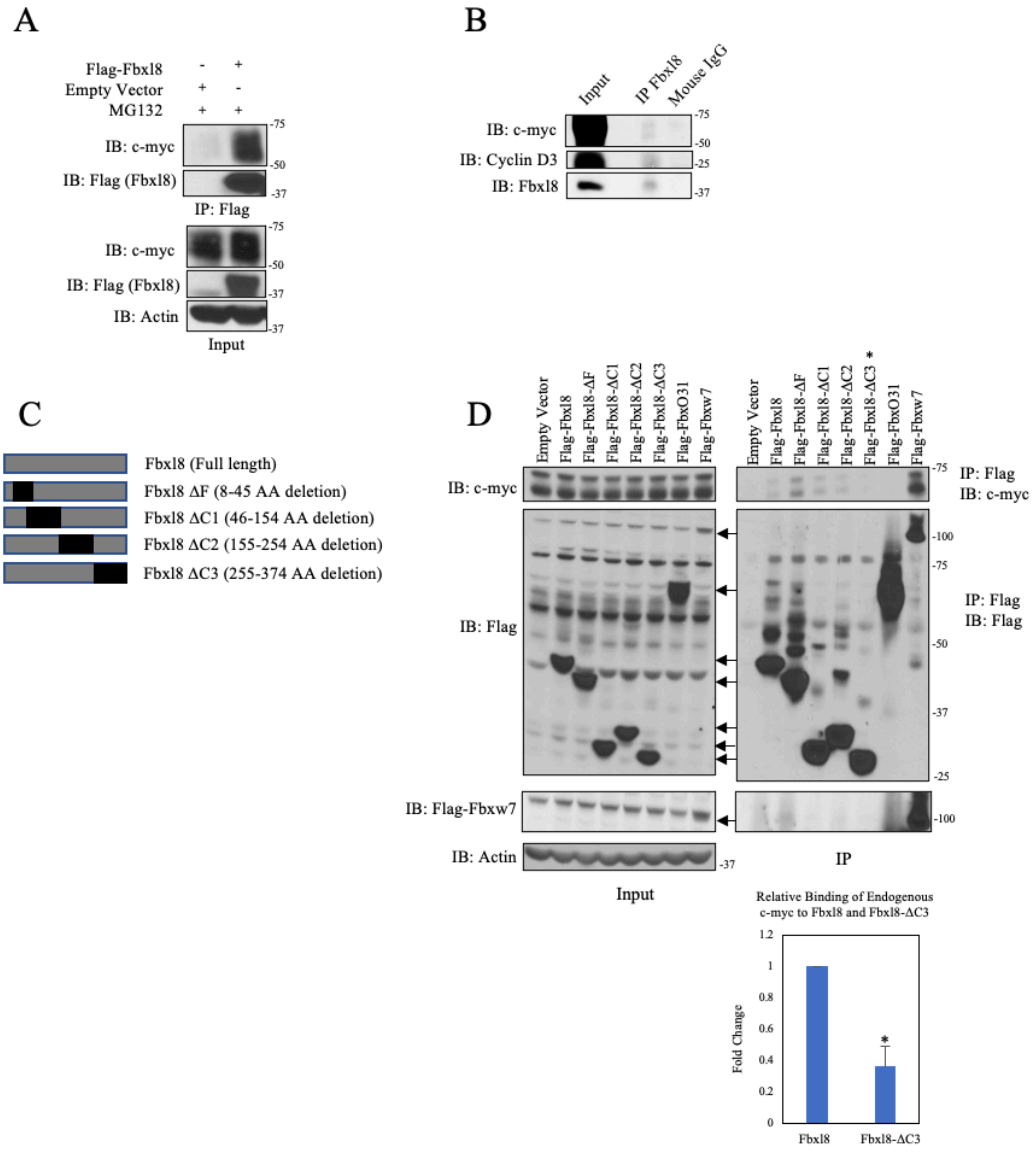

Figure 3.1: C-myc associates with Fbxl8 in vivo.

a. Lysates from U2OS cells transfected with an empty vector or Flag-Fbxl8 and treated with MG132 (10um) for 6 hours were immune precipitated with anti-Flag antibodies. Immune complexes were analyzed by western blot.

b. Lysates from U2OS cells were immune precipitated with anti-Fbxl8 antibody crosslinked to Protein A Sepharose beads. Immune complexes were analyzed for c-myc and Cyclin D3 by western blot.

c. Schematic model of deletion mutants of Flag tagged Fbxl8 construct.

d. Lysates from U2OS cells transfected with an empty vector, Flag-Fbxl8, deletion mutants, and treated with a proteasome inhibitor MG132 (10um) for 6 hours were immune precipitated with anti-Flag beads. Immune complexes were analyzed by western blot. Densitometric quantification of binding between endogenous c- myc and ectopic Fbxl8-ΔC3 relative to ectopic wildtype Fbxl8 control (Ratio Paired t-test, p-value < 0.05; N=3).

SCF^{Fbxl8} polyubiquitylates c-myc independent of phosphorylation at threonine 58 and serine 62

Canonical c-myc polyubiquitylation is catalyzed in an Fbxw7 dependent fashion (Grim J et al., 2008). Binding of Fbxw7 with c-myc is dependent upon phosphorylation of serine 62 (S62) and threonine 58 (T58) residues by Erk1/2 and GSK3β. [13] C-myc is stabilized upon phosphorylation of S62 by ERK.[10] [11] However, phosphorylation of S62 serves as a priming event for the subsequent phosphorylation of the T58 residue by GSK3β[12] after which the S62 residue is then dephosphorylated by PP2A. [15]
Threonine 58 phosphorylated c-myc is recognized by SCF^{Fbxw7}, polyubiquitylated, and degraded by the 26S proteasome. [13, 14] It is currently unknown if Fbxl8 and Fbxw7 compete for shared c-myc populations and if Fbxl8 has other substrates aside from cyclin D3.

To evaluate the potential role of SCF^{Fbxl8} in c-myc metabolism, we first assessed whether Fbxl8-c-myc binding was regulated by T58/S62 phosphorylation. We compared binding of Fbxl8 with V5 tagged wild type c-myc versus either c-mycT58A or c-mycS62A. We also evaluated binding of Fbxw7 with c-myc mutants as a control. Complexes were precipitated from U2OS cells expressing relevant expression plasmids. Complexes were collected by precipitation with antibody directed to the V5 tag and followed by western blot analysis. As previously published, Fbxw7 binding to c-myc was abolished by mutation of either S62 or T58 (Fig 3.3A). Strikingly, Fbxl8 associated with c-myc independent of S62 or T58 (Fig 3.3A) suggesting Fbxl8 might regulate c-myc in a phosphorylation independent fashion.

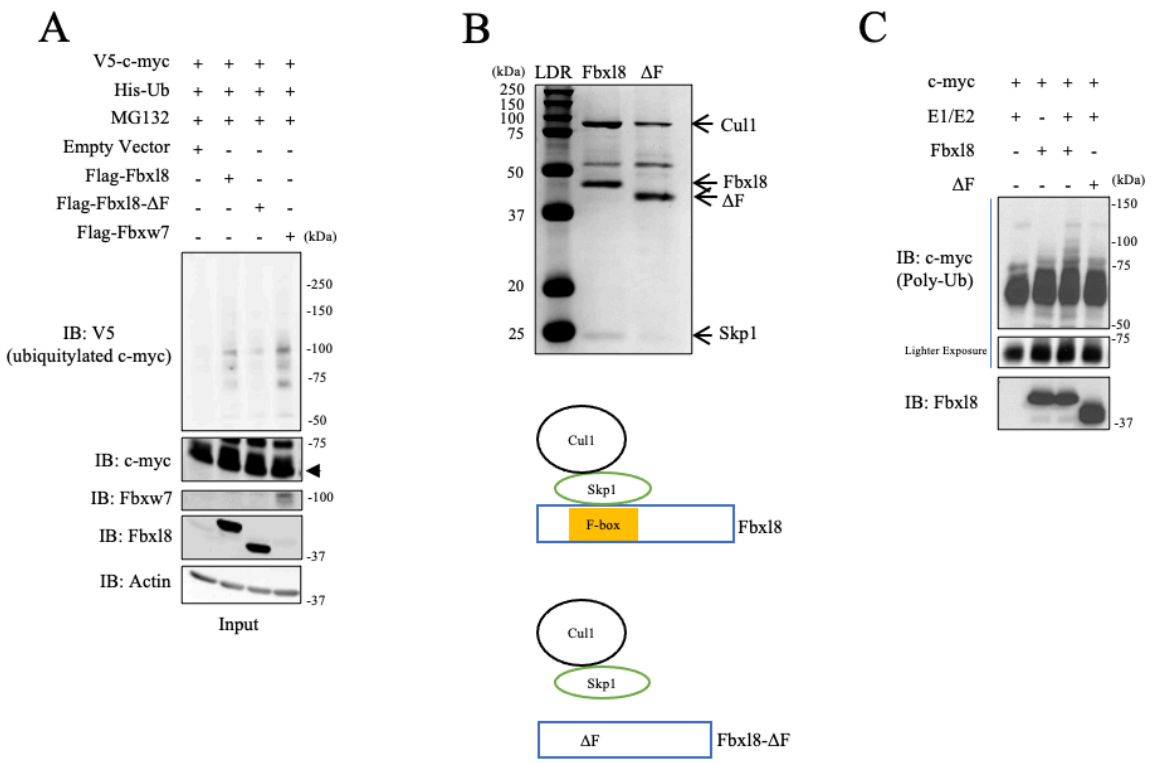

Figure 3.2: C-myc is a SCF^{Fbxl8} substrate.
a. Lysates from U2OS cells co-transfected with His-Ub, pBABE-c-myc, and either Fbxl8, Fbxl8-F, Fbxw7 or Empty Vector were treated with MG132 (20um) for 6 hours prior to immune precipitation with anti-His beads. Immune complexes were analyzed by western blot for ubiquitinated c-myc (anti c-myc), F-box proteins (anti-Flag), and β-actin was a loading control.
b. Coomassie stain verifying purified SCF (Skp1-Cul1-F-box) complexes from SF9 cells for Fbxl8 and Fbxl8-ΔF.
c. In vitro ubiquitylation assay was performed in reaction mixtures containing the presence or absence of indicated mixture components. Lysates from assays were analyzed by western blot using antibodies against indicated proteins.

To further evaluate the role of c-myc phosphorylation in the context of regulation by Fbxl8, we next determined the contribution of T58 and S62 for polyubiquitylation by SCF^{Fbxl8} both in vivo and in vitro. We evaluated c-myc versus c-mycT58A or c-mycS62A polyubiquitylation by either Fbxw7 or Fbxl8 in U2OS cells. While Fbxw7, as previous published, efficiently promoted wild type c-myc polyubiquitylation, and failed to trigger ubiquitylation of either c-mycT58A or c-mycS62A (Fig 3.3B). In contrast, Fbxl8 expression efficiently promoted polyubiquitylation of both wild type and mutant c-myc (Fig 3.3C). Analogous with the in vivo analysis, purified SCF^{Fbxl8} polyubiquitylated c-myc independent of S62 and T58 (Fig 3.3D) demonstrating that SCF^{Fbxl8} catalyzes c-myc ubiquitylation independent of canonical phosphorylation sites. This observation was further complemented with Fbxl8 overexpression reducing protein levels of overexpressed c-myc-T58A and c-myc-S62A (Fig 3.3E)

Fbxl8 regulates c-myc accumulation in a 26S Proteasome-Dependent Manner.

Because ubiquitylation frequently regulates protein degradation, we assessed the impact of Fbxl8 on c-myc accumulation. HEK293T cells were transfected with either V5 tagged c-myc and Fbxl8 c-myc levels were followed by western blot. Expression Fbxl8 significantly reduced levels of c-myc (Fig 3.4A). We subsequently evaluated the impact of expression of wild type Fbxl8 versus Fbxl8-ΔF on endogenous c-myc. Expression of wild type Fbxl8 reduced c-myc levels in a 26S proteasome dependent manner (Fig 3.4B). To determine if differential accumulation of c-myc reflects protein degradation, we measured c-myc half-life following Fbxl8 knockdown in both human U2OS cells and in murine

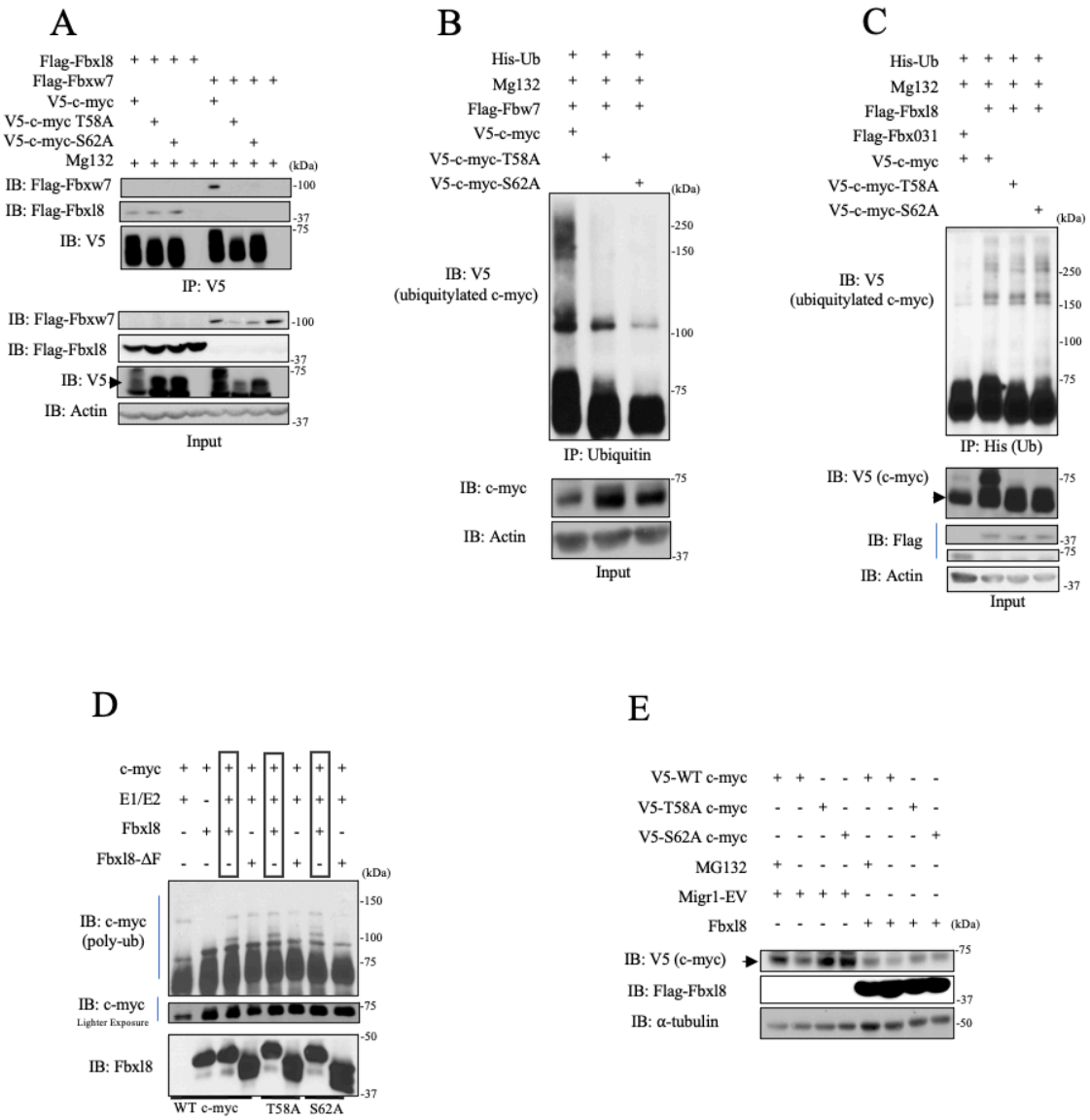

Figure 3.3 SCF^{Fbxl8} polyubiquitylates c-myc independent of phosphorylation at threonine 58 and serine 62

a. Lysates from U2OS cells transfected with either Flag-Fbxl8, Flag-Fbxw7 along with c-myc and c-myc phosphomutants and treated with MG132 (20 um) for 6 hours were immune precipitated with anti-V5 beads. Immune complexes were analyzed by western blot.

b. Lysates from U2OS cells co transfected with His-Ub, His-V5-c-myc WT, T58A or S62A, and either Fbxl8 or Empty Vector were treated with MG132 (20um) for 6 hours prior to immunoprecipitation with anti-His beads. Immune complexes were analyzed by western blot for ubiquitinated c-myc and c-myc phospho-mutants (anti-V5), F-box proteins (anti-Flag), and β-actin as a loading control.

c. Lysates from U2OS cells co transfected with His-Ub, His-V5-c-myc WT, T58A or S62A, and Fbxw7 were treated with MG132 (20um) for 6 hours prior to immunoprecipitation of ubiquitin with TUBEs (Tandem Ubiquitin Binding Entities). Immune complexes were analyzed by western blot for ubiquitinated c-myc and c-myc phospho-mutants (anti-V5) and β-actin as a loading control.

d. In vitro ubiquitylation assay was performed in reaction mixtures containing the presence or absence of indicated mixture components. Lysates from assays were analyzed by western blot using antibodies against indicated proteins.

fibroblasts. As expected, Fbxl8 knockdown significantly extended the half-life of c-myc in both cell types (Fig 3.4C).

We next addressed the relative contribution of Fbxl8 and Fbxw7 to c-myc accumulation. Initially, we tested 3 independent shRNA targeting Fbxl8 relative to knockdown of Fbxw7 and noted similar accumulation of c-myc under all knockdown conditions (Fig 3.4D). Because Fbxw7 and Fbxl8 target different populations of c-myc (phosphorylated versus unphosphorylated), we hypothesized that concurrent knockdown of both would have an additive impact on c-myc accumulation. Indeed, knockdown of both Fbxl8 and Fbxw7 significantly increased c-myc levels above that observed with knockdown of either individual F-box protein (Fig 3.4E).

Fbxl8 knockout elevates c-myc and Accelerates G1/S Phase Transition.

C-myc is an immediate early gene and c-myc accumulation is necessary for cell cycle progression. Overexpression of c-myc can accelerate cell division primarily during the G1 to S-phase interval. We obtained conditional knock out mice generated by Cyagen wherein exon 3 (which encodes the F-box domain) of the Fbxl8 gene is flanked by LoxP sequences (Fig 3.5A). A detailed description of the phenotype of Fbxl8 knockout mice will be provided subsequently. For the current work, we generated murine embryonic fibroblasts (MEFs) from mouse embryos homozygous for floxed Fbxl8 alleles ($Fbxl8^{f/f}$). MEFs were infected with control retrovirus or retrovirus encoding Cre recombinase after which we assess levels of Fbxl8 and c-myc. Expression of Cre reduced Fbxl8 levels below detection levels and triggered elevation of c-myc protein (Fig 3.5A). To address the impact of Fbxl8 knockout on cell cycle progression, $Fbxl8^{f/f}$ and $Fbxl8^{-/-}$ MDFs were arrested in G0/G1 via serum starvation and contact inhibition. Cell cycle reentry was analyzed at 0-24

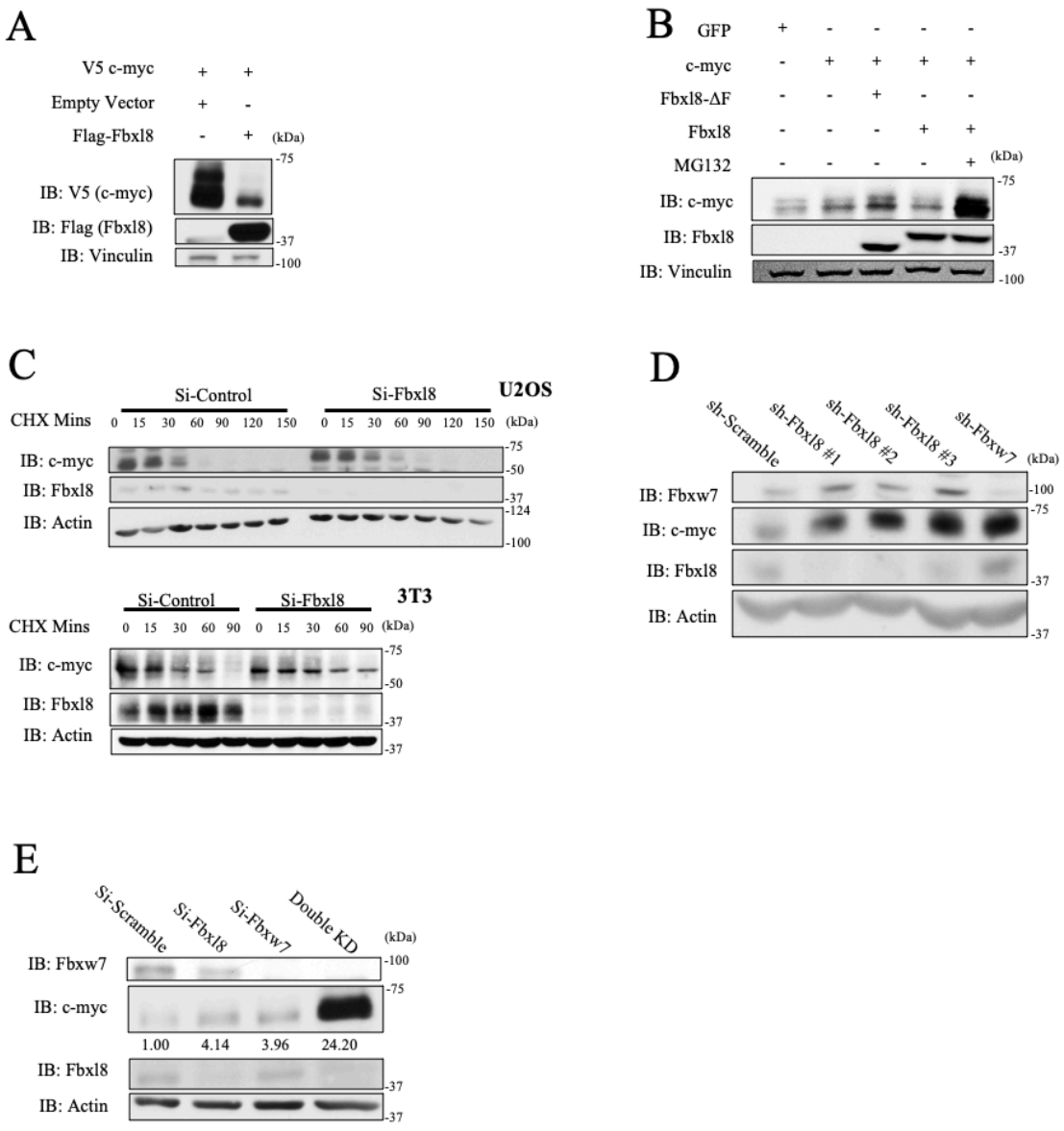

Figure 3.4 Fbxl8 regulates c-myc accumulation in a proteasome dependent manner
a. Lysates from 293T cells were transfected with either an empty vector or Fbxl8, along with wildtype c-myc. Exogenous c-myc levels were analyzed via western blot along with Fbxl8 and Vinculin.
b. Lysates from 293T cells transfected with either GFP or c-myc along with Fbxl8 or Fbxl8-ΔF were analyzed via western blot.
c. Lysates from 3T3 and U2OS treated with either si-Control or si-Fbxl8 and cycloheximide 100μg/mL over indicated time periods and analyzed via western blot for endogenous c-myc, Fbxl8, and Vinculin.
d. Lysates from U2OS cells infected with either scramble shRNA, sh-Fbxl8, or sh-Fbxw7. endogenous c-myc, Fbxl8, and β-actin were analyzed via western blot.
e. Lysates from U2OS cells treated with si-Scramble si-Fbxl8, or si Fbxw7 for 3 days and analyzed by western blot for endogenous c-myc, Fbxl8, Fbxw7, and β-actin.

hours following mitogenic stimulation (Fig. 3.5B-C). As expected, Fbxl8-/- MEFs exhibited an accelerated G1 to S phase transition along with higher c-myc protein levels (Fig 3.5D). Inhibition of c-myc in Fbxl8-/- cells vastly reduced G1/S phase transition (Appendix M), substantiating evidence that Fbxl8's activity on the cell cycle is additionally mediated through c-myc protein levels.

Reduced Fbxl8 levels correlate with poor survival in cancer patients.

Given that Fbxl8 negatively regulates two oncogenes, cyclin D3[110] and c-myc, we hypothesized that Fbxl8 levels might be reduced in certain cancers. We therefore assessed Fbxl8 levels in the TCGA data base. While we did not observe a high frequency of recurrent mutations in Fbxl8, we noted that expression of Fbxl8 was significantly reduced in several cancers (Fig 3.6A). C-myc is frequently overexpressed in Diffuse Large B-cell Lymphoma (DLBCL) (Fig 3.6B) while cyclin D3 is often mutated or overexpressed in Uterine Corpus Endometrial Carcinoma (UCEC) subtypes (Fig 3.6C). We therefore assessed patient survival versus Fbxl8 levels in these two cancer types. Indeed, reduced Fbxl8 levels correlated with poor patient prognosis (Fig 3.6D-E). While correlative, this is consistent with the role of Fbxl8 as an antagonist of key tumor drivers and suggests that its loss may in fact contribute to tumor progression.

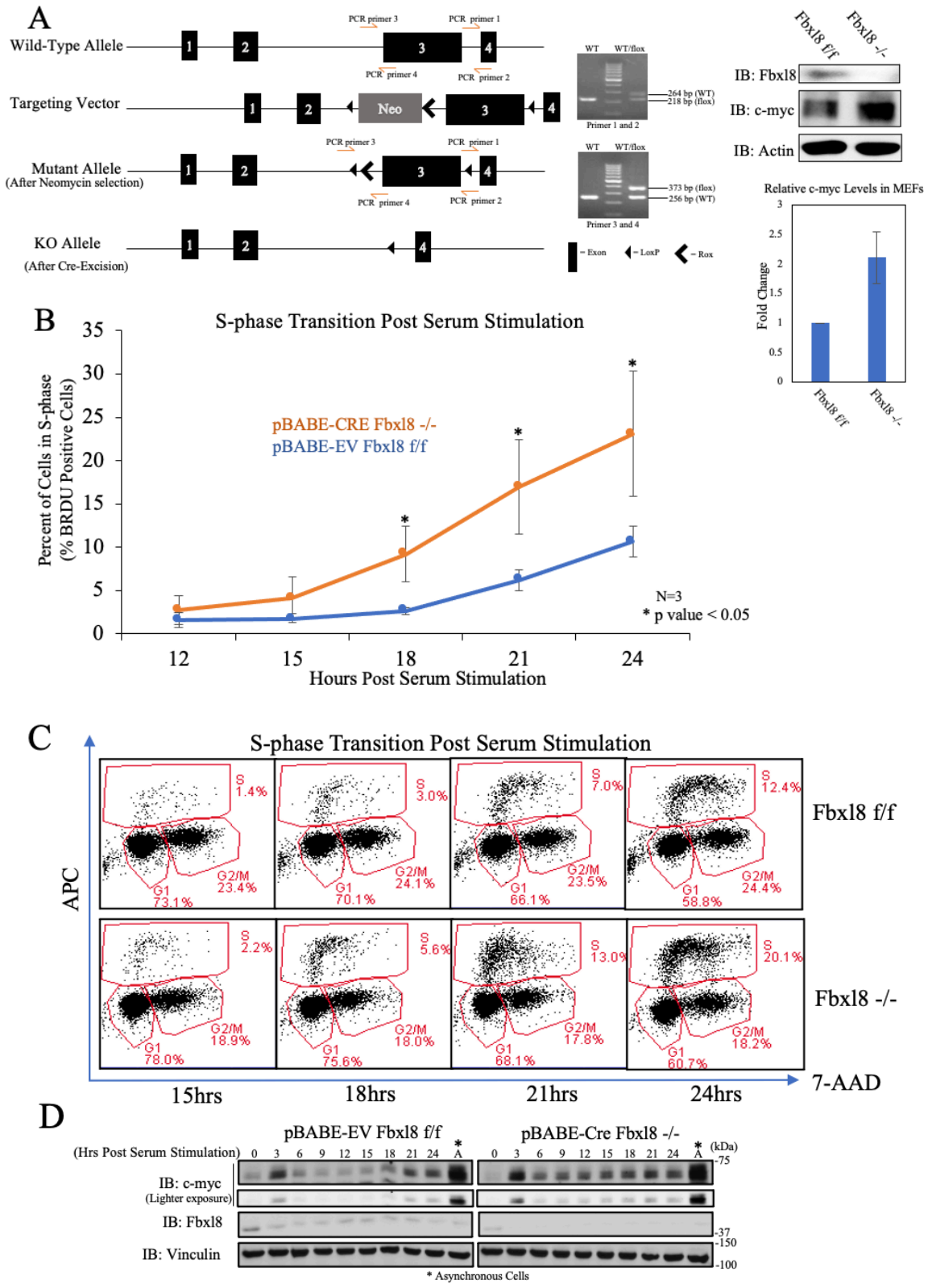
A
Wild-Type Allele
Targeting Vector
Neo
Mutant Allele
(After Neomycin selection)
KO Allele
(After Cre-Excision)
PCR primer 1
PCR primer 2
PCR primer 3
PCR primer 4
WT
WT/flox
264 bp (WT)
218 bp (flox)
Primer 1 and 2
373 bp (flox)
256 bp (WT)
Primer 3 and 4
Exon
LoxP
Rox
Fbxl8 f/f
Fbxl8 -/-
IB: Fbxl8
IB: c-myc
IB: Actin
Relative c-myc Levels in MEFs
Fold Change
B
S-phase Transition Post Serum Stimulation
Percent of Cells in S-phase
(% BRDU Positive Cells)
pBABE-CRE Fbxl8 -/-
pBABE-EV Fbxl8 f/f
N=3
* p value < 0.05
Hours Post Serum Stimulation
C
S-phase Transition Post Serum Stimulation
APC
7-AAD
Fbxl8 f/f
Fbxl8 -/-
S 1.4%
G2/M 23.4%
G1 73.1%
S 3.0%
G2/M 24.1%
G1 70.1%
S 7.0%
G2/M 23.5%
G1 66.1%
S 12.4%
G2/M 24.4%
G1 58.8%
S 2.2%
G2/M 18.9%
G1 78.0%
S 5.6%
G2/M 18.0%
G1 75.6%
S 13.0%
G2/M 17.8%
G1 68.1%
S 20.1%
G2/M 18.2%
G1 60.7%
15hrs
18hrs
21hrs
24hrs
D
pBABE-EV Fbxl8 f/f
pBABE-Cre Fbxl8 -/-
(Hrs Post Serum Stimulation)
0 3 6 9 12 15 18 21 24 A
(kDa)
IB: c-myc
(Lighter exposure)
IB: Fbxl8
IB: Vinculin
* Asynchronous Cells

Figure 3.5

Figure 3.5: Fbxl8 excision accelerates G1/S phase transition

a. Schematic for generation of conditional knockout Fbxl8 allele. Lysates from $Fbxl8^{f/f}$ and $Fbxl8^{-/-}$ MEFs were analyzed by western blot to determine Fbxl8 and c-myc protein levels after Fbxl8 ablation from the genome.

b. $Fbxl8^{f/f}$ and $Fbxl8^{-/-}$ murine embryonic fibroblasts arrested at G0/G1 by contact inhibition and serum starvation for 36 hours. S-phase entry was assessed by BRDU incorporation (30min) and FACS at 12, 15, 18, 21, and post release. Quantification of BRDU positive cells mean ± SD, $*p < 0.05$ (two-tailed Student's *t* test, $n = 3$).

c. Flow cytometry data of specified timepoints post serum stimulation.

d. Western analysis of lysates from (b) for c-myc, Fbxl8, and Vinculin.

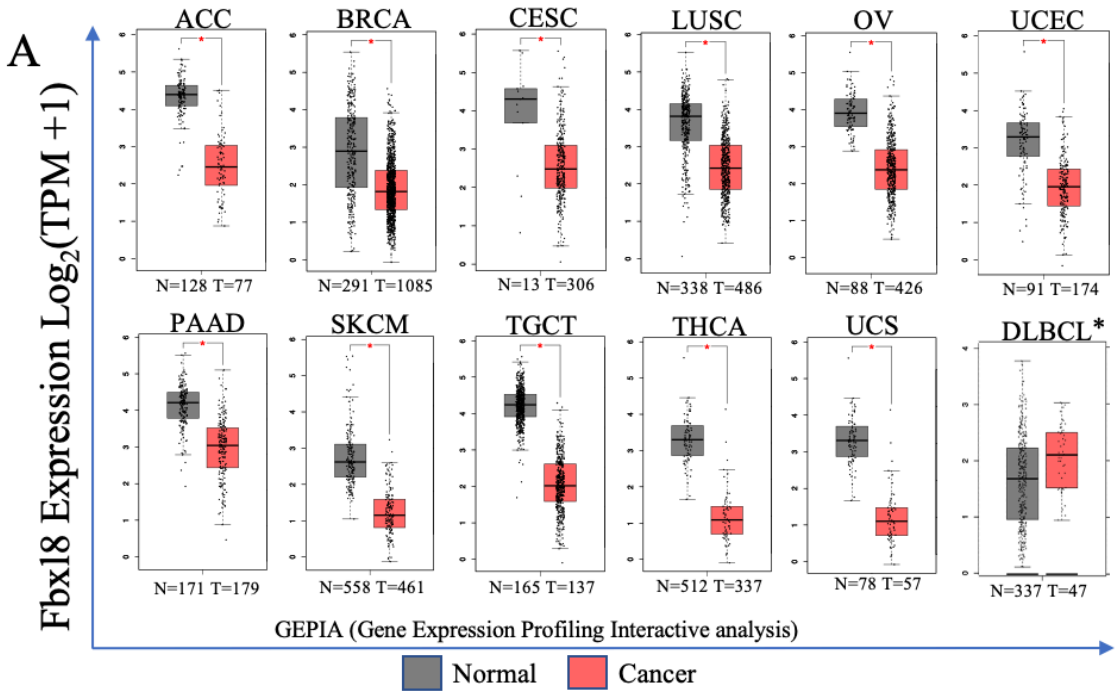

Cancers types with significantly reduced Fbxl8 Expression: ACC (Adenoid Cystic Carcinoma), BRCA (Breast Cancer), CESC (cervical squamous and endocervical adenocarcinoma), LUSC (Lung Squamous Carcinoma), OV (Ovarian Cancer), PAAD (Pancreatic adenocarcinoma), SKCM (Skin Cutaneous Melanoma), TCGT (Tenosynovial Giant Cell Tumor), THCA (Thyroid Cancer), UCS (Uterine Carcinoma), UCEC (Uterine Corpus Endometrial Carcinoma). *DLBCL (Diffuse Large B Cell Lymphoma) does not have significantly reduced Fbxl8 expression.

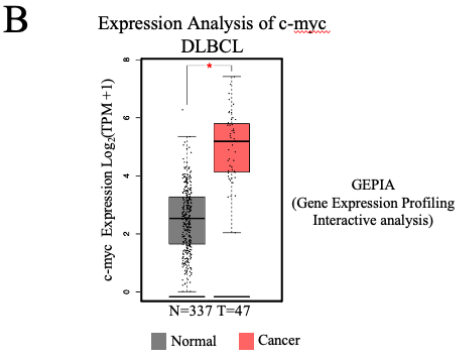

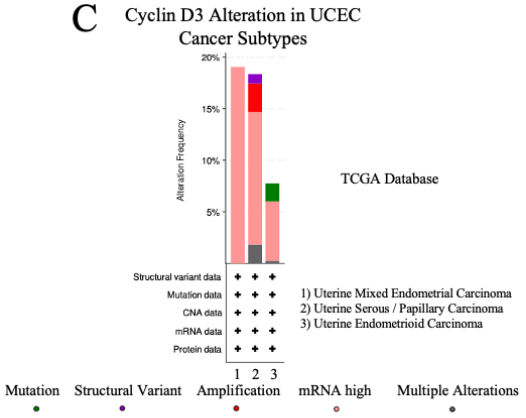

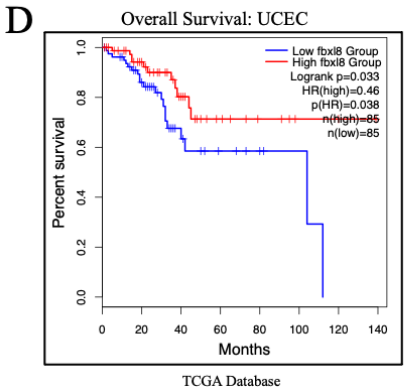

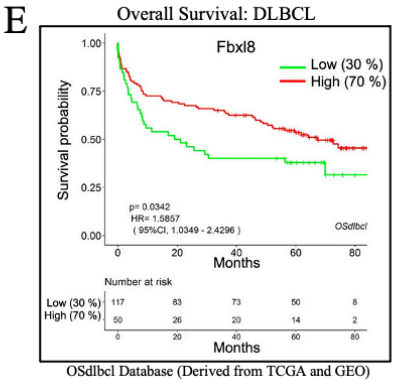

Figure 3.6

Figure 3.6: Reduced Fbxl8 levels correlate with poor survival in cancer patients
a. Fbxl8 expression analysis for various cancer types comparing normal versus tumor tissue in patients. Cancer types include ACC (Adenoid Cystic Carcinoma), BRCA (Breast Cancer), CESC (cervical squamous and endocervical adenocarcinoma), LUSC (Lung Squamous Carcinoma), OV (Ovarian Cancer), PAAD (Pancreatic adenocarcinoma), SKCM (Skin Cutaneous Melanoma), TCGT (Tenosynovial Giant Cell Tumor), THCA (Thyroid Cancer), UCS (Uterine Carcinoma), UCEC (Uterine Corpus Endometrial Carcinoma), and DLBCL (Diffuse Large B-cell Lymphoma).
b. C-myc expression analysis for DLBCL comparing normal versus tumor tissue in patients.
c. Alteration frequency of Cyclin D3 in uterine corpus endometrial carcinoma (UCEC).
d. Kaplan–Meier survival curve for overall survival in diffuse large B-cell lymphoma (DLBCL) patients with low and high expression of Fbxl8.
e. Kaplan–Meier survival curve for overall survival in uterine corpus endometrial carcinoma patients with low and high expression of Fbxl8.

Chapter 4: Discussion and Future Directions

Discussion

In this investigation c-myc and Cyclin D3 were identified as substrates of E3 ligase ubiquitin ligase Fbxl8. D-type cyclins function as mitogenic sensors that integrate growth factor signaling with cell division and proliferation. It is therefore of little surprise that all three D-type cyclins are dysregulated in human cancers. Cyclin D3 is overexpressed in specific human cancers and is subject to point mutations specifically in Burkitt's lymphoma [123]; the specific residue targeted, Thr-283 has been implicated in regulating cyclin D3 protein destruction [122]. Given the prevalence of D3 mutations in Burkitt's lymphoma, it is striking that little is known about post-translational modification of cyclin D3. We have therefore identified Fbxl8 as the specificity subunit of an SCF E3 ligase that specifically recognizes and polyubiquitylates Thr-283 phosphorylated cyclin D3 thereby triggering its proteasome-dependent degradation (Chapter 2 Fig. 7d). It is of importance to note that while SCF^{Fbxl8} neither binds nor regulates accumulation of cyclin D1, our data support a role for SCF^{Fbxl8} in regulating cyclin D2 indirectly. We were unable to observe the direct interaction of cyclin D2 and Fbxl8, and to reconstitute direct ubiquitylation of cyclin D2 with SCF^{Fbxl8} suggesting that while it can regulate cyclin D2 in vivo indirectly, there is either another ubiquitin-ligase that specifically regulates its degradation or a critical secondary specificity factor that specifies cyclin D2 is yet to be identified. Functional analyses using either knockdown of Fbxl8 or overexpression of wild type or mutant Fbxl8 demonstrated its role in regulating the G1-S phase transition. This result is consistent with its role as a negative regulator of cyclin D3 given that overexpression of either cyclin D accelerates the G1- S phase transition [113]. Importantly, cyclin D3T283A, a

nonphosphorylable mutant, rescued Fbxl8 overexpression mediated cell proliferation attenuation, indicating that Fbxl8-cyclin D3 axis plays a critical role in regulating lymphoma cell proliferation. However, cyclin D3T283A mutant partially rescued Fbxl8 induced hematopoietic cell growth inhibition (Chapter 2 Fig. 5g). This suggests that Fbxl8 may have other substrates that promote hematopoietic transformation. While SCF-Fbxl2 has been implicated as a potential regulator of cyclin D3, regulation by Fbxl2 is independent of cyclin phosphorylation [124, 125]. More importantly, inactivation of Fbxl2 results in a mitotic defect suggesting its predominant substrate functions during mitosis, independent of either cyclin D3 or D2 although we observed the binding of Fbxl2 and cyclin D3 (Yoshida et al, Appendix A). Fbxl8 overexpression dramatically suppressed oncogene induced transformation in vitro and lymphoma progression in vivo. Consistently, we found that cyclin D3 expression is negatively correlated with Fbxl8 expression in human lymphomas and low level of Fbxl8 correlates poor overall survival for lymphoma patients, supporting our conclusion that Fbxl8-cyclin D3 axis has a critical role in regulating cell cycle and tumorigenesis. CDK4/6 inhibitors are being used for many clinical trials and the efficacy has been assessed in many types of cancers where cyclin D1 is overexpressed [126, 127]. Our data demonstrate that cyclin D3T283A accumulates in the nucleus and promotes oncogene-induced tumorigenesis in hematopoietic cells, reflecting increased CDK activity. Indeed, Rb is highly phosphorylated by knockdown of Fbxl8. Importantly, cells harboring either a D3T283A allele or overexpressing WT D3 were more responsive to palbociclib treatment than parental cells. This supports the notion that Fbxl8-cyclin D3 axis might be a potential novel biomarker to predict the efficacy of CDK4/6i in lymphomas.

In summary, Fbxl8 regulates cell cycle progression and lymphoma cell proliferation through cyclin D3. Thus, either loss of Fbxl8 or gain of a cyclin D3 mutation that stabilizes cyclin D3 protein level will accelerate cell cycle progression and lymphoma cell growth consistent Fbxl8 functioning as a tumor suppressor (Chapter 2 Fig. 7d).

C-myc is a potent oncoprotein and overexpression of wild type c-myc triggers cancer in model systems [21] and this occurs in many human cancers [18] where it is considered a driver oncogene. Given the predominant pro-tumor function of c-myc, it is not surprising that c-myc functions as an integrative convergence for extracellular stimuli and as a master regulator of many downstream cellular responses and pathways. Regulation of c-myc occurs at multiple levels including transcription, translation and protein degradation.[128] The c-myc protein is highly labile and a common feature of labile regulators of cell growth and survival is ubiquitin-dependent post-translational regulation. While c-myc ubiquitylation can be catalyzed by several E3 ligases including Skp2 [62], HUWE1 [65], and Fbxw7 [129], where Fbxw7 is the primary regulator of c-myc ubiquitin-dependent degradation. In addition, c-myc degradation is most closely associated with phosphorylation of key residues; phosphorylation of such residues generates a phospho-degron recognized by downstream E3 ligases. However, this begs the question of whether and how is unphosphorylated c-myc degraded. We have found that Fbxl8 functions to recognize unmodified c-myc and thereby regulate underphosphorylated pools of c-myc. Fbxl8 binds directly to unphosphorylated c-myc and coordinates polyubiquitylation of unphosphorylated c-myc in vitro and in vivo. Loss of Fbxl8 promotes c-myc overexpression and accelerates G1 phase progression. Finally, concurrent loss of Fbxl8 and Fbxw7 have an additive impact on c-myc levels consistent with them targeting distinct

population of c-myc for degradation. Our results suggest that Fbxw7 and Fbxl8 work in concert to maintain homeostatic c-myc levels.

Canonical c-myc degradation is dictated by ERK and GSK3β kinases that sequentially phosphorylate c-myc at T58 and S62 residues. Mutation of either residue inhibits Fbxw7 binding and stabilizes c-myc resulting in a dramatic increase in transcription of downstream target genes. This increase in pro-proliferative c-myc targets is clearly a driver of cancer as genetic inactivation of c-myc [130] or use of Brd4 inhibitors [131] which also reduce c-myc levels have significant anti-tumor activities.

While c-myc is clearly a tumor promoter, too much uncontrolled c-myc can be toxic. There are a variety of potential c-myc activities that when unchecked can trigger cell death including disruption of DNA replication origin priming [132] DNA damage [133] and proteotoxicity [134]. Proteotoxicity is reflected in c-myc's function to regulate ribosome levels and overall rates of protein synthesis via its activity in polymerase I transcription [135] and recruitment of polymerase II [35] . Elegant work has revealed that protein translation checkpoints that limit protein translation rates are essential for the survival of c-myc overexpressing tumor cells [136]. This highlights the importance of maintaining a critical threshold of c-myc protein in both normal and tumor cells for overall survival. Our data demonstrating regulation of unphosphorylated c-myc and phospho-c-myc by distinct E3 ligase pathways highlights new depth and importance to the context of c-myc turnover. The role of Fbxl8 in tumors with inactive Fbxw7 requires further investigation to ascertain the relative importance of the SCF^{Fbxl8} ligase in this context and whether there are therapeutic opportunities.

Future Directions

There are still many unanswered questions surrounding Fbxl8 and c-myc. The first question deals with the specific lysine linkages being tagged onto c-myc. We see that in vitro ubiquitination of c-myc by Fbxl8 occurs with both K48 and K63 linkages (Appendix N). This is not expected as traditionally only the K48 linkages are associated with degradation. Recent studies have confirmed however that K48 and K63 heterotypic linkages can enhance degradation of a targeted substrate; This warrants further investigation via in vivo ubiquitin assays to see if these in vitro findings can be recapitulated. Overall, however the fact that Fbxl8's heterotypic polyubiquitin chains differ from those of Fbxw7 (K48 only) drives the question of what the function of these heterotypic chains are outside of canonical protein degradation signaling. This can more properly be assessed through observing the status of c-myc target genes when either Fbxl8 or Fbxw7 is knocked down or overexpressed. These findings would help bridge the link between the different ubiquitin linkages and broader c-myc transcriptional programs.

The second aspect of Fbxl8 activity that needs elucidation, is the existence of other essential post translational modifications on c-myc. In this investigation is c-myc degradation occurred independent of canonical T58 and S62 phosphorylation status. However, the dependence of Fbxl8 activity on total phosphorylation status of c-myc has yet to be assessed. New literature suggests the existence of a new degron (T244) on c-myc responsible for Fbxw7 mediated degradation [8]. This now calls into question if c-myc's T244 degron is relevant to Fbxl8 function. Outside of phosphorylation status it is also unknown if other post translational modifications (i.e., acetylation, SUMOylation, glycosylation) on c-myc are crucial for Fbxl8 activity.

The next aspect of Fbxl8 activity worthy of addressing deals with its localization. Canonical c-myc degradation is localized in the nucleus by Fbxw7 alpha. However, we showed Fbxl8 is exclusively cytoplasmic and that knocking it out promotes accumulation of nuclear c-myc (Appendix O). It is well known that blocking the proteasome causes nuclear c-myc accumulation; it is also known that c-myc does indeed shuttle between the nucleus and cytoplasm [137]. The fact that Fbxl8 is localized in a compartment outside of where canonical c-myc degradation takes place further substantiates Fbxl8 and Fbxw7 actions on a distinct c-myc populations. However, is this c-myc population exported population from the nucleus? Or is it newly synthesized c-myc being trafficked to the nucleus. These questions are important to understanding the reason for having cytoplasmic E3 ligase that negatively downregulates c-myc. The only documented cytoplasmic metabolism of c-myc is in the context of calpain dependent protein digestion. This results in the production of the "myc-nick" which is in fact a cleaved c-myc protein lacking its nuclear localization signal. This truncated isoform has been implicated in microtubule assembly and muscle cell differentiation. There is still however no study that identifies c-myc as a substrate for degradation in a cytoplasmic compartment. Fbxl8's exclusive localization to the cytoplasm warrants further investigation into where Fbxl8 activity is taking place and on which pool of c-myc is being acted on. Use of nuclear transport inhibitors and immune fluorescence can be employed help in this part of the investigation. This is also important when considering that knocking out both F-box proteins results in a seemingly synergistic incease in c-myc protein levels. This suggests the activation of a pathway independent of proteasomal degradation but still related to these F-box proteins functional roles. Levels of c-myc transcription were unchanged when Fbxl8 however

translation was not assessed. Fbxl8 may very well regulate c-myc translation elements that exhibit crosstalk with Fbxw7 activity, resulting in such a significant increase in c-myc protein levels.

We are already aware of regulator proteins that oppose Fbxw7 activity. β-TrCP ubiquitylation of c-myc stabilizes c-myc and in turn prevents its degradation in the latter part of S-phase. USP28 directly counteracts Fbxw7 by directly deubiquitylating c-myc. These two opposing elements to Fbxw7, give a holistic picture behind the regulation of canonical c-myc degradation. However, it is still unknown if there are any proteins or E3 ligases that directly or indirectly antagonize Fbxl8 function; it is also unknown if Fbxw7 competes with Fbxl8 for c-myc substrate. In vitro affinity assays and in vivo co immune precipitation experiments could give insight into this query.

Further exploration in the activity of Fbxl8 in other phases of the cell cycle is also warranted. In this study c-myc protein levels increase significantly during the G1/S phase transition when Fbxl8 is excised knocked out. This increase in c-myc corresponds to an accelerated cell cycle progression as well. However, the G1/S phase is not the only phase where c-myc is relevant and Fbxl8 is expressed ubiquitously throughout the cell cycle. New studies show that a population of unphosphorylated c-myc bound to microtubules during mitosis contributes to chemotherapeutic resistance [138]. Understanding Fbxl8's activity in this phase of the cell cycle along with others is imperative given its ability to ubiquitylate unphosphorylated and phosphorylated c-myc.

Characterization of c-myc transcriptional activity is largely uncharacterized in the context of Fbxl8 regulation. To better understand other cellular programs being activated on the Fbxl8 axis; RNA-seq should be done in $Fbxl8^{f/f}$ and $Fbxl8^{-/-}$ cells specifically re-

entering G1/S, since this is where the difference in c-myc levels was the most pronounced. This would uncover the transcriptional program dictated by the Fbxl8-c-Myc axis of regulation and further elucidate the role of Fbxl8 in the context of cell cycle re-entry.

Analysis of Fbxl8 in the context of Fbxw7 loss is also worthy of investigation. Being that both F-box proteins share c-myc as a substrate, and that Fbxw7 is mutated in 31% of all human cancers, it provokes the question if Fbxl8 could have any compensatory response when Fbxw7 is inactive and if Fbxl8 upregulation in this context could impact c-myc levels. Jurkat, CEM and HSB-2 cell lines would be the first place to start as these lymphoma cells lines express high levels of c-myc and have mutated Fbxw7. Fbxl8 is additionally mutated in Jurkat cells while Loucy cells have an Fbxl8 mutation with no Fbxw7 mutation. Observing c-myc levels and overall biological phenotypes upon manipulation of Fbxl8 and Fbxw7 these cell lines with would give insight into Fbxl8 function in a T cell lymphoma context.

Assessment of in vivo consequences of Fbxl8 excision must also be assessed. This is currently being done with a conditional knockout mouse model. This mouse model consists of a single Cre-recombinase allele and two floxed Fbxl8 alleles. It is also unknown if Fbxl8 excision has any developmental consequences if excised in utero. Understanding this would give key insights into Fbxl8's biological and physiological role. Current cohorts of mice are now being monitored pathological abnormalities and malignant transformation. It's currently unknown if these mice can spontaneously develop tumors or if they will only do so in conjunction more rapidly with an oncogenic driver, such as Eμ-*Myc or* Kras. Affected tissues with a consistent and discernible phenotype will be analyzed at the transcriptional level and protein level for all known Fbxl8 substrates with an additional

focus around c-myc driven transcriptional programs and downstream signaling pathways. Once a clear tumor phenotype is characterized methods to reintroduce Fbxl8 pharmacologically (or treatment with an Fbxl8 agonist) should be employed to assess Fbxl8's tumor suppressive and therapeutic potential.

Methods to pharmacologically augment Fbxl8 activity should also be thoroughly explored, especially since Fbxl8 is now shown to operate on unphosphorylated c-myc populations where Fbxw7 cannot operate. This starts with understanding Fbxl8's binding to c-myc at a pharmacokinetic level. The first step is to compile a series of crystal structure and NMR data sets of Fbxl8 associating with the SCF complex along with SCF^{Fbxl8} associating with the c-myc substrate of various phosphorylation statuses. This approach will allow us to determine if Fbxl8 operates in a dimeric fashion or a single unit in the context of each version of phosphorylated c-myc. If the function is dimeric then the pharmacokinetic studies can be applied to augmenting Fbxl8 dimerization activity. If dimerization is not required than kinetic studies can be more directed to augmenting Fbxl8 binding and ubiquitylation activity on c-myc. Once this crucial structural data is compiled large scale pharmacological screens can be conducted. This structural data will also help assess the existence of various binding pockets or domains that can be stabilized and/or augment Fbxl8 binding affinity with c-myc.

From these large-scale pharmacological screens, a shortlist of Fbxl8 candidate agonists should be tested in immortalized Fbxl8 f/f MEFs to confirm if colony formation and malignant transformation is reduced in the presence of the Fbxl8 agonist. The Fbxl8 knockout MEFs would operate as the negative control in this experiment and would also help resolve any non-specific effects of the agonists. The agonists that prove successful

could then be tested on cancer cell lines with high c-myc protein levels and/or with mutated Fbxw7. Parameters like proliferation rate, apoptosis, viability, and transformation potential can all be assessed to determine if the Fbxl8 agonist has any potency in a malignant setting and in an Fbxw7 deficient setting. In tandem, Kras V12D and Eμ-Myc models with and without Fbxl8 alleles can be treated with Fbxl8 agonists to assess its effect on tumor growth and tumor progression in a living organism.

Any candidate Fbxl8 pharmacological agonist should then be tested in the context of tumors which high levels of c-myc and cyclin D3 levels. We currently do not know if Fbxl8 has a preference between these two substrates. Cyclin D3 is a c-myc target gene and understanding on which substrate Fbxl8 has a stronger affinity would be instrumental into understanding the mechanism behind any observable phenotype caused by treatment with an Fbxl8 phenotypic agonist.

Looking at Fbxl8 in a broader context, there is still little known about the existence of other substrate targets. Many F-box proteins have redundant substrates along with compensatory functions. This over the years have has made scientists aware of the larger F-box interactome and its many unknown pathways that may or may not play crucial roles in a tumorigenic context. A deep understanding of the F-box interactome and its relationship with c-myc degradation will help better resolve Fbxl8's more unique role as c-myc regulator. Being that c-myc is a promiscuous transcription factor, and a convergence point for many cellular signals and has a plethora of down-stream targets, it is imperative that we uncover of all Fbxl8's other substrate targets.

Chapter 5 Materials and Methods

Cell culture, transfection, infection, cell cycle analyses and CRISPR-Cas9 knockout

NIH3T3 and 293T cells were cultured in Dulbecco's modified Eagle's medium (DMEM) supplemented with 10% fetal bovine serum (FBS), 100 units/ml of penicillin, and 100 mg/ml of streptomycin (Corning). U2OS cells were cultured in McCoy's 5A medium supplemented with 10% fetal bovine serum (FBS), 100 units/ml of penicillin, and 100 mg/ml of streptomycin (Corning). For transfection, expression plasmids were transfected into cells with lipofectamine (ThermoFisher Scientific) or PolyJet (SignaGen Laboratories) reagents according to the manufacturer's instructions. For siRNA transfection, siRNA was introduced into cells with Lipofectamine RNAiMAX (ThermoFisher Scientific) according to the manufacturer's instructions. siRNA for control and Fbxl8 (SMARTpool: siGENOME Fbxl8 siRNA) were purchased from Dharmacon. For viral production, viral expression plasmids and packaging plasmids were co-transfected into 293T cells with lipofectamine (ThermoFisher Scientific). Virus supernatants harvested 48–72 h after transfection were used to infect cells with polybrene (10 μg/mL). See supplementary material for cell cycle analyses and CRISPR-Cas9 knockout.

Western analyses and Mass spectrometry analyses

In Chapter 2 cells were lysed in EBC buffer (50 mM Tris pH 8.0, 120 mM NaCl, 1 mM EDTA, 0.5% NP40) containing 1 mM phenylmethylsulfonyl fluoride, 20 U/ml aprotinin, 1 μM leupeptin, 1 mM dithiothreitol, 0.1 mM NaF, 0.1 mM Sodium orthovanadate, and 10 mM β-glycerophosphate. Proteins were resolved by SDS-PAGE,

transferred to membrane, and immunoblotted with the indicated antibodies. See supplementary material for information of antibodies. Membranes were incubated with horseradish peroxidase-conjugated anti-mouse or rabbit antibodies and signals were developed with the ECL system (PerkinElmer) according to the manufacturer's instructions. See supplementary material for mass spectrometry analysis. 293T expressing Flag-Tagged Fbxl8 (wildtype) or Flag-Tagged Fbxl8ΔF (mutant) cells were harvested and subsequently lysed in Tween 20 lysis buffer (50 mM HEPES (pH 8.0), 150 mM NaCl, 2.5 mM EGTA, 1 mM EDTA, 0.1% Tween 20) with protease and phosphatase inhibitors (1 mM PMSF, 20 U/ml aprotinin, 5 mg/ml leupeptin, 1 mM DTT, 0.4 mM NaF, and 10 mM b-glycerophosphate). Fbxl8 complexes were purified using FLAG M2 Agarose (Sigma), separated by SDS Page, and stained with Pierce Silver Stain (Thermoscientific). Gel pieces were cut and submitted to the Taplin Mass Spectroscopy Facility to determine peptide fragment sequences and hence protein identity of co-immunoprecipitated proteins. Spectral matches were manually examined and multiple peptides per protein were required.

In chapter 3 sells were lysed in EBC buffer (50 mM Tris pH 8.0, 120 mM NaCl, 1 mM EDTA, 0.5% NP40) containing 1mM phenylmethylsulfonyl fluoride, 20 U/ml aprotinin, 1μM leupeptin, 1mM dithiothreitol, 0.1mM NaF, 0.1mM Sodium orthovanadate, and 10mM β-glycerophosphate. Proteins were resolved by SDS-PAGE, transferred to the membrane, and immunoblotted with the indicated antibodies; Fbxl8 (Santa Cruz), Fbxw7 (Bethyl Laboratories), c-myc (Cell Signaling, Cyclin D3 (Cell Signaling), Actin (Sigma), Vinculin (Cell Signaling), Anti-Flag (Sigma), and anti-V5 Sigma). Proteins of interest were detected with horseradish peroxidase-conjugated anti-mouse or rabbit antibodies and signals were visualized with the ECL system (Perkin Elmer).

In vitro binding assay

1 × 106 sf9 insect cells were infected with baculovirus expressing Flag-Fbxl8 or Flag-Fbxo4 for 1 h and harvested 40 h post infection. 1 × 106 sf9 insect cells were infected with baculovirus expressing cyclins along with CDK4 for 1 h and harvested 40 h after infection. Harvested cells were lysed in Tween20 lysis buffer (50 mM HEPES (pH 8.0), 150 mM NaCl, 2.5 mM EGTA, 1 mM EDTA, 0.1% Tween 20) with inhibitors for protease and phosphatase (1 mM PMSF, 20 U/ml aprotinin, 5 mg/ml leupeptin, 1 mM DTT, 0.4 mM NaF, 10 mM b-glycerophosphate, and 100 nM okadaic acid) for 30 min. Flag-Fbxl8 or Flag-Fbxo4 was immunoprecipitated from sf9 lysates using anti Flag beads (Sigma Cat No. A2220). The beads were washed with Tween20 lysis buffer and FlagFbxl8 or Flag-Fbxo4 was purified. Purified Flag-Fbxl8 or FlagFbxo4 was incubated with Cyclin D3/CDK4 or cyclin D2/ CDK4 purified from sf9 cells for 4 h and Flag beads were washed with Tween20 lysis buffer for 5 times. Immune complexes were analyzed by western blot.

Co-Immunoprecipitations assays

U2OS cells were transfected with Flag-Fbxl8, Flag-Fbxl8-ΔF/ΔC mutants, with Flag-Fbxw7 and Fbxo31 for 5 hours and harvested 40 hours post-transfection. Harvested cells were lysed in EBC buffer with inhibitors (1 mM PMSF, 20 U/ml aprotinin, 5 mg/ml leupeptin, 1 mM DTT, 0.4 mM NaF, and 10 mM b-glycerophosphate) for protease and phosphatase for 30 minutes. Flag tagged F box proteins were precipitated from cell lysates using anti-Flag beads (Sigma Cat No. A2220). The beads were washed with EBC lysis buffer and F-box proteins were purified. Endogenous binding was conducted by harvesting U2OS cells 5 hours after MG132 treatment. Fbxl8 was precipitated from lysates using

Protein A/G beads (Pierce) crossing linked to Anti-Fbxl8 antibodies (Santa Cruz) via disuccinimidyl suberate.

Ubiquitylation assay

For in vivo ubiquitination assay (chapter 2), NIH3T3 or HEK293T cells were transfected with indicated plasmids (Detail plasmids are described in the figure legends) for 40 h and treated with MG132 (20 μm) for 4 h. The supernatants of cell lysates in 0.2% SDS with RIPA buffer were subjected to immunoprecipitation with antibodies against HA or Flag followed by western analysis to detect the ubiquitinated proteins. For the in-vivo ubiquitination assay (chapter 3), U2OS Cells were transfected with indicated plasmids (Detailed plasmids are described in figure legends) for 40 hours and treated with MG132 (10um) for 6 hours. Cell lysates in EBC buffer were subjected to immunoprecipitation with antibodies against His tagged ubiquitin followed by western analysis to detect the ubiquitinated protein targets.

For in vitro ubiquitination (chapter 2), SCF components including Fbxl8, Cul1, Skp1, Roc1 were purified from 293T cells and incubated with purified cyclin D3/CDK4 from sf9 cells in the presence of E1/E2 enzymes, ubiquitin, and ATP at 37 °C for 60 min. Insect sf9 (1×10^8) cells were infected with baculoviral Flag-Fbxl8 or Flag-ΔF along with remaining SCF components (Skp1, Cul1, and Rbx1) for 1 hour and harvested 40 hours post transfection. Cells were lysed in Tween 20 lysis buffer Harvested cells were lysed in Tween20 lysis buffer (50 mM HEPES (pH 8.0), 150 mM NaCl, 2.5 mM EGTA, 1 mM EDTA, 0.1% Tween 20) with inhibitors for protease and phosphatase (1 mM PMSF, 20 U/ml aprotinin, 5 mg/ml leupeptin, 1 mM DTT, 0.4 mM NaF, and 10 mM b-

glycerophosphate) for 2hours. Flag-Fbxl8 or Flag-ΔF was immunoprecipitated from sf9 lysates using anti Flag beads (Sigma Cat No. A2220). The beads were washed 5 times with Tween 20 lysis buffer and Flag-Fbxl8 or Flag-Fbxl8-ΔF was purified. Purified F-box proteins were incubated with c-myc substrate purified from 293T cells for 2 hours at 37 degrees. Protein complexes were analyzed by western blot.

For in vitro ubiquitylation (chapter 3), sf9 (1×10^8) insect cells were infected with baculoviral Flag-Fbxl8 or Flag-ΔF along with remaining SCF components (Skp1, Cul1, and Rbx1) for 1 hour and harvested 40 hours post transfection. Cells were lysed in Tween 20 lysis buffer Harvested cells were lysed in Tween20 lysis buffer (50 mM HEPES (pH 8.0), 150 mM NaCl, 2.5 mM EGTA, 1 mM EDTA, 0.1% Tween 20) with inhibitors for protease and phosphatase (1 mM PMSF, 20 U/ml aprotinin, 5 mg/ml leupeptin, 1 mM DTT, 0.4 mM NaF, and 10 mM b-glycerophosphate) for 2hours. Flag-Fbxl8 or Flag-ΔF was immunoprecipitated from sf9 lysates using anti Flag beads (Sigma Cat No. A2220). The beads were washed 5 times with Tween 20 lysis buffer and Flag-Fbxl8 or Flag-Fbxl8-ΔF was purified. Purified F-box proteins were incubated with c-myc substrate purified from 293T cells for 2 hours at 37 degrees. Protein complexes were analyzed by western blot.

qRT-PCR analysis

Total RNA was isolated using the RNeasy Micro Kit (Qiagen) and reverse transcribed using iScript cDNA Synthesis Kit (Bio-Rad) according to the manufacturer's instructions. qRT-PCR was performed with SsoAdvanced Universal SYBR Green Supermix (Bio-Rad) and the data were normalized by GAPDH. Immunofluorescence staining Cells were fixed in 4% paraformaldehyde, permeabilized in 0.5% Triton X-100,

stained with rabbit polyclonal and mouse monoclonal antibodies, incubated with Alexa Fluor 488 or 594-conjugated anti-mouse/rabbit IgG (Life Technologies), and mounted with ProLong Gold sntifade reagent with DAPI (Invitrogen)

Transformation assay in soft agar

2500 cells infected with H-rasV12 or c-Myc were seeded in agarose medium (Lonza) (0.4% low melting point agarose as a lower layer and 0.8% agarose as a top layer) on 6-well plates. Cells were grown in 37 °C, 5% CO2 for 21–26 days and colonies were quantified.

Colony formation assay in methylcellulose

Bone marrow cells were aseptically isolated from 5-fluorouracil (5-FU; 150 mg/kg) treated C57BL/6 mice. After red blood cells were removed by using ACK lysis buffer (Lonza), 2 × 104 nucleated cells were plated in triplicates into methylcellulose medium (MethoCult3234; Stem Cell Technologies) supplemented with 50 ng/mL FLT3L, 50 ng/mL SCF, 10 ng/mL IL3, 10 ng/mL IL6, and 10 ng/mL IL7 (Stem Cell Technologies). The colony numbers were counted every 7 days and re-plated for next round of serial replating.

Xenograft

2 × 106 CA46 cells were subcutaneously injected into 8- weeks-old SCID mice with matrigel (BD). Tumor volumes were measured by caliper every 2 days and calculated by the following formula V = (length × width × height)/2. Mice were sacrificed and the

tumor size was measured when tumors reached 10 mm. Care of experimental animals was in accordance with institutional guidelines.

Immunohistochemistry staining and tissue micro array

Lymphoma tissues from xenograft were fixed with 4% PFA, dehydrated, and embedded in paraffin followed by sectioned with a microtome. H&E sections and tissue microarray slides (US Biomax, Inc.) were blocked with 10% goat serum, incubated with the primary antibodies, and subsequently incubated with biotinylated antibodies. Signal was developed with ABC substrate kit (Vector) followed by DAB reaction (Vector), and counterstained with Hematoxylin (Thermo Scientific). The Ki-67 antibody (ab15580) was purchased from Abcam. Fbxl8 antibody (NBP2-34012) was obtained from Novus Biologicals. Cyclin D3 (DCS22) and pRb (S780) were purchased from Cell Signaling Technology and Santa Cruz, respectively. The IHC score in each core was defined by following formula Intensity = (staining positive population (1 to 3) × staining intensity (1 to3)). The IHC scores 1–2, 3–5, and 6–9 was defined as expression of low, medium, and high, respectively.

Statistics, sample size and randomization: The error bars represent standard deviation (SD) of the mean and significance was defined as a p value less than 0.05 with two-tailed, unless otherwise specified. The normality and equal variance of data were evaluated by Shapiro–Wilk test and F-test, respectively. When two groups were normally distributed, the parametric test was applied such as Student's t test for equal variance and Welch's t-test for unequal variance. When group was not normally distributed, non-parametric test such as Wilcoxon rank-sum test was applied. At least three independent

experiments were performed to obtain reproducibility with statistical significance. Sample size and P value were described in figure legends. All samples and animals were randomly allocated to the groups and all investigators were blinded to the group allocation during the experiments.

Generation of Fbxl8 Knockout Allele

Murine embryonic fibroblasts (MEFs) were generated from conditional knockout mice provided by Cyagen. The Fbxl8 allele, specifically exon 3 (which encodes the F-box domain) in these mice is flanked with LoxP sites sensitive to Cre-Recombinase activity. Mouse embryos from a pregnant $Fbxl8^{f/f}$ mother were harvested at day 14 and cells were passed every 3 days until immortalization as dictated by the 3T9 protocol. Immortalized $Fbxl8^{f/f}$ MEFs were then infected with pBABE-Cre recombinase viral particles and excision of Fbxl8 alleles was analyzed via western blot. Primers for genotyping the excision of the allele are:

5’AGTCAACGGAGCCCCTAAAGAGAC’3

5’CGAAACAGAGGATTGAACCCAGTGT’3

Transfection, infection, and Cell Cycle analysis

For transfection, expression plasmids were transfected into cells with lipofectamine (ThermoFisher Scientific or PolyJet (SigmaGen Laboratories) reagent according to the manufacturer’s instructions. For viral production, viral expression plasmids were co-transfected into 293T cells with lipofectamine (ThermoFisher Scientific). Virus supernatants were harvested 48 to 72 hours after transfection and used to infect cells with

polybrene (10ug/ul). For cell cycle experiments, NIH 3T3 cells were synchronized in G0/G1 phase by contact inhibition or DMEM containing 0.1% FBS for 36 hours at high density. Cell cycle were released from G0/G1 phase by splitting cells with DMEM containing 10% FBS. $Fbxl8^{f/f}$ and $Fbxl8^{-/-}$ Cells were harvested, fixed, and stained using Cytofix and Permeabilization Plus reagents from APC BRDU Flow Kit (BD Pharmingen). For BRDU detection, cells were cultured in medium containing 10uM BRDU for 30 minutes, fixed with Cytofix and Permeabilization Plus reagents (BD Pharmingen) and stained with an anti-BRDU monoclonal antibody conjugated with APC and 7-AAD for DNA staining. Cell cycle distribution and BRDU positive Cells were measured with a BD Accuri C6 Plus Flow Cytometer.

References:

1. Llombart, V. and M.R. Mansour, *Therapeutic targeting of "undruggable" MYC.* EBioMedicine, 2022. **75**: p. 103756.
2. Li, Z., et al., *A global transcriptional regulatory role for c-Myc in Burkitt's lymphoma cells.* Proc Natl Acad Sci U S A, 2003. **100**(14): p. 8164-9.
3. Wahlstrom, T. and M.A. Henriksson, *Impact of MYC in regulation of tumor cell metabolism.* Biochim Biophys Acta, 2015. **1849**(5): p. 563-9.
4. Delgado, M.D. and J. Leon, *Myc roles in hematopoiesis and leukemia.* Genes Cancer, 2010. **1**(6): p. 605-16.
5. Jiang, J., et al., *Direct Phosphorylation and Stabilization of MYC by Aurora B Kinase Promote T-cell Leukemogenesis.* Cancer Cell, 2020. **37**(2): p. 200-215 e5.
6. Madden, S.K., et al., *Taking the Myc out of cancer: toward therapeutic strategies to directly inhibit c-Myc.* Mol Cancer, 2021. **20**(1): p. 3.
7. Gregory, M.A. and S.R. Hann, *c-Myc proteolysis by the ubiquitin-proteasome pathway: stabilization of c-Myc in Burkitt's lymphoma cells.* Mol Cell Biol, 2000. **20**(7): p. 2423-35.
8. Welcker, M., et al., *Two diphosphorylated degrons control c-Myc degradation by the Fbw7 tumor suppressor.* Sci Adv, 2022. **8**(4): p. eabl7872.
9. Farrell, A.S. and R.C. Sears, *MYC degradation.* Cold Spring Harb Perspect Med, 2014. **4**(3).
10. Bachireddy, P., P.K. Bendapudi, and D.W. Felsher, *Getting at MYC through RAS.* Clin Cancer Res, 2005. **11**(12): p. 4278-81.
11. Sears, R.C., *The life cycle of C-myc: from synthesis to degradation.* Cell Cycle, 2004. **3**(9): p. 1133-7.
12. Gregory, M.A., Y. Qi, and S.R. Hann, *Phosphorylation by glycogen synthase kinase-3 controls c-myc proteolysis and subnuclear localization.* J Biol Chem, 2003. **278**(51): p. 51606-12.
13. Welcker, M., et al., *The Fbw7 tumor suppressor regulates glycogen synthase kinase 3 phosphorylation-dependent c-Myc protein degradation.* Proc Natl Acad Sci U S A, 2004. **101**(24): p. 9085-90.
14. Yada, M., et al., *Phosphorylation-dependent degradation of c-Myc is mediated by the F-box protein Fbw7.* EMBO J, 2004. **23**(10): p. 2116-25.
15. Yeh, E., et al., *A signalling pathway controlling c-Myc degradation that impacts oncogenic transformation of human cells.* Nat Cell Biol, 2004. **6**(4): p. 308-18.
16. Beaulieu, M.E., F. Castillo, and L. Soucek, *Structural and Biophysical Insights into the Function of the Intrinsically Disordered Myc Oncoprotein.* Cells, 2020. **9**(4).
17. Varmus, H.E., *The molecular genetics of cellular oncogenes.* Annu Rev Genet, 1984. **18**: p. 553-612.
18. Kalkat, M., et al., *MYC Deregulation in Primary Human Cancers.* Genes (Basel), 2017. **8**(6).
19. Taub, R., et al., *Translocation of the c-myc gene into the immunoglobulin heavy chain locus in human Burkitt lymphoma and murine plasmacytoma cells.* Proc Natl Acad Sci U S A, 1982. **79**(24): p. 7837-41.
20. Ghazzaui, N., et al., *Emu and 3'RR transcriptional enhancers of the IgH locus cooperate to promote c-myc-induced mature B-cell lymphomas.* Blood Adv, 2020. **4**(1): p. 28-39.

21. Adams, J.M., et al., *The c-myc oncogene driven by immunoglobulin enhancers induces lymphoid malignancy in transgenic mice.* Nature, 1985. **318**(6046): p. 533-8.
22. Abrams, H.D., L.R. Rohrschneider, and R.N. Eisenman, *Nuclear location of the putative transforming protein of avian myelocytomatosis virus.* Cell, 1982. **29**(2): p. 427-39.
23. Kelly, K., et al., *Cell-specific regulation of the c-myc gene by lymphocyte mitogens and platelet-derived growth factor.* Cell, 1983. **35**(3 Pt 2): p. 603-10.
24. Bentley, D.L. and M. Groudine, *A block to elongation is largely responsible for decreased transcription of c-myc in differentiated HL60 cells.* Nature, 1986. **321**(6071): p. 702-6.
25. Laird-Offringa, I.A., et al., *Poly(A) tail shortening is the translation-dependent step in c-myc mRNA degradation.* Mol Cell Biol, 1990. **10**(12): p. 6132-40.
26. Land, H., L.F. Parada, and R.A. Weinberg, *Tumorigenic conversion of primary embryo fibroblasts requires at least two cooperating oncogenes.* Nature, 1983. **304**(5927): p. 596-602.
27. Vaux, D.L., S. Cory, and J.M. Adams, *Bcl-2 gene promotes haemopoietic cell survival and cooperates with c-myc to immortalize pre-B cells.* Nature, 1988. **335**(6189): p. 440-2.
28. Strasser, A., et al., *Novel primitive lymphoid tumours induced in transgenic mice by cooperation between myc and bcl-2.* Nature, 1990. **348**(6299): p. 331-3.
29. Hanahan, D. and R.A. Weinberg, *The hallmarks of cancer.* Cell, 2000. **100**(1): p. 57-70.
30. Armelin, H.A., et al., *Functional role for c-myc in mitogenic response to platelet-derived growth factor.* Nature, 1984. **310**(5979): p. 655-60.
31. Amati, B., et al., *Oncogenic activity of the c-Myc protein requires dimerization with Max.* Cell, 1993. **72**(2): p. 233-45.
32. McMahon, S.B., M.A. Wood, and M.D. Cole, *The essential cofactor TRRAP recruits the histone acetyltransferase hGCN5 to c-Myc.* Mol Cell Biol, 2000. **20**(2): p. 556-62.
33. McMahon, S.B., et al., *The novel ATM-related protein TRRAP is an essential cofactor for the c-Myc and E2F oncoproteins.* Cell, 1998. **94**(3): p. 363-74.
34. Cheng, S.W., et al., *c-MYC interacts with INI1/hSNF5 and requires the SWI/SNF complex for transactivation function.* Nat Genet, 1999. **22**(1): p. 102-5.
35. Cowling, V.H. and M.D. Cole, *The Myc transactivation domain promotes global phosphorylation of the RNA polymerase II carboxy-terminal domain independently of direct DNA binding.* Mol Cell Biol, 2007. **27**(6): p. 2059-73.
36. Cleveland, J.L., et al., *Negative regulation of c-myc transcription involves myc family proteins.* Oncogene Res, 1988. **3**(4): p. 357-75.
37. Grignani, F., et al., *Negative autoregulation of c-myc gene expression is inactivated in transformed cells.* EMBO J, 1990. **9**(12): p. 3913-22.
38. Facchini, L.M. and L.Z. Penn, *The molecular role of Myc in growth and transformation: recent discoveries lead to new insights.* FASEB J, 1998. **12**(9): p. 633-51.
39. Obaya, A.J., M.K. Mateyak, and J.M. Sedivy, *Mysterious liaisons: the relationship between c-Myc and the cell cycle.* Oncogene, 1999. **18**(19): p. 2934-41.
40. Schuhmacher, M., et al., *Control of cell growth by c-Myc in the absence of cell division.* Curr Biol, 1999. **9**(21): p. 1255-8.
41. Ngo, C.V., et al., *An in vivo function for the transforming Myc protein: elicitation of the angiogenic phenotype.* Cell Growth Differ, 2000. **11**(4): p. 201-10.

42. Dews, M., et al., *Augmentation of tumor angiogenesis by a Myc-activated microRNA cluster.* Nat Genet, 2006. **38**(9): p. 1060-5.
43. Pelengaris, S., M. Khan, and G.I. Evan, *Suppression of Myc-induced apoptosis in beta cells exposes multiple oncogenic properties of Myc and triggers carcinogenic progression.* Cell, 2002. **109**(3): p. 321-34.
44. Evan, G.I., et al., *Induction of apoptosis in fibroblasts by c-myc protein.* Cell, 1992. **69**(1): p. 119-28.
45. de Alboran, I.M., E. Baena, and A.C. Martinez, *c-Myc-deficient B lymphocytes are resistant to spontaneous and induced cell death.* Cell Death Differ, 2004. **11**(1): p. 61-8.
46. Maclean, K.H., et al., *c-Myc augments gamma irradiation-induced apoptosis by suppressing Bcl-XL.* Mol Cell Biol, 2003. **23**(20): p. 7256-70.
47. Egle, A., et al., *Bim is a suppressor of Myc-induced mouse B cell leukemia.* Proc Natl Acad Sci U S A, 2004. **101**(16): p. 6164-9.
48. Conacci-Sorrell, M. and R.N. Eisenman, *Post-translational control of Myc function during differentiation.* Cell Cycle, 2011. **10**(4): p. 604-10.
49. Ohtake, F., et al., *K63 ubiquitylation triggers proteasomal degradation by seeding branched ubiquitin chains.* Proc Natl Acad Sci U S A, 2018. **115**(7): p. E1401-E1408.
50. Nandi, D., et al., *The ubiquitin-proteasome system.* J Biosci, 2006. **31**(1): p. 137-55.
51. Deshaies, R.J., *SCF and Cullin/Ring H2-based ubiquitin ligases.* Annu Rev Cell Dev Biol, 1999. **15**: p. 435-67.
52. Sailo, B.L., et al., *FBXW7 in Cancer: What Has Been Unraveled Thus Far?* Cancers (Basel), 2019. **11**(2).
53. Yeh, C.H., M. Bellon, and C. Nicot, *FBXW7: a critical tumor suppressor of human cancers.* Mol Cancer, 2018. **17**(1): p. 115.
54. Popov, N., et al., *Ubiquitylation of the amino terminus of Myc by SCF(beta-TrCP) antagonizes SCF(Fbw7)-mediated turnover.* Nat Cell Biol, 2010. **12**(10): p. 973-81.
55. Lippens, G., I. Landrieu, and C. Smet, *Molecular mechanisms of the phospho-dependent prolyl cis/trans isomerase Pin1.* FEBS J, 2007. **274**(20): p. 5211-22.
56. Chuang, H.H., et al., *Targeting Pin1 for Modulation of Cell Motility and Cancer Therapy.* Biomedicines, 2021. **9**(4).
57. Farrell, A.S., et al., *Pin1 regulates the dynamics of c-Myc DNA binding to facilitate target gene regulation and oncogenesis.* Mol Cell Biol, 2013. **33**(15): p. 2930-49.
58. Popov, N., et al., *The ubiquitin-specific protease USP28 is required for MYC stability.* Nat Cell Biol, 2007. **9**(7): p. 765-74.
59. Sun, X.X., R.C. Sears, and M.S. Dai, *Deubiquitinating c-Myc: USP36 steps up in the nucleolus.* Cell Cycle, 2015. **14**(24): p. 3786-93.
60. Chakravorty, D., A. Ghosh, and S. Saha, *Computational approach to target USP28 for regulating Myc.* Comput Biol Chem, 2020. **85**: p. 107208.
61. von der Lehr, N., et al., *The F-box protein Skp2 participates in c-Myc proteosomal degradation and acts as a cofactor for c-Myc-regulated transcription.* Mol Cell, 2003. **11**(5): p. 1189-200.
62. Kim, S.Y., et al., *Skp2 regulates Myc protein stability and activity.* Mol Cell, 2003. **11**(5): p. 1177-88.
63. Hydbring, P., A. Castell, and L.G. Larsson, *MYC Modulation around the CDK2/p27/SKP2 Axis.* Genes (Basel), 2017. **8**(7).

64. Bretones, G., et al., *SKP2 oncogene is a direct MYC target gene and MYC down-regulates p27(KIP1) through SKP2 in human leukemia cells.* J Biol Chem, 2011. **286**(11): p. 9815-25.
65. Adhikary, S., et al., *The ubiquitin ligase HectH9 regulates transcriptional activation by Myc and is essential for tumor cell proliferation.* Cell, 2005. **123**(3): p. 409-21.
66. Peter, S., et al., *Tumor cell-specific inhibition of MYC function using small molecule inhibitors of the HUWE1 ubiquitin ligase.* EMBO Mol Med, 2014. **6**(12): p. 1525-41.
67. Choi, S.H., et al., *Myc protein is stabilized by suppression of a novel E3 ligase complex in cancer cells.* Genes Dev, 2010. **24**(12): p. 1236-41.
68. Petroski, M.D. and R.J. Deshaies, *Function and regulation of cullin-RING ubiquitin ligases.* Nat Rev Mol Cell Biol, 2005. **6**(1): p. 9-20.
69. Jamal, A., et al., *The G1 phase E3 ubiquitin ligase TRUSS that gets deregulated in human cancers is a novel substrate of the S-phase E3 ubiquitin ligase Skp2.* Cell Cycle, 2015. **14**(16): p. 2688-700.
70. Izumi, H. and Y. Kaneko, *Trim32 facilitates degradation of MYCN on spindle poles and induces asymmetric cell division in human neuroblastoma cells.* Cancer Res, 2014. **74**(19): p. 5620-30.
71. Nicklas, S., et al., *A complex of the ubiquitin ligase TRIM32 and the deubiquitinase USP7 balances the level of c-Myc ubiquitination and thereby determines neural stem cell fate specification.* Cell Death Differ, 2019. **26**(4): p. 728-740.
72. Dias, D.C., et al., *CUL7: A DOC domain-containing cullin selectively binds Skp1.Fbx29 to form an SCF-like complex.* Proc Natl Acad Sci U S A, 2002. **99**(26): p. 16601-6.
73. Koch, H.B., et al., *Large-scale identification of c-MYC-associated proteins using a combined TAP/MudPIT approach.* Cell Cycle, 2007. **6**(2): p. 205-17.
74. Paul, I., et al., *The ubiquitin ligase CHIP regulates c-Myc stability and transcriptional activity.* Oncogene, 2013. **32**(10): p. 1284-95.
75. Ballinger, C.A., et al., *Identification of CHIP, a novel tetratricopeptide repeat-containing protein that interacts with heat shock proteins and negatively regulates chaperone functions.* Mol Cell Biol, 1999. **19**(6): p. 4535-45.
76. Vaquero, A., et al., *SirT2 is a histone deacetylase with preference for histone H4 Lys 16 during mitosis.* Genes Dev, 2006. **20**(10): p. 1256-61.
77. Fraga, M.F., et al., *Loss of acetylation at Lys16 and trimethylation at Lys20 of histone H4 is a common hallmark of human cancer.* Nat Genet, 2005. **37**(4): p. 391-400.
78. Liu, P.Y., et al., *The histone deacetylase SIRT2 stabilizes Myc oncoproteins.* Cell Death Differ, 2013. **20**(3): p. 503-14.
79. Kim, B.Y., et al., *NEMO stabilizes c-Myc through direct interaction in the nucleus.* FEBS Lett, 2010. **584**(22): p. 4524-30.
80. Kim, B.Y., et al., *Phosphorylation and stabilization of c-Myc by NEMO renders cells resistant to ionizing radiation through up-regulation of gamma-GCS.* Oncol Rep, 2011. **26**(6): p. 1587-93.
81. Vervoorts, J., et al., *Stimulation of c-MYC transcriptional activity and acetylation by recruitment of the cofactor CBP.* EMBO Rep, 2003. **4**(5): p. 484-90.
82. Patel, J.H., et al., *The c-MYC oncoprotein is a substrate of the acetyltransferases hGCN5/PCAF and TIP60.* Mol Cell Biol, 2004. **24**(24): p. 10826-34.
83. Yuan, J., K. Minter-Dykhouse, and Z. Lou, *A c-Myc-SIRT1 feedback loop regulates cell growth and transformation.* J Cell Biol, 2009. **185**(2): p. 203-11.

84. Salghetti, S.E., et al., *Regulation of transcriptional activation domain function by ubiquitin.* Science, 2001. **293**(5535): p. 1651-3.
85. Zhang, Q., et al., *Domain-specific c-Myc ubiquitylation controls c-Myc transcriptional and apoptotic activity.* Proc Natl Acad Sci U S A, 2013. **110**(3): p. 978-83.
86. Nesbit, C.E., J.M. Tersak, and E.V. Prochownik, *MYC oncogenes and human neoplastic disease.* Oncogene, 1999. **18**(19): p. 3004-16.
87. Minella, A.C. and B.E. Clurman, *Mechanisms of tumor suppression by the SCF(Fbw7).* Cell Cycle, 2005. **4**(10): p. 1356-9.
88. Knuutila, S., et al., *DNA copy number losses in human neoplasms.* Am J Pathol, 1999. **155**(3): p. 683-94.
89. Akhoondi, S., et al., *FBXW7/hCDC4 is a general tumor suppressor in human cancer.* Cancer Res, 2007. **67**(19): p. 9006-12.
90. Kajiro, M., et al., *The ubiquitin ligase CHIP acts as an upstream regulator of oncogenic pathways.* Nat Cell Biol, 2009. **11**(3): p. 312-9.
91. Hemann, M.T., et al., *Evasion of the p53 tumour surveillance network by tumour-derived MYC mutants.* Nature, 2005. **436**(7052): p. 807-11.
92. Malempati, S., et al., *Aberrant stabilization of c-Myc protein in some lymphoblastic leukemias.* Leukemia, 2006. **20**(9): p. 1572-81.
93. Zhang, X., et al., *Mechanistic insight into Myc stabilization in breast cancer involving aberrant Axin1 expression.* Proc Natl Acad Sci U S A, 2012. **109**(8): p. 2790-5.
94. Farrell, A.S., et al., *Targeting inhibitors of the tumor suppressor PP2A for the treatment of pancreatic cancer.* Mol Cancer Res, 2014. **12**(6): p. 924-39.
95. Mannava, S., et al., *PP2A-B56alpha controls oncogene-induced senescence in normal and tumor human melanocytic cells.* Oncogene, 2012. **31**(12): p. 1484-92.
96. Sablina, A.A. and W.C. Hahn, *SV40 small T antigen and PP2A phosphatase in cell transformation.* Cancer Metastasis Rev, 2008. **27**(2): p. 137-46.
97. Eichhorn, P.J., M.P. Creyghton, and R. Bernards, *Protein phosphatase 2A regulatory subunits and cancer.* Biochim Biophys Acta, 2009. **1795**(1): p. 1-15.
98. Khanna, A., et al., *MYC-dependent regulation and prognostic role of CIP2A in gastric cancer.* J Natl Cancer Inst, 2009. **101**(11): p. 793-805.
99. Come, C., et al., *CIP2A is associated with human breast cancer aggressivity.* Clin Cancer Res, 2009. **15**(16): p. 5092-100.
100. Westermarck, J. and W.C. Hahn, *Multiple pathways regulated by the tumor suppressor PP2A in transformation.* Trends Mol Med, 2008. **14**(4): p. 152-60.
101. Cristobal, I., et al., *Overexpression of SET is a recurrent event associated with poor outcome and contributes to protein phosphatase 2A inhibition in acute myeloid leukemia.* Haematologica, 2012. **97**(4): p. 543-50.
102. Christensen, D.J., et al., *SET oncoprotein overexpression in B-cell chronic lymphocytic leukemia and non-Hodgkin lymphoma: a predictor of aggressive disease and a new treatment target.* Blood, 2011. **118**(15): p. 4150-8.
103. Janghorban, M., et al., *Targeting c-MYC by antagonizing PP2A inhibitors in breast cancer.* Proc Natl Acad Sci U S A, 2014. **111**(25): p. 9157-62.
104. Soucek, L., et al., *Modelling Myc inhibition as a cancer therapy.* Nature, 2008. **455**(7213): p. 679-83.
105. Davis, A.C., et al., *A null c-myc mutation causes lethality before 10.5 days of gestation in homozygotes and reduced fertility in heterozygous female mice.* Genes Dev, 1993. **7**(4): p. 671-82.

106. Wiese, K.E., et al., *The role of MIZ-1 in MYC-dependent tumorigenesis.* Cold Spring Harb Perspect Med, 2013. **3**(12): p. a014290.
107. van Wezel, T., et al., *Expression analysis of candidate breast tumour suppressor genes on chromosome 16q.* Breast Cancer Res, 2005. **7**(6): p. R998-1004.
108. Chang, S.C., et al., *Human FBXL8 Is a Novel E3 Ligase Which Promotes BRCA Metastasis by Stimulating Pro-Tumorigenic Cytokines and Inhibiting Tumor Suppressors.* Cancers (Basel), 2020. **12**(8).
109. Chang, S.C., et al., *A Novel Signature of CCNF-Associated E3 Ligases Collaborate and Counter Each Other in Breast Cancer.* Cancers (Basel), 2021. **13**(12).
110. Yoshida, A., et al., *Fbxl8 suppresses lymphoma growth and hematopoietic transformation through degradation of cyclin D3.* Oncogene, 2021. **40**(2): p. 292-306.
111. Matsushime, H., et al., *Colony-stimulating factor 1 regulates novel cyclins during the G1 phase of the cell cycle.* Cell, 1991. **65**.
112. Lin, D.I., et al., *Phosphorylation-dependent ubiquitination of cyclin D1 by the SCF(FBX4-alphaB crystallin) complex.* Mol Cell, 2006. **24**.
113. Quelle, D.E., et al., *Overexpression of mouse D-type cyclins accelerates G1 phase in rodent fibroblasts.* Genes Dev, 1993. **7**.
114. Alt, J.R., et al., *Phosphorylation-dependent regulation of cyclin D1 nuclear export and cyclin D1-dependent cellular transformation.* Genes Dev, 2000. **14**.
115. Baldin, V., et al., *Cyclin D1 is a nuclear protein required for cell cycle progression in G1.* Genes Dev, 1993. **7**.
116. Diehl, J.A., et al., *Glycogen synthase kinase-3beta regulates cyclin D1 proteolysis and subcellular localization.* Genes Dev, 1998. **12**.
117. Bu, Y., et al., *A PERK-miR-211 axis suppresses circadian regulators and protein synthesis to promote cancer cell survival.* Nat Cell Biol, 2018. **20**.
118. Li, Y., et al., *PRMT5 is required for lymphomagenesis triggered by multiple oncogenic drivers.* Cancer Discov, 2015. **5**.
119. Dong, H., et al., *OSdlbcl: an online consensus survival analysis web server based on gene expression profiles of diffuse large B-cell lymphoma.* Cancer Med, 2020. **9**.
120. Sherr, C.J., D. Beach, and G.I. Shapiro, *Targeting CDK4 and CDK6: from discovery to therapy.* Cancer Discov, 2016. **6**.
121. Anders, L., et al., *A systematic screen for CDK4/6 substrates links FOXM1 phosphorylation to senescence suppression in cancer cells.* Cancer Cell, 2011. **20**.
122. Casanovas, O., et al., *P38SAPK2 phosphorylates cyclin D3 at Thr-283 and targets it for proteasomal degradation.* Oncogene, 2004. **23**.
123. Schmitz, R., et al., *Burkitt lymphoma pathogenesis and therapeutic targets from structural and functional genomics.* Nature, 2012. **490**.
124. Chen, B.B., et al., *F-box protein FBXL2 exerts human lung tumor suppressor-like activity by ubiquitin-mediated degradation of cyclin D3 resulting in cell cycle arrest.* Oncogene, 2012. **31**.
125. Chen, B.B., et al., *F-box protein FBXL2 targets cyclin D2 for ubiquitination and degradation to inhibit leukemic cell proliferation.* Blood, 2012. **119**.
126. Sherr, C.J., D. Beach, and G.I. Shapiro, *Targeting CDK4 and CDK6: From Discovery to Therapy.* Cancer Discov, 2016. **6**(4): p. 353-67.
127. Anders, L., et al., *A systematic screen for CDK4/6 substrates links FOXM1 phosphorylation to senescence suppression in cancer cells.* Cancer Cell, 2011. **20**(5): p. 620-34.

128. Meyer, N. and L.Z. Penn, *Reflecting on 25 years with MYC.* Nat Rev Cancer, 2008. **8**(12): p. 976-90.
129. Sato, M., et al., *MYC is a critical target of FBXW7.* Oncotarget, 2015. **6**(5): p. 3292-305.
130. Felsher, D.W., *MYC Inactivation Elicits Oncogene Addiction through Both Tumor Cell-Intrinsic and Host-Dependent Mechanisms.* Genes Cancer, 2010. **1**(6): p. 597-604.
131. Mertz, J.A., et al., *Targeting MYC dependence in cancer by inhibiting BET bromodomains.* Proc Natl Acad Sci U S A, 2011. **108**(40): p. 16669-74.
132. Srinivasan, S.V., et al., *Cdc45 is a critical effector of myc-dependent DNA replication stress.* Cell Rep, 2013. **3**(5): p. 1629-39.
133. McMahon, S.B., *MYC and the control of apoptosis.* Cold Spring Harb Perspect Med, 2014. **4**(7): p. a014407.
134. Zhang, T., et al., *MYC and the unfolded protein response in cancer: synthetic lethal partners in crime?* EMBO Mol Med, 2020. **12**(5): p. e11845.
135. Arabi, A., et al., *c-Myc associates with ribosomal DNA and activates RNA polymerase I transcription.* Nat Cell Biol, 2005. **7**(3): p. 303-10.
136. Nagy, P., et al., *Myc-driven overgrowth requires unfolded protein response-mediated induction of autophagy and antioxidant responses in Drosophila melanogaster.* PLoS Genet, 2013. **9**(8): p. e1003664.
137. Arabi, A., et al., *Accumulation of c-Myc and proteasomes at the nucleoli of cells containing elevated c-Myc protein levels.* J Cell Sci, 2003. **116**(Pt 9): p. 1707-17.
138. Becker, S., et al., *Destruction of a Microtubule-Bound MYC Reservoir during Mitosis Contributes to Vincristine's Anticancer Activity.* Mol Cancer Res, 2020. **18**(6): p. 859-872.

Appendix A: Fbxl8 interacts with and regulates cyclin D3 in a phosphorylation dependent manner.

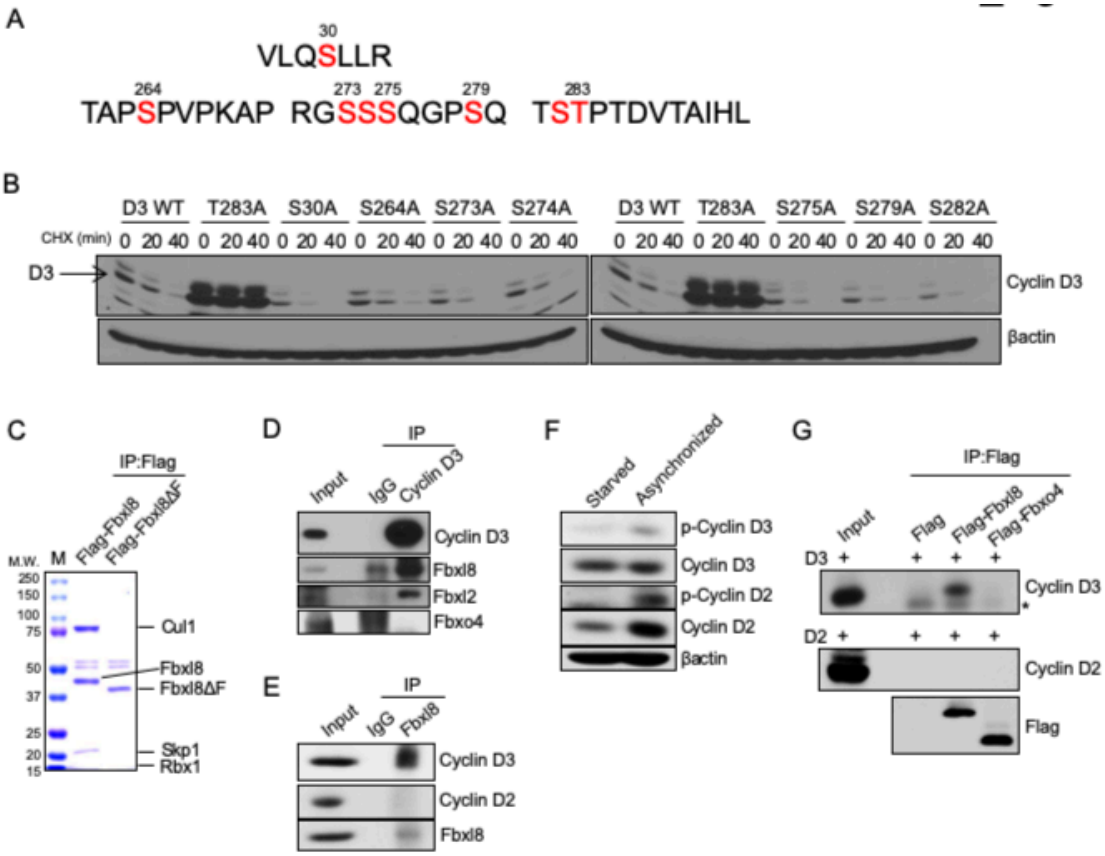

a. Phosphorylated residues (red) in cyclin D3 identified by mass spec.

b. Lysates from NIH3T3 cells transfected with cyclin D3 (WT), T283A, S30A, S264A, S273A, S274A, S275A, S279A and treated with 100ug/mL of cycloheximide (CHX) for the indicated time periods were analyzed by western blot using antibodies against cyclin D3 and Actin. Only Thr-283 is required for rapid degradation of cyclin D3.

c. Lysates from sf9 cells infected with Cul1, Skp1, Rbx1, and Flag-Fbxl8 or Flag-Fbxl8-ΔF were immunoprecipitated with anti Flag beads. Immune complexes were analyzed by Coomassie Brilliant Blue staining for SCF components (Cul1, Skp1, and Rbx1).

d. Lysates from NIH3T3 cells treated with proteasome inhibitor MG132 (20uM) for 4 hours were immunoprecipitated with antibodies against normal IgG and or Cyclin D3. Immune complexes were analyzed for cyclin D3, Fbxo4, Fbxl8, and Fbxl2.

e. Lysates from Raji cells with proteasome inhibitor MG132 (20uM) for 4 hours were immunoprecipitated with antibodies against normal IgG or Fbxl8. Immune complexes were analyzed for cyclin D3, cyclin D2, and Fbxl8.

f. Lysates from serum starved and asynchronized NIH 3T3 were analyzed by western blot using antibodies against p-cyclin D3 (T283), cyclin D3, p-cyclin D2 (T280), cyclin D2, and Actin.

g. Immune complexes from sf9 cells infected with cyclin D3/CDK4 or cyclin D2/CDK4 for 4 hours. *In vitro* binding was assessed by western blot for cyclin D3, cyclin D2, and, Flag. (*indicates non-specific band)

Appendix B: Fbxl8 regulates cyclin D3 stability

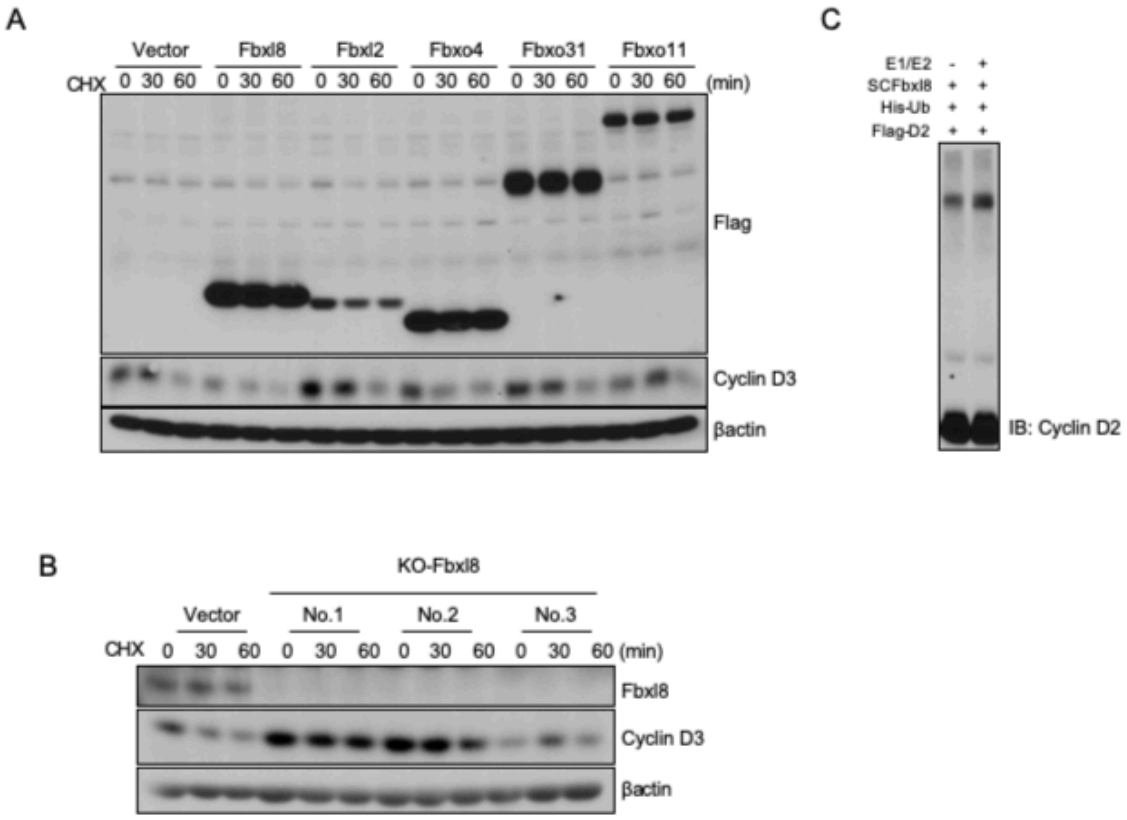

a. Lysates from U2OS cells transfected with ectopic Fbxl8, Fbxl2, Fbxo4, Fbxo31, or Fbx011 and treated with cycloheximide (CHX) as indicated time periods were analyzed by western blot using antibodies against Flag, cyclin D3, cyclin D2, cyclin D1, and Actin.

b. Lysates from CRISPR-mediated knockout cell lines (clones 1, 2, and 3) in NIH3T3 cells treated with CHX as indicated time periods were analyzed by western blot using antibodies against Fbxl8, cyclin D3, cyclin D2, and cyclin D1, and Actin.

c. In vitro ubiquitylation assays were performed in reaction mixtures containing the presence or absence of the indicated reaction mixture components. Lysates from assays were analyzed by western blot using antibody against cyclin D2.

Appendix C: Fbxl8 regulates the G1-S phase transition

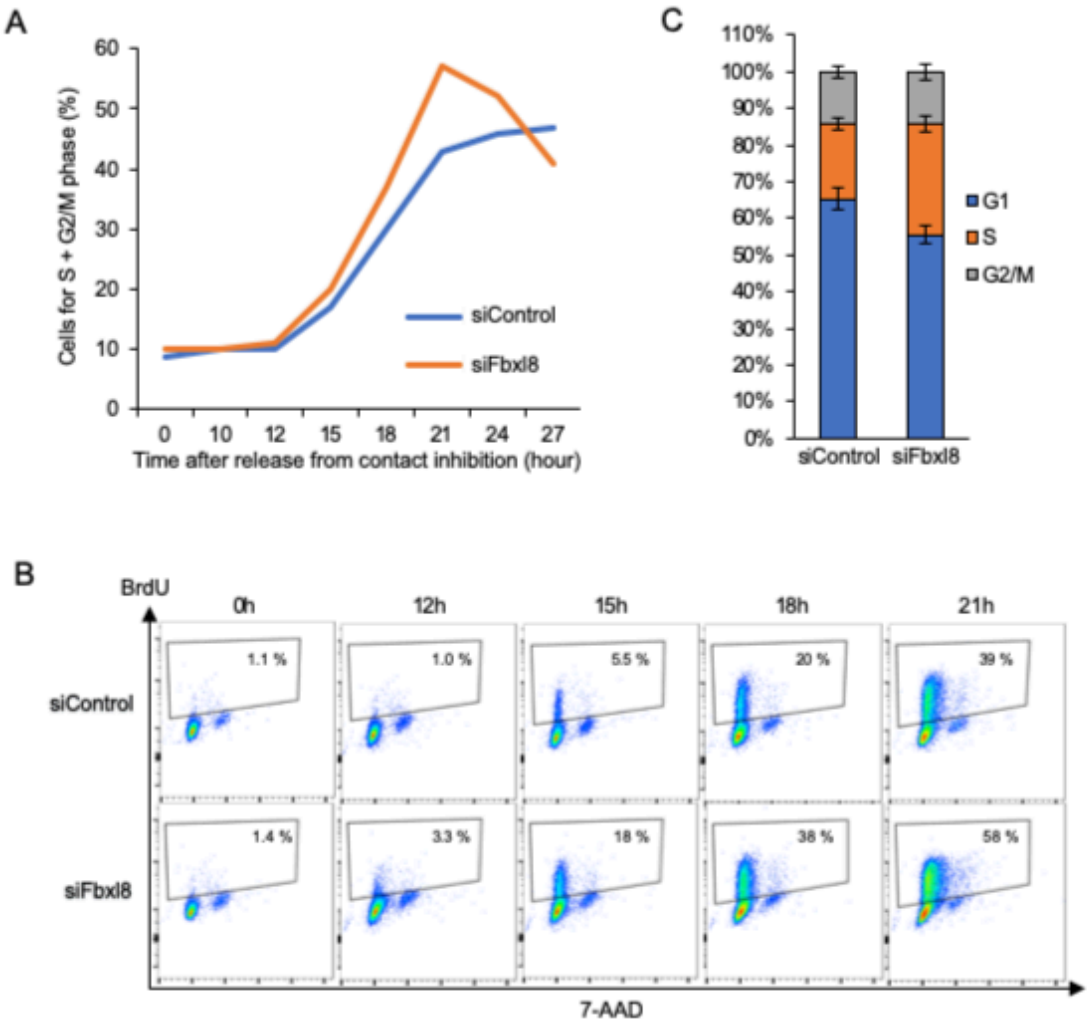

NIH3T3 cells were transfected with siControl or siFbxl8 and arrested at G0/G1 by contact inhibition for 36 hours:

a. Cell cycle was analyzed 10, 12,15,18,21, 24, and 27 hours after release from G0/G1 phase. Quantification of cells in S/G2+M phase was shown.

b. S phase entry was assessed by BrdU incorporation assay (30min) using cells 0, 12, 15, 18, 21 hours after release from G0/G1 phase. Representative FACS profiles were shown.

c. NIH 3T3 cells were transfected with siControl or siFbxl8. Cell cycle distribution was measured by BrdU incorporation Assay

Appendix D: Fbxl8 G1-S transition through cyclin D3

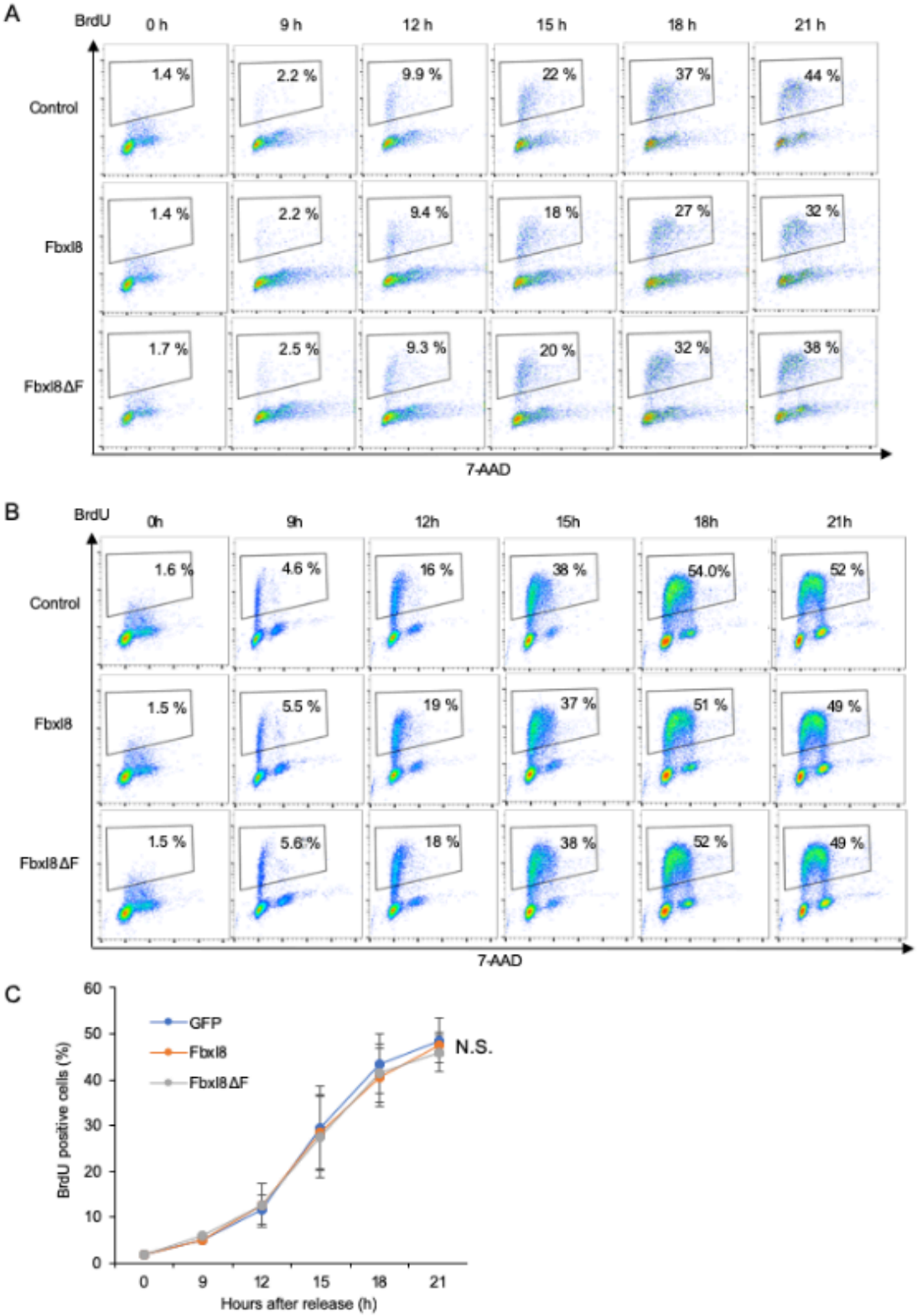

D

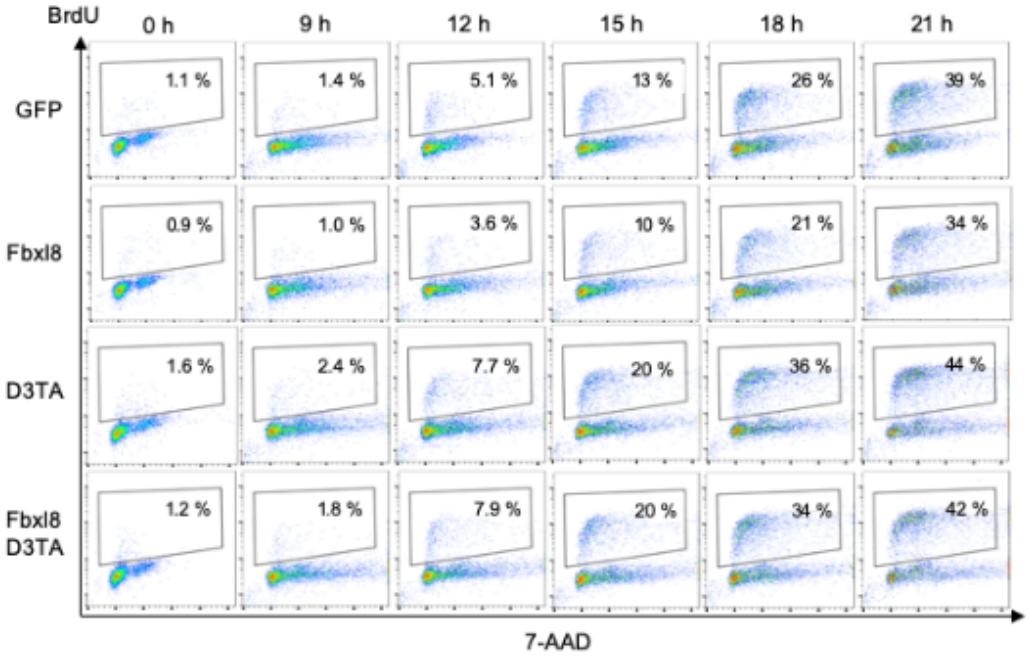

NIH3T3 cells (a,b) were transfected with MigR1 IRES-GFP, MigR1-Fbxl8 RES-GFP or MigR1-Fbxl8-ΔF IRES-GFP and arrested at G0/G1 by serum starvation for 36 hours. GFP and BrdU double positive cells (a) and GFP negative and BrdU positive cells (b) were analyzed 0, 9, 12, 15, 18, and 21, hours after release from G0/G1 phase by resplitting cells in DMEM with 10% FBS. Representative FACS profile were shown.

c. Quantification of GFP positive and Brdu positive cells from (b); mean +/- SD, N.S., Not significant (two tailed student T-test, n=3)

d. NIH 3T3 cells were transfected with MigR1 IRES-GFP, MigR1-Fbxl8 IRES-GFP, MigR1-cyclinD3TA IRES-GFP, or MigR1-Fbxl8 IRES-GFP + MigR1-cyclinD3TA IRES-GFP and arrested at G0/G1 phase by serum starvation for 36 hours. GFP and BrdU double positive cells were analyzed 9, 12, 15, 18, 21, after release from G0/G1 phase by re-splitting cells in DMEM with 10%FBS. Representative FACS profiles were shown

Appendix E: Subcellular localization of cyclin D3 during cell division

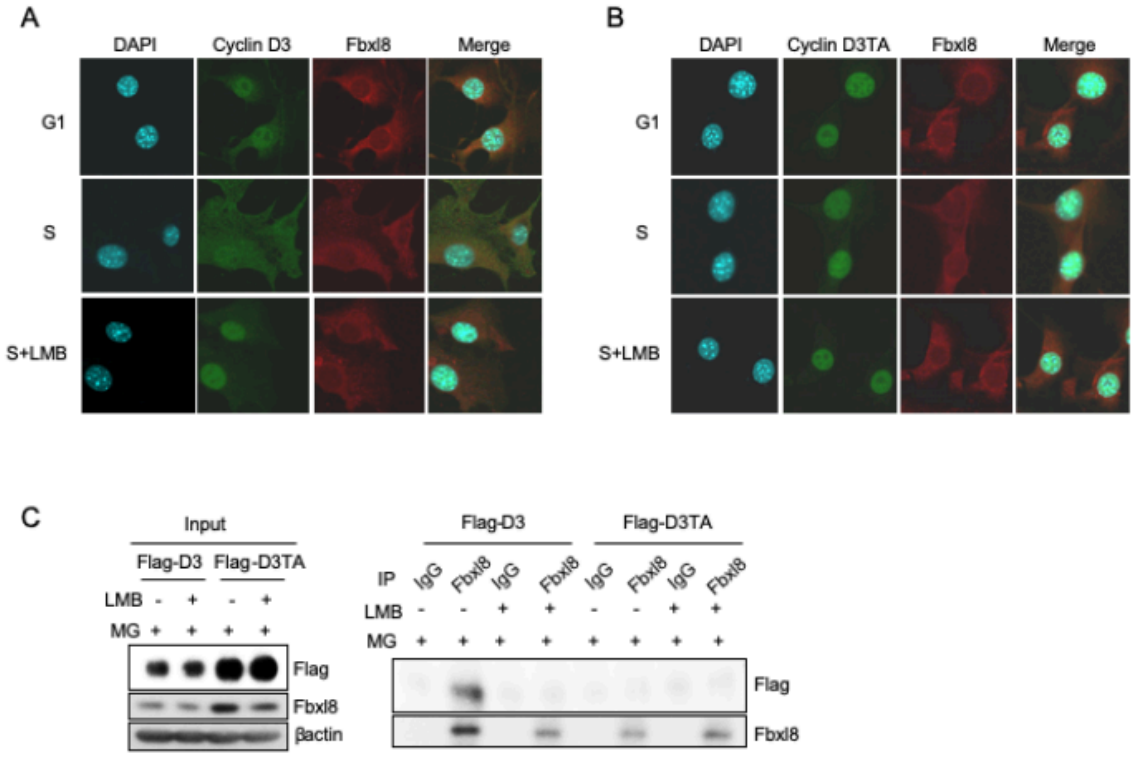

NIH3T3 cells (a,b) were transfected with previously sequenced Flag tagged cyclin D3 (a) or Flag tagged cyclin D3T283A (b), and arrested at G0/G1 phase by serum starvation for 36 hours. Localization of cyclin D3 and Fbxl8 were assessed by immunofluorescence in cell at midG1 (8 hours) and S phase (16 hours) with or without treatment of leptomycin B (10ng/mL), an inhibitor of nuclear export, for 2 hours after release from, G0/G1 phase by re-splitting cells in DMEM with 10% FBS. Representative pictures were shown.

c. NIH3T3 cells were infected with previously sequenced Flag tagged cyclin D3 or Flag D3283A and arrested at G0/G1 phase by serum starvation for 36 hours. Binding of cyclin D3 or cyclin D3TA and Fbxl8 in cells at S phase (16 hours) with or without treatment of Leptomycin B (10ng/mL) for 2 hours with a proteasome inhibitor MG132 (20uM) for 4 hours.

Appendix F: Cyclin D3 is overexpressed in c-myc driven Tumors

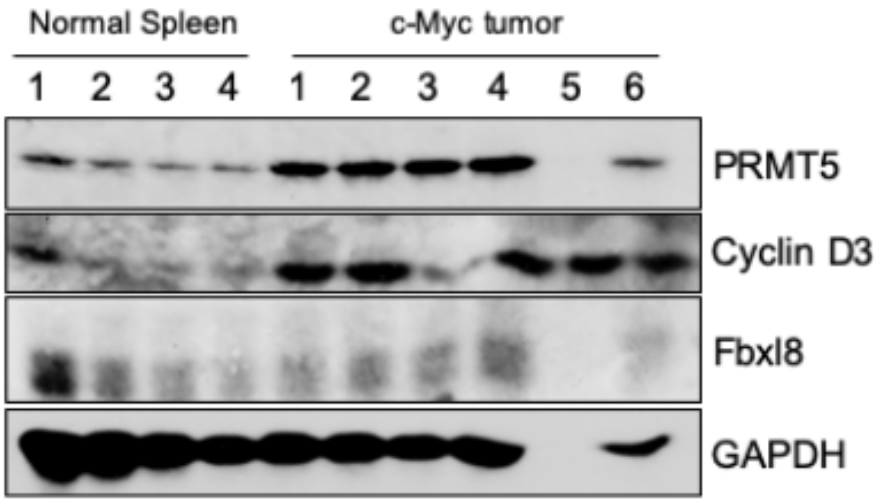

Bone marrow cells isolated from 5-FU (150mg/kg) treated mice were retrovirally transduced with MigR1/c-Myc in the presence of IL-3, IL-6, and stem cell factor (SCF) and then transplanted into lethally irradiated (900 rad) recipient mice. Lysates from c-Myc driven tumors and normal spleens cells were analyzed by western blot using antibodies against PRMT5, cyclin D3, Fbxl8, and GAPDH.

Appendix G: Fbxl8 regulates lymphoma cell proliferation through cyclin D3

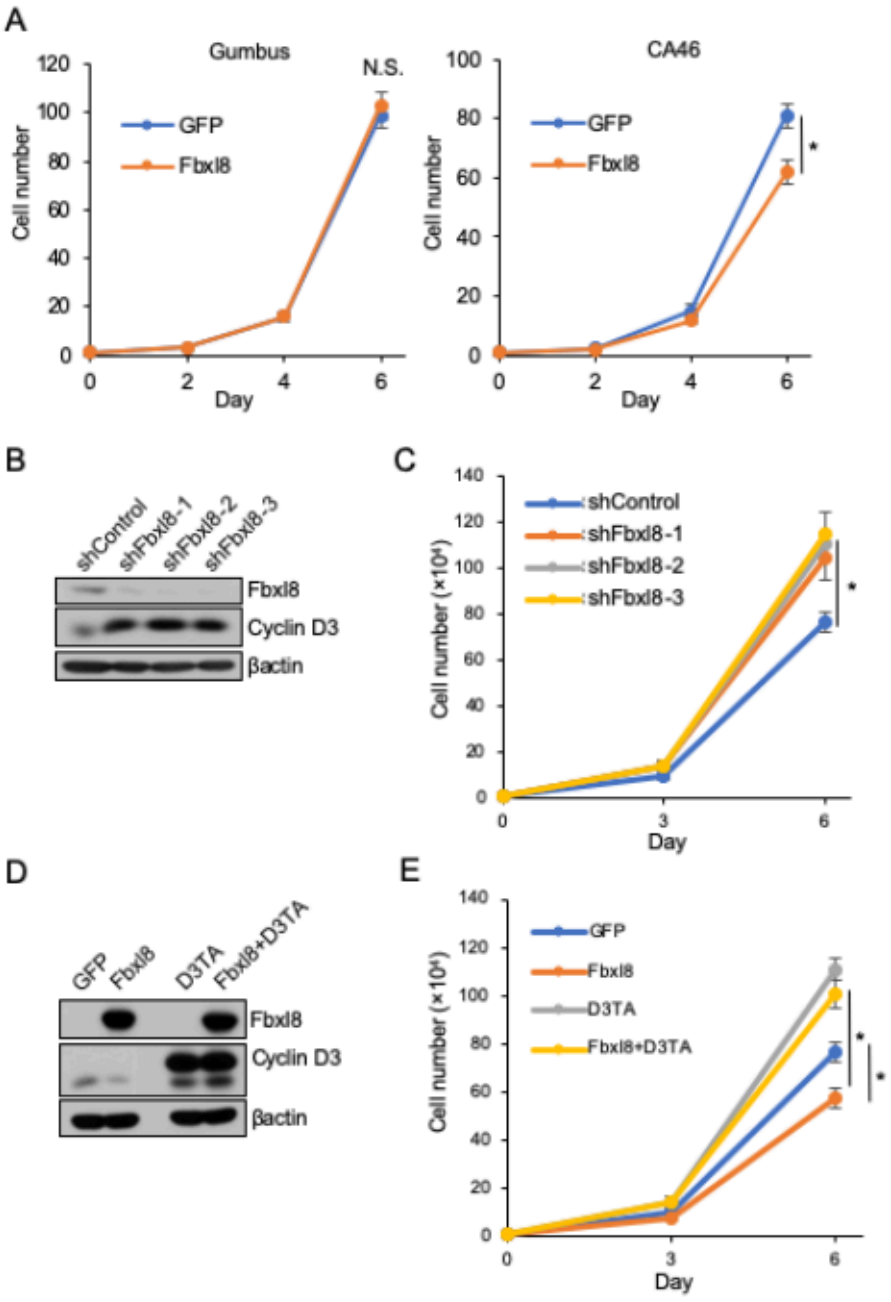

a. 10,000 Gumbus cells or CA46 cells infected with GFP or GFP/Flag-Fbxl8 were plated, and cell numbers were counted every 2 days. Data represents +/- SD, * $p<0.05$ (two tailed student t-tests, n=3).

b. Lysates from CA46 cells infected with sh-Control and shFbxl8s (1-3) were analyzed by western blot using antibodies against Fbxl8, cyclin D3, and actin.

c. 10,000 cells from B were plated and cell numbers were counted every 3 days. Data represents mean +/- SD *$p<0.05$ (two tailed Student t-Test, n=3)

d. Lysates from CA46 cells infected with GFP, Fbxl8, cyclin D3TA, or cyclin D3 + Fbxl8 were analyzed by western blot using antibodies against Fbxl8, cyclin D3, and Actin.

e. 10,000 CA46 cells from (d) were plated every and counted every 3 days. Data represents mean +/- SD * $p=<0.05$ (two tailed student t-test, n=3)

Appendix H: Cyclin D3 overexpression renders cells to susceptible to Palbociclib

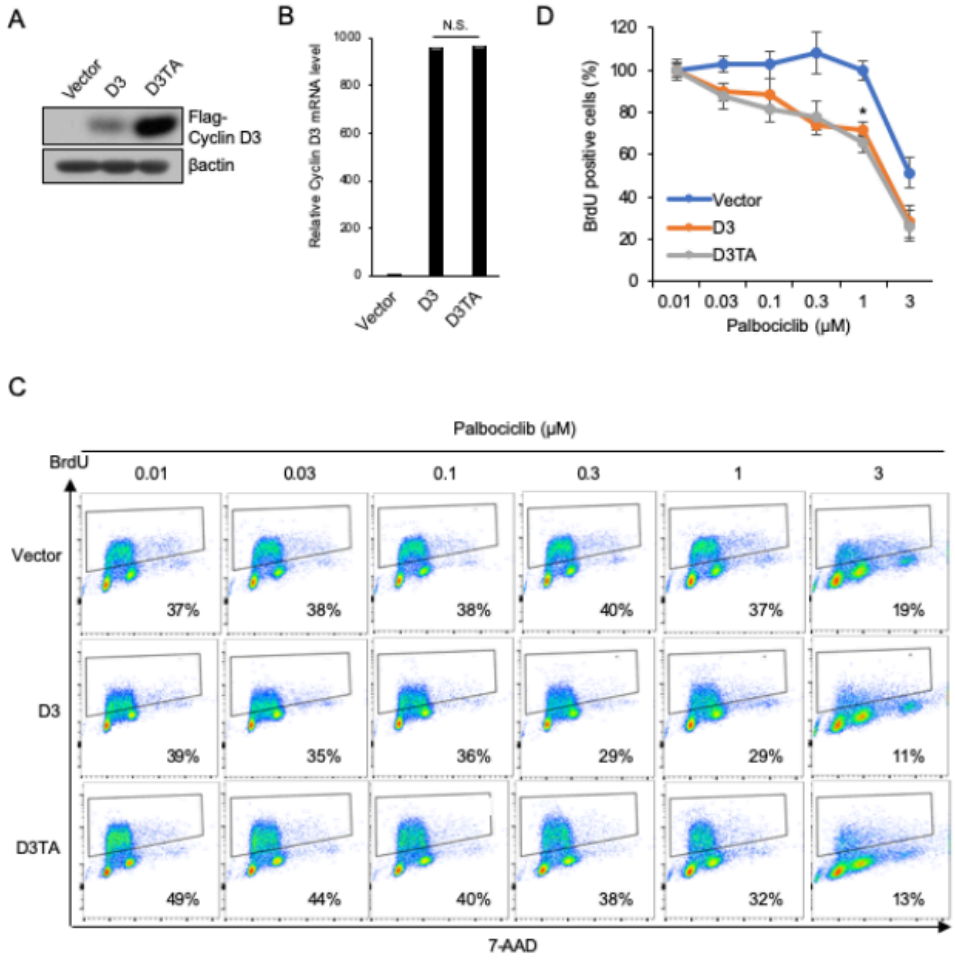

a. Lysates from NIH 3T3 cells infected with vector, Flag-cyclin D3, or Flag-cyclin D3TA were analyzed by western blot using antibodies against Flag and Actin.

b. QPCR analysis of samples from (a) using a set of primer for cyclin D3. Data from normalized by GAPDH and represent mean +/- SD. NS., Not Significant (n=3).

c. NIH3T3 cells from (a) were subjected to BrdU incorporation for 40 min post Palbociclib treatment for 2 days at different concentrations (0.01, 0.03, 0.1, 0.3, 1 and 3uM). BrdU and DNA content were determined by anti-BrdU (Y axis) and 7-AAD (X axis) respectively and analyzed by FACS.

d. Quantification of BrdU positive cells from [c] mean +/- SD *$p<0.05$ (n=3).

Appendix I: p38 or GSK3ß marginally regulate cyclin D3 phosphorylation

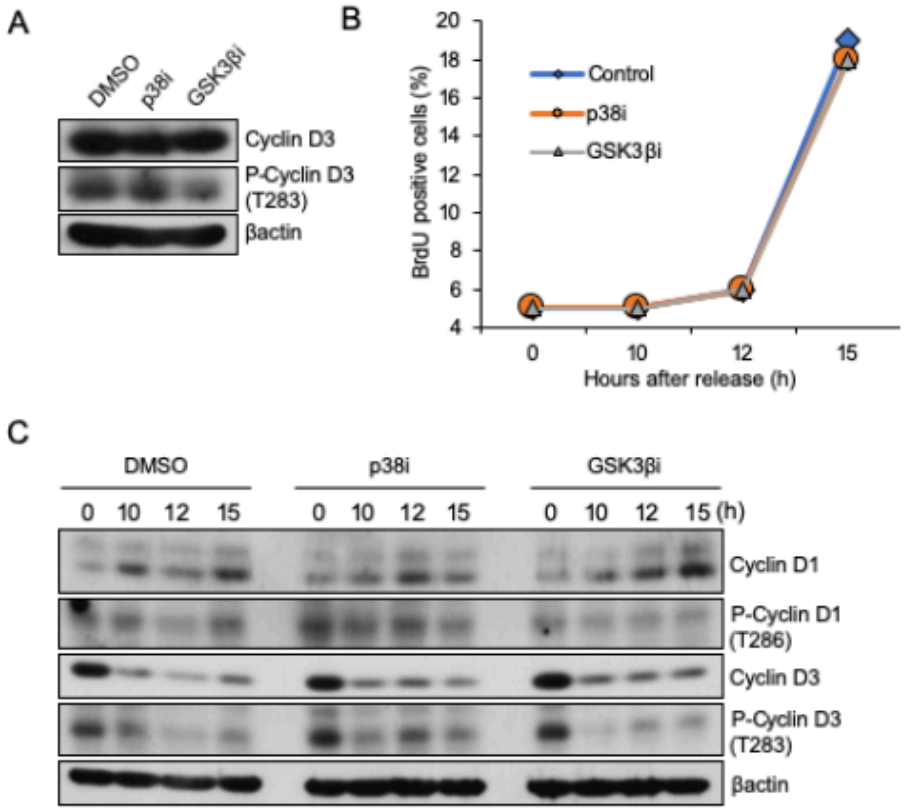

a. Western analysis of lysates from CA46 cells treated with DMSO, SB203580 (p38 inhibitor 10uM) or SB216763 (GSK3ß inhibitor 10uM) for 2 hours for phospho-cyclin D3, cyclin D2, and Actin.

b. NIH3T3 cells were arrested at G0/G1 by contact inhibition for 36 hours. Following release by replating at low density, the S-phase population was analyzed at 0, 10, 12, and 15 hours by BrdU incorporation assay. Quantification of BrdU positive cells were shown. DMSO, SB203580 (p38 inhibitor 10uM) or SB216763 (GSK3ß inhibitor 10uM) were treated 2 hours prior to analysis.

c. Western Analysis of lysates from (b) for phospho-cyclin D3 (T283), cyclin D3, phosphor-cyclin D1 (T286), cyclin D1, and actin.

Appendix J: Mass Spectroscopy Analysis

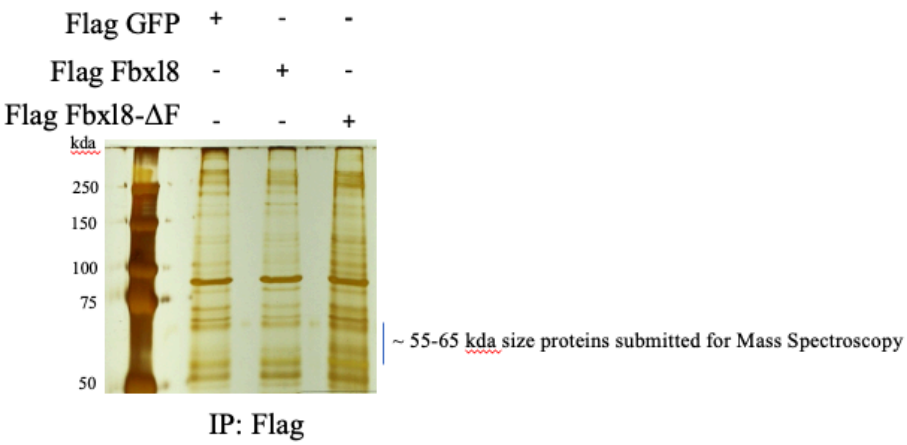

c-myc Sequence Homology

>P01108_MYC_MOUSE Myc proto-oncogene protein OS=Mus musculus GN=Myc PE=1 SV=1

MPLNVNFTNR NYDLDYDSVQ PYFICDEEEN FYHQQQQSEL QPPAPSEDIW KKFELLPTPP LSPSRRSGLC SPSYVAVATS FSPREDDDGG GGNFSTADQL
EMMTELLGGD MVNQSFICDP DDETFIKNII IQDCMWSGFS AAAKLVSEKL ASYQAARKDS TSLSPARGHS VCSTSSLYLQ DLTAAASECI DPSVVFPYPL
NDSSSPKSCT SSDSTAFSPS SDSLLSSESS PRASPEPLVL HEETPPTTSS DSEEEQEDEE EIDVVSVEKR QTPAKRSESG SSPSRGHSKP PHSPLVLKRC
HVSTHQHNYA APPSTRKDYP AAKRAKLDSG RVLKQISNNR KCSSPRSSDT EENDKRRTHN VLERQRRNEL KRSFFALRDQ IPELENNEKA PKVVILKKAT
AYILSIQADE HKLTSEKDLL RKRREQLKHK LEQLRNSGA

POSITION	SEQUENCE (click to highlight)	SEARCH: 30059 60498 Scan.Charge	Score	ΔScore	Ions
53-65	FELLPTPPLSPSR				
	K.FELLPTPPLSPSR.A	8710.2	1.76	0.128	8/24
150-157	LASYQAAR				
	K.LASYQAAR.K	525.2	1.94	0.26	10/14

Protein Coverage	
21 AA	4.78 %

293T expressing Flag-Tagged Fbxl8 (wildtype) or Flag-Tagged Fbxl8-ΔF (mutant) cells were harvested and subsequently lysed. Fbxl8 complexes were purified using FLAG M2 Agarose (Sigma), separated by SDS Page, and stained with Pierce Silver Stain (Thermo scientific). Samples were submitted for mass spectroscopy to determine peptide fragment sequences and hence protein identity of co-immunoprecipitated proteins. Spectral matches were manually examined and multiple peptides per protein were required.

Appendix K: Cell Cycle Analysis Strategy

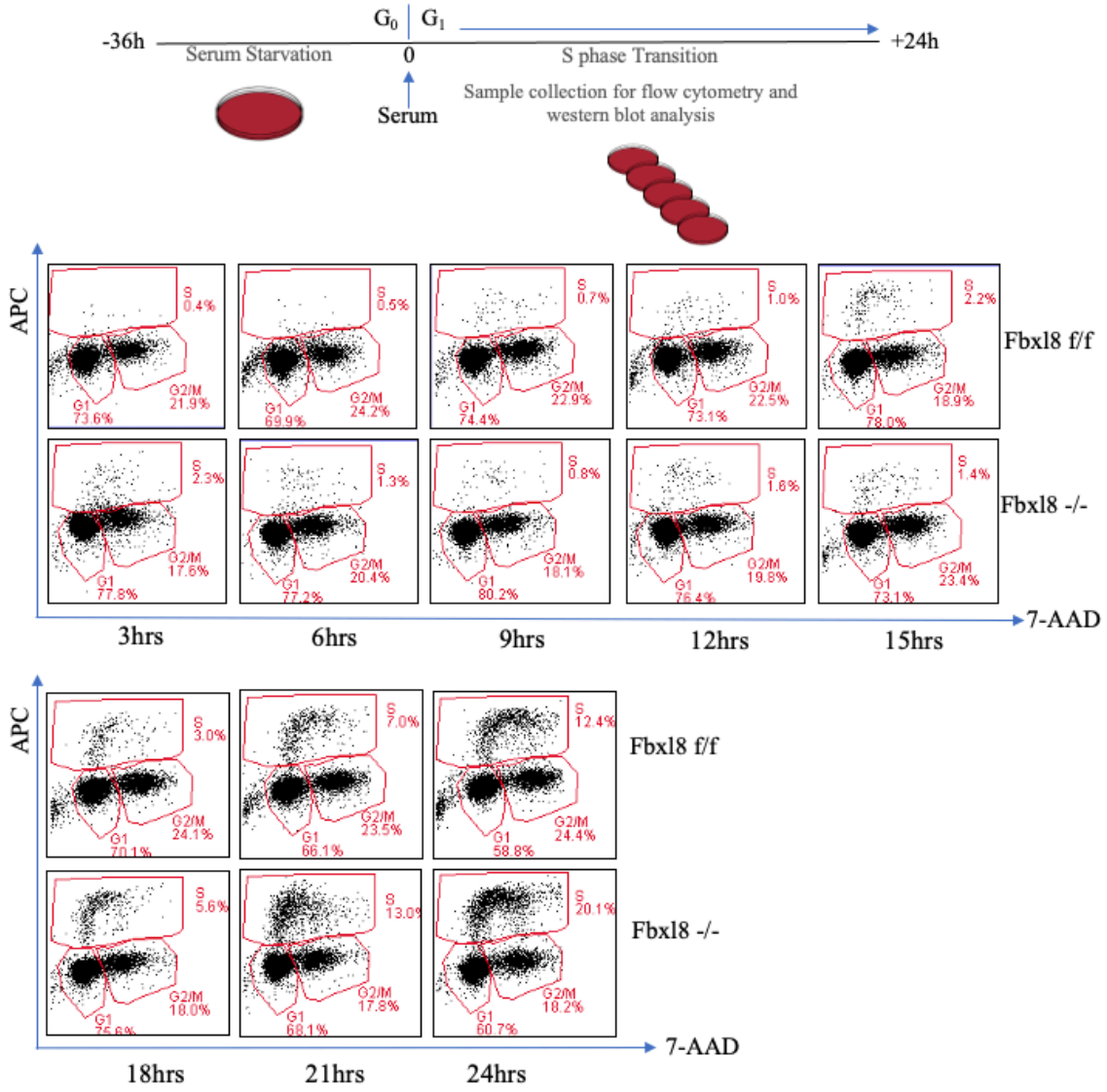

Experimental strategy assessing changes in G1/S phase of cell cycle. Fbxl8 knockout on cell cycle progression, Fbxl8$^{f/f}$ and Fbxl8$^{-/-}$ MDFs were arrested in G0/G1 via serum starvation and contact inhibition. Cell cycle reentry was analyzed at 0-24 hours following mitogenic stimulation.

Appendix L: Single color controls for G1/S phase transition

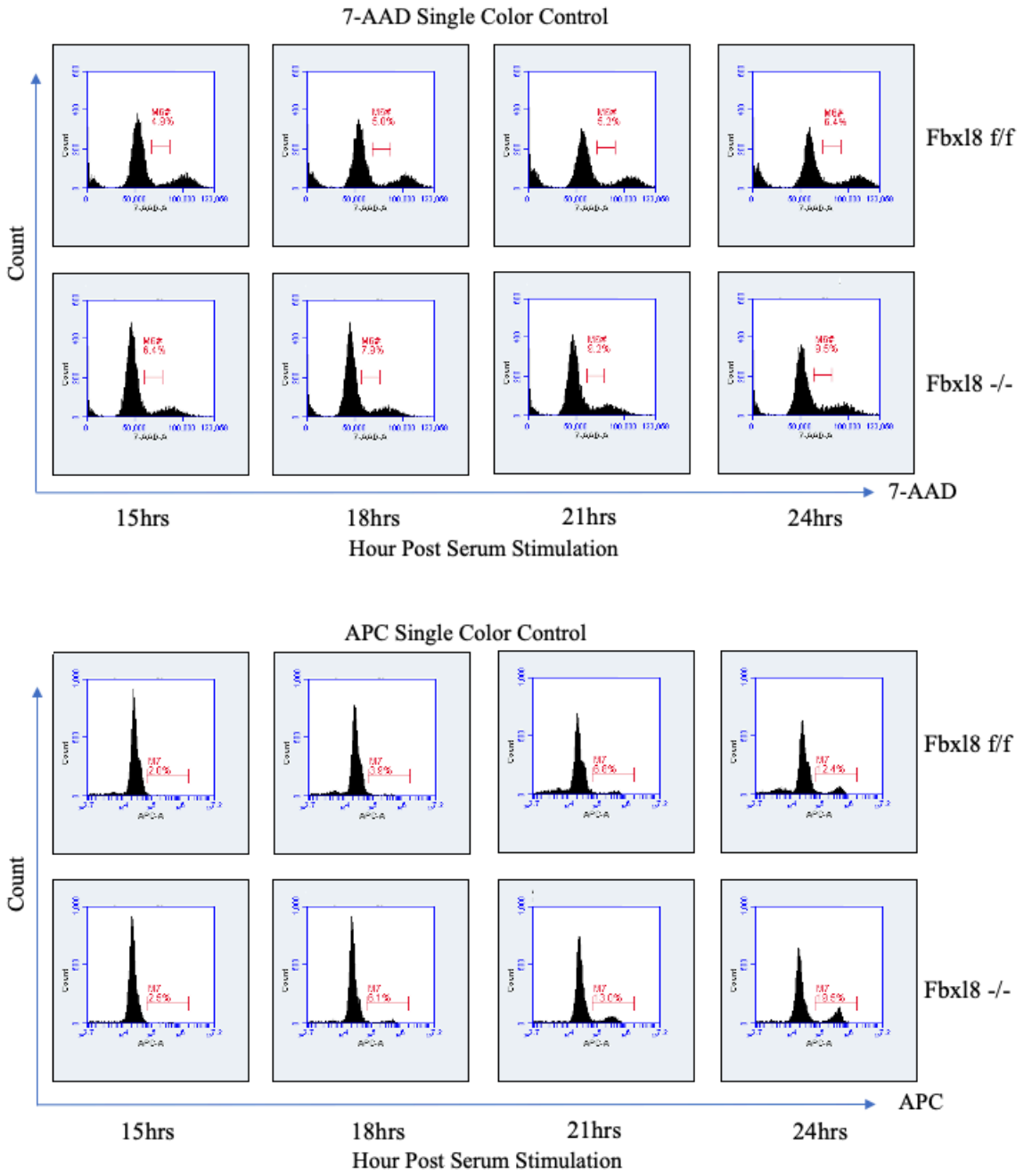

Single color controls (APC and 7-AAD) for 15, 18 21, and 24-hour time points for Fbxl8$^{+/+}$ and Fbxl8$^{-/-}$.

Appendix M: Cell Cycle Analysis Strategy for si-c-myc knock down cells

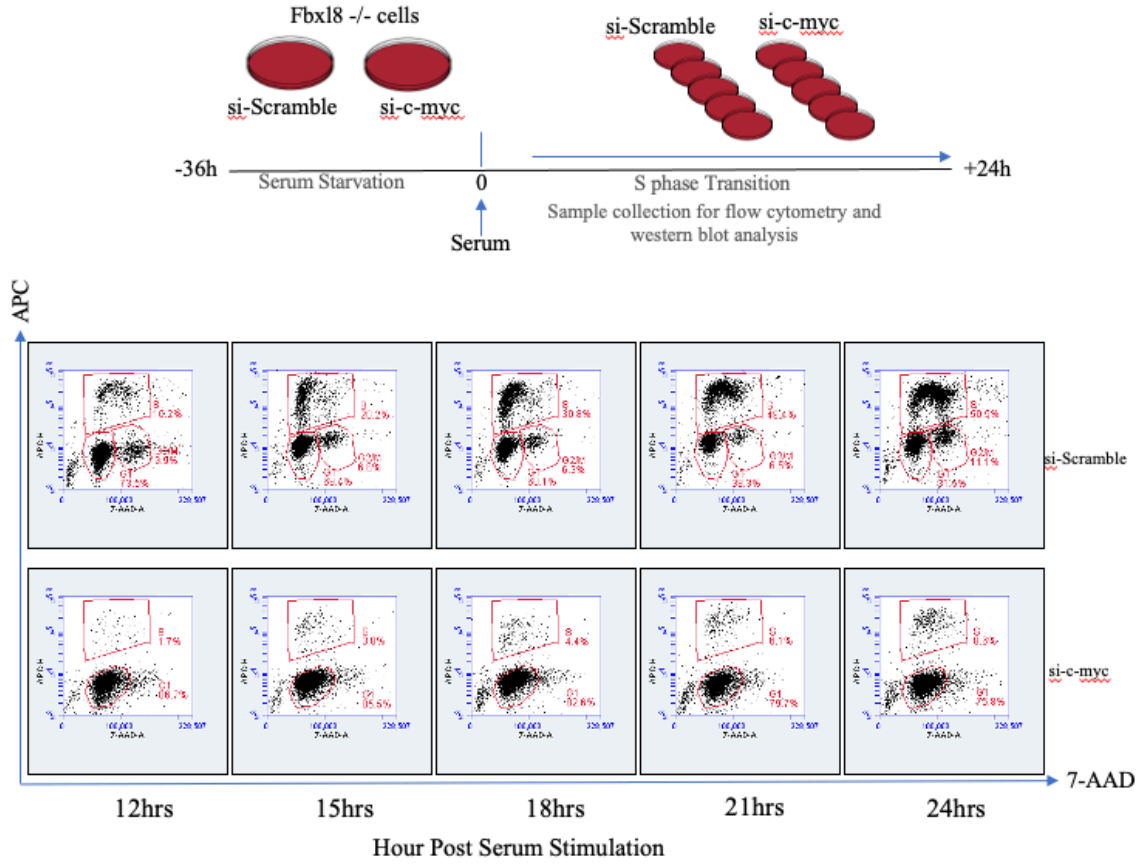

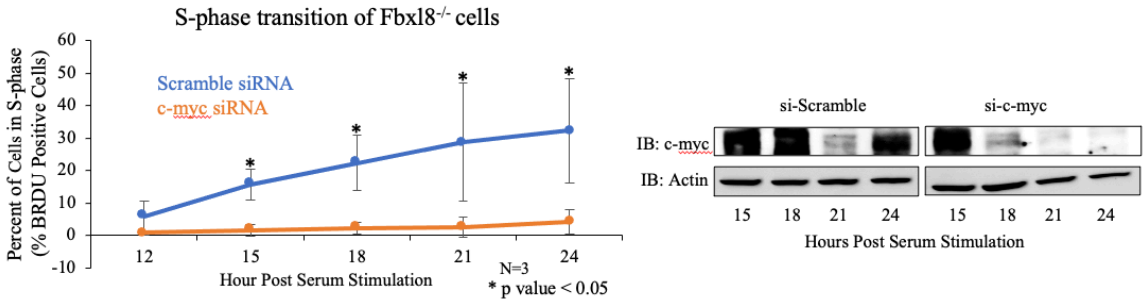

Fbxl8$^{-/-}$ cells treated with si-Scramble and si-c-myc were synchronized via serum starvation and harvested from 12-24 hours. Samples were analyzed for western blot and flow cytometry to confirm c-myc knock down and S-phase transition.

Appendix N: In Vitro Ubiquitylation Assay with K48 and K63 linkages

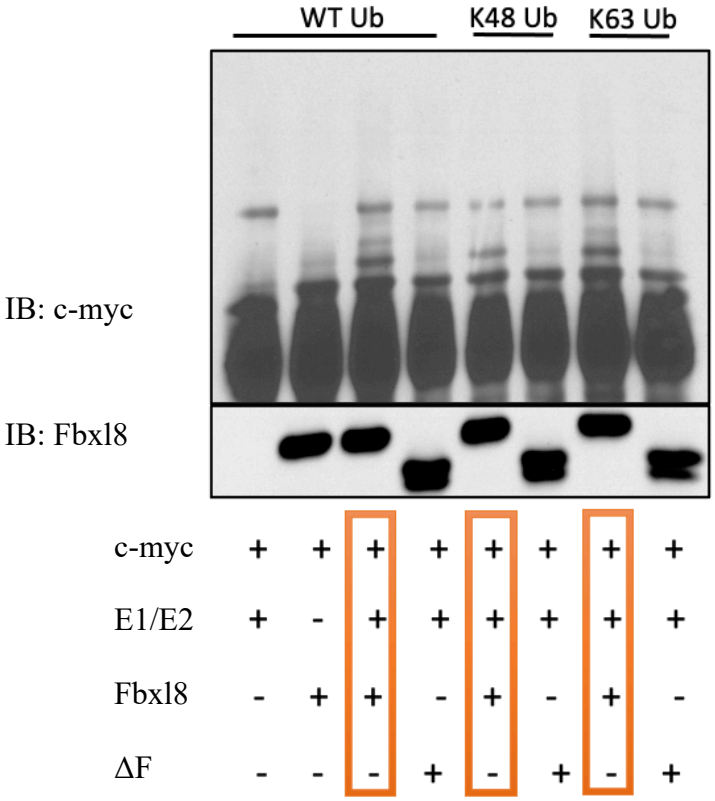

In vitro ubiquitylation assay was performed to detect ubiquitylation of c-myc by Fbxl8 with WT, K48 only, and K63 only ubiquitin.

Appendix O: Fractionation of Fbxl8 f/f and Fbxl8 -/- MEFS 15 hours post serum stimulation

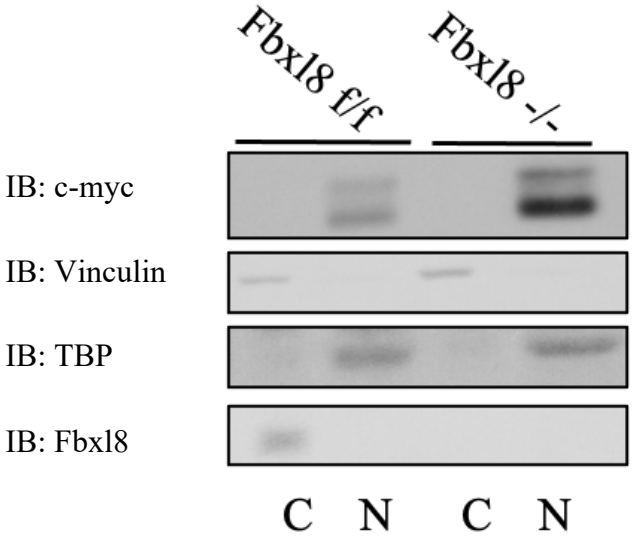

MEF cells treated synchronized via serum starvation and harvested 15 hours post serum stimulation. Samples were analyzed for western blot to observed where c-myc was accumulating after Fbxl8 excision from the genome.